UNIVERSITAT POLITÈCNICA DE CATALUNYA
BARCELONATECH
Escola Superior d'Enginyeries Industrial,
Aeroespacial i Audiovisual de Terrassa

BACHELOR FINAL THESIS

Aerodynamic study of the evolution of a Formula 1 front wing with the change in regulations between the 2021 and 2022 seasons

Document:

Report

Author:

Arenas Canalda, Pau

Director/Co-director:

Nualart Nieto, Pau

Degree:

Bachelor in Aerospace Technology Engineering

Examination session:

Spring, 2023

Abstract

The objective of this final degree thesis is to comprehensively analyze and compare the evolution of the 2021 and 2022 front wings in the context of Formula 1. This study combines theoretical insights into fluid dynamics and Computational Fluid Dynamics (CFD) with an examination of the historical development of the sport, focusing specifically on front wing design.

The thesis begins by providing a theoretical introduction to fluid dynamics and CFD, establishing the foundation necessary to understand the principles governing the aerodynamics of Formula 1 vehicles. Furthermore, a historical overview of Formula 1 is presented, highlighting key milestones and technological advancements that have influenced front wing design throughout the years.

To conduct a thorough analysis, the two front wings are visually compared, allowing for a preliminary assessment of their differences in terms of shape, features, and design philosophy. Subsequently, four CFD simulations are carried out, enabling a more detailed evaluation of the aerodynamic performance of each front wing variant.

The results obtained from the CFD simulations are analyzed and interpreted to extract meaningful conclusions. The impact of the regulatory changes implemented in 2022 on the aerodynamic behavior of the front wings is thoroughly evaluated, shedding light on the effectiveness of these modifications in reducing turbulence and enhancing overall performance.

The conclusions drawn from this study provide valuable insights into the evolution and comparative performance of the 2021 and 2022 front wings. The findings not only contribute to a deeper understanding of the aerodynamic characteristics of these components but also offer valuable guidance for future design iterations.

The present thesis aims to bridge the gap between theoretical knowledge and practical application by utilizing CFD simulations as a powerful tool for analyzing the aerodynamic performance of the front wings. This work lays the foundation for further research and development in the field of Formula 1 aerodynamics, encouraging continuous innovation and advancements in front wing design to achieve optimal performance and a competitive edge.

Resum

L'objectiu d'aquesta tesi final de grau és analitzar i comparar de manera exhaustiva l'evolució dels alerons davanters de 2021 i 2022 en el context de la Fórmula 1. Aquest estudi combina coneixements teòrics sobre la dinàmica de fluids i la Dinàmica de Fluids Computacional (CFD) amb un anàlisi del desenvolupament històric de l'esport, centrant-se específicament en el disseny de l'aleró davanter.

La tesi comença proporcionant una introducció teòrica a la dinàmica de fluids i CFD, establint les bases necessàries per comprendre els principis que regeixen l'aerodinàmica dels vehicles de Fórmula 1. A més, es presenta una visió històrica de la Fórmula 1, destacant les fites clau i els avenços tecnològics que han influït en el disseny de l'aleró davanter al llarg dels anys.

Per dur a terme un anàlisi exhaustiu, els dos alerons davanters es comparen visualment, permetent una avaluació preliminar de les seves diferències en termes de forma, característiques i filosofia de disseny. Posteriorment, es realitzen quatre simulacions CFD, que permeten una avaluació més detallada del rendiment aerodinàmic de cada variant de l'aleró davanter.

Els resultats obtinguts de les simulacions CFD s'analitzen i s'interpreten per extreure conclusions significatives. S'avalua a fons l'impacte dels canvis normatius implementats l'any 2022 en el comportament aerodinàmic dels alerons davanters, donant llum a l'efectivitat d'aquestes modificacions per reduir la turbulència i millorar el rendiment global.

Les conclusions extretes d'aquest estudi proporcionen informació valuosa sobre l'evolució i el rendiment comparatiu dels alerons de 2021 i 2022. Les conclusions no només contribueixen a una comprensió més profunda de les característiques aerodinàmiques d'aquests components, sinó que també ofereixen una guia valuosa per a futures iteracions de disseny.

La present tesi pretén reduir la bretxa entre el coneixement teòric i l'aplicació pràctica mitjançant la utilització de simulacions CFD com una potent eina per analitzar el rendiment aerodinàmic dels alerons davanters. Aquest treball posa les bases per a més investigació i desenvolupament en el camp de l'aerodinàmica de la Fórmula 1, fomentant la innovació contínua i els avenços en el disseny de l'aleró davanter per aconseguir un rendiment òptim i un avantatge competitiu.

Resumen

El objetivo de esta tesis final de grado es analizar y comparar de forma exhaustiva la evolución de los alerones delanteros de 2021 y 2022 en el contexto de la Fórmula 1. Este estudio combina conocimientos teóricos sobre la dinámica de fluidos y la Dinámica de Fluidos Computacional (CFD) con un análisis del desarrollo histórico del deporte, centrándose específicamente en el diseño del alerón delantero.

La tesis comienza proporcionando una introducción teórica a la dinámica de fluidos y CFD, estableciendo las bases necesarias para comprender los principios que rigen la aerodinámica de los vehículos de Fórmula 1. Además, se presenta una visión histórica de la Fórmula 1, destacando los hitos clave y los avances tecnológicos que han influido en el diseño del alerón delantero a lo largo de los años.

Para realizar un análisis exhaustivo, los dos alerones delanteros se comparan visualmente, permitiendo una evaluación preliminar de sus diferencias en términos de forma, características y filosofía de diseño. Posteriormente, se realizan cuatro simulaciones CFD, que permiten una evaluación más detallada del rendimiento aerodinámico de cada variante del alerón delantero.

Los resultados obtenidos de las simulaciones CFD se analizan y interpretan para extraer conclusiones significativas. Se evalúa a fondo el impacto de los cambios normativos implementados en 2022 en el comportamiento aerodinámico de los alerones delanteros, dando luz a la efectividad de estas modificaciones para reducir la turbulencia y mejorar el rendimiento global.

Las conclusiones extraídas de este estudio proporcionan información valiosa sobre la evolución y el rendimiento comparativo de los alerones de 2021 y 2022. Las conclusiones no sólo contribuyen a una comprensión más profunda de las características aerodinámicas de estos componentes, sino que también ofrecen una guía valiosa para futuras iteraciones de diseño.

La presente tesis pretende reducir la brecha entre el conocimiento teórico y la aplicación práctica mediante la utilización de simulaciones CFD como una potente herramienta para analizar el rendimiento aerodinámico de los alerones delanteros. Este trabajo sienta las bases para mayor investigación y desarrollo en el campo de la aerodinámica de la Fórmula 1, fomentando la innovación continua y los avances en el diseño del alerón delantero para conseguir un rendimiento óptimo y una ventaja competitiva.

Contents

List of Figures

List of Tables

List of abbreviations

CAD:	Computer Aided Design
CFD:	Computational Fluid Dynamics
DNS:	Direct Numerical Simulation
DRS:	Drag Reduction System
F1:	Formula 1
LES:	Large Eddy Simulation
FIA:	Fédération Internationale de l'Automobile
RANS:	Reynolds Average Navier Stokes

Glossary

Dirty air: Also known as turbulent wake, is the disturbed air left behind a car, that hampers the aerodynamic flow of cars directly behind it.

Downforce: downward aerodynamic force that pushes a car's tires onto the track surface, increasing traction and cornering ability.

Drag: force that opposes the motion of an object through a fluid, such as air or water, acting in the direction of the fluid flow.

Ground effect: Exploit of the Venturi effect in the floor of a car.

Slipstream: Utilizing other car's turbulent wake to decrease drag when driving in straight sections.

Venturi effect: Decrease in fluid pressure that occurs when a fluid travels through a constricted section of a pipe.

Chapter 1

Introduction

1.1 Object

The aim of this project is to analyze two Formula 1 (F1) front wings from an aerodynamic standpoint, given the change in the technical regulations implemented in the 2022 season. The analysis will use advanced Computational Fluid Dynamics (CFD) simulations to model the airflow around each wing and to measure various performance parameters, such as downforce and drag. By comparing the results from the two wings, the project seeks to quantify the changes in design that the new regulation has produced.

1.2 Scope

This project will include the following set of work packages:

- An analysis of the theoretical framework regarding aerodynamics, with a focus on principles present in F1 cars.
- A description of the computational foundation of CFD solvers and its theoretical background.
- An overview of the aerodynamic evolutions throughout F1 history.
- A run-through the new regulation of 2022 and its key changes versus 2021.
- An exploded view of the parts of a front wing, with a comparison of the 2021 and 2022 designs.
- The 3D design using CAD software of the two front wings to be studied.
- Numerical simulations on both wings using CFD software under different boundary conditions.
- A convergence study of the simulations done.
- An analysis of the results obtained and drawing of conclusions.
- The budget of the project.

The following elements are beyond the scope and will not be included:

- Structural analysis of the front wings.
- Numerical simulations under *slipstream* or *dirty air* conditions.
- Prototyping and experimental studies.

1.3 Requirements

In general traits, the required knowledge to develop this project is:

- Basic knowledge of fluid mechanics and aerodynamics, in order to comprehend the mathematical framework of the procedures and the explanation and clarification of the outcomes.
- Basic knowledge of CAD software, in order to design the geometries used for the analysis.
- Basic knowledge of CFD software, in order to carry out the simulations.

Next, the following technical requirements have been established for the project:

- The 3D models of the front wings must be designed using the CAD software *Solidworks*.
- The CFD simulations must be carried out using open-source software.
- The 3D models must be created following the FIA technical regulations of 2021 and 2022.

Finally, the project must meet the following formal requirements:

- All the documentation and results must be written in English.
- The report and all the deliverables must be developed using the given templates.
- The scope of the project must be equivalent to a workforce of 300 hours.

1.4 Rationale

Throughout history, F1 cars have evolved massively in the aerodynamic field, from the first vehicles with no aerodynamic elements, which relied solely on mechanical grip, to today's single-seaters, which are able to generate enough aerodynamic downforce to drive upside down in a tunnel. However, these aerodynamic elements that generate large amounts of downforce lose an important amount of efficiency when working out of laminar flow, and yet they generate turbulent downstream airflow. This prevents cars from following each other closely which, combined with its growing length, width, and weight, makes it increasingly difficult to see overtakes other than those that take place on long straights, and with the help of DRS.

For this reason, on the 2022 season, the FIA implemented one of the biggest technical regulation changes in F1 history, to reduce the turbulent wake generated by the cars in order to enhance on-track battles and thus

improve the show. This change involved the simplification of all aerodynamic elements and the return of the *ground effect* —intended to compensate for the loss of downforce due to aerodynamic simplification—, while maintaining the lower turbulent wake.

This project focuses on the modifications that the front wing has undergone and aims to quantify the loss of aerodynamic loads that it has experienced compared to the previous technical regulation. This quantification is just a component of understanding the regulation change, but it plays a vital role in comprehending how the new designs will function in unison.

Chapter 2

Background

2.1 Fluid dynamics

Fluid dynamics is a branch of physics that studies the motion and behavior of fluids, which includes both liquids and gases. The study of fluid dynamics is based on the fundamental laws of physics that govern the behavior of fluids, expressed by a set or partial differential equations known as the Navier-Stokes equations (2.1.9). These equations relate the velocity, pressure, and density of a fluid to its motion and the forces acting upon it.

However, solving the Navier-Stokes equations analytically is very challenging, excepting a few idealized and simplified cases, and for more complex fluid flows, numerical methods and computational simulations are commonly used to approximate the solutions. These methods involve dividing the fluid domain into a finite set of points or elements and using numerical approximations to solve the equations at each point or element. While these methods cannot provide exact solutions, they can provide highly accurate approximations of the behavior of fluids under different conditions.

One important application of fluid dynamics is in the field of aerodynamics, which studies the motion of air and other gases and how they interact with solid objects, such as aircraft and vehicles. It seeks to understand the forces and pressures exerted by moving air on these objects, and how those forces and pressures can be controlled and manipulated for practical applications. Consequently, aerodynamics is extremely important in F1, as it is one of the key factors that determine the performance of an F1 car.

2.1.1 Boundary Layer

In fluid dynamics, the boundary layer refers to a thin layer of fluid that forms near a solid surface, where the fluid experiments with frictional forces. Due to this interaction, the fluid adheres to the surface and moves along with it, causing the known "no-slip" condition. This states that the velocity of the fluid in contact with the surface is zero. However, as the distance from the surface is increased, the fluid experiences a shearing force from the adjacent layers of fluid, which causes the fluid to accelerate and generates a velocity gradient.

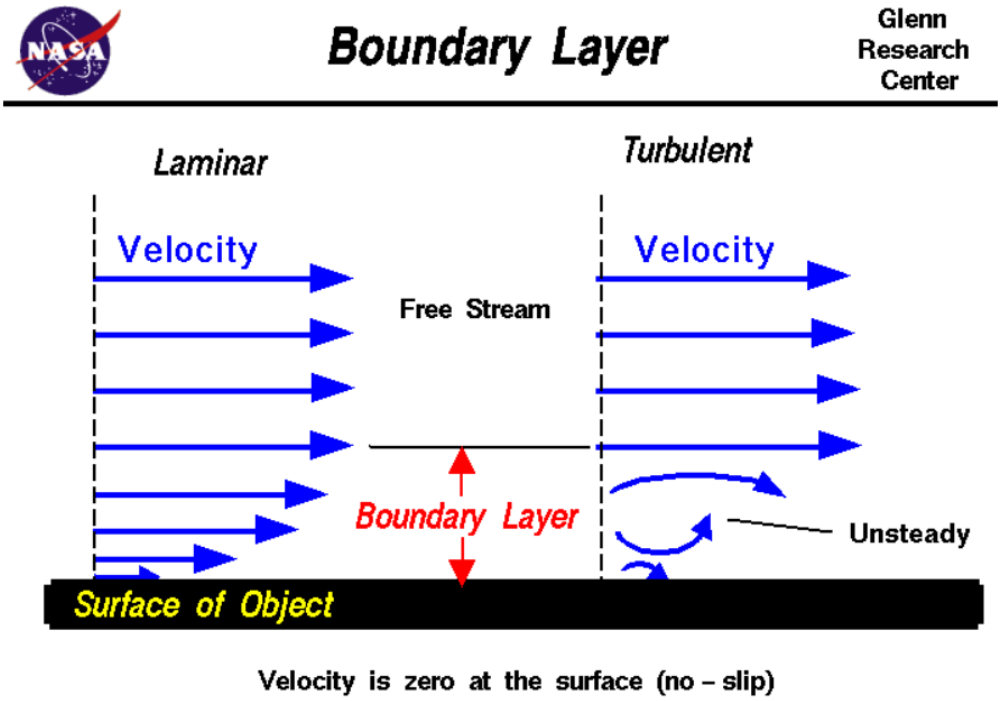

Figure 2.1: Representation of the boundary layer created between a fluid and a surface. *Source: [1].*

When the boundary layer detaches from the surface too early, it creates turbulence and separation of airflow, resulting in increased drag and decreased lift. By keeping the boundary layer attached for as long as possible, the aerodynamic performance of the object can be improved. This is achieved through various means, such as shaping the surface to promote smooth airflow and reducing the pressure gradient along the surface.

The thickness and behavior of the boundary layer also depend on the Reynolds number. The Reynolds number is a dimensionless number used in fluid dynamics to characterize the flow regime. This number determines whether the flow is laminar or turbulent. At low Reynolds numbers, the flow tends to be smooth and laminar, with a thin and predictable boundary layer. However, as the Reynolds number increases, the flow becomes more turbulent, resulting in a thicker and more unpredictable boundary layer. The equation of the Reynolds number can be seen next:

$$Re = \frac{\rho u L}{\mu} \tag{2.1}$$

where ρ is the density of the fluid, u refers to its speed, L is a characteristic linear dimension and μ corresponds to the dynamic viscosity of the fluid.

2.1.2 Aerodynamic Forces

The term aerodynamic forces refer to the forces that are exerted on an object as it moves through a fluid, such as air. These forces appear as a result of the interaction of the body and the fluid and are the main focus of the study of aerodynamics [2].

The first type of aerodynamic force is Lift, which acts perpendicular to the direction of motion. This force

is responsible for keeping airplanes in the air, or F1 vehicles attached to the ground. Lift is caused by the difference in pressure between the top and bottom surfaces of an object, as air flows around it, and is described by Bernoulli's principle. The shape of the object causes the air flowing over the top to move faster, creating a lower pressure area, while the air underneath moves slower, creating a higher pressure area and thus, a difference in pressure that generates the resulting force.

On the other hand, Drag is a force that acts parallel to the direction of motion and opposes it. It is generated by the friction of the fluid as it flows over the object's surface. The shape of the object has a large impact on the resulting drag, but it also depends on the velocity and viscosity of the fluid.

Additionally, other forces that can occur are thrust and weight. Thrust is a forward force generated by a propulsion system, and weight is a downward force generated due to gravity. A simplified representation of these aerodynamic forces can be seen in Figure 2.2.

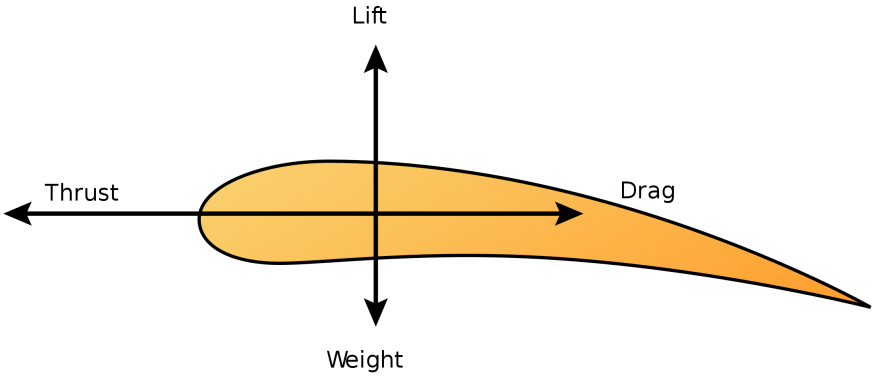

Figure 2.2: Aerodyamic forces on an airfoil. *Source: Wikipedia.*

This representation shows an airfoil shape, which is a shaped design to provide lift as air flows over it and is commonly used in the design of aircraft wings. However, in F1 cars the goal is to generate downwards lift, which is called downforce. This can be achieved, in a very simplified way, by inverting the airfoil design shown in Figure 2.2, and is one of the key design points of F1 cars.

2.1.3 Compressible and Incompressible flow

In fluid dynamics studies, the nature of the flow is key to understand its behavior. That is why it is important to determine the type of flow to be studied, and how this affects the equations that describe it [3].

Incompressible flow refers to the flow of a fluid where the density remains relatively constant throughout the flow field. This means that the fluid's volume does not significantly change as it moves. In an incompressible flow, changes in pressure and velocity are inversely related according to Bernoulli's principle. Incompressible flow is commonly observed in low-speed or subsonic flows, such as the flow of liquids or gases at low velocities, where the density changes are negligible.

On the other hand, compressible flow refers to the flow of a fluid where significant changes in density occur

due to variations in pressure and velocity. In compressible flow, the density of the fluid is not assumed to be constant, and compressibility effects play a crucial role. Compressible flow is commonly encountered in high-speed flows or flows involving gases, especially when approaching or exceeding the speed of sound. Examples include supersonic flows around aircraft or gas flows in rocket nozzles.

The compressibility of a fluid is often evaluated using a nondimensional raito called the Mach number, which represents the ratio between the flow velocity and the speed of sound. The transition from incompressible to compressible flows occur at around $Mach$ 0.3, so for values lower than this the flow can be considered incompressible, and for higher Mach numbers, the compressibility effects must be taken into account.

2.1.4 Laminar and Turbulent flow

When the fluid moves over a surface, its motion can take one of two forms: laminar or turbulent flow. Understanding the differences between laminar and turbulent flow is important, as it allows us to characterize the behavior of fluids in a more precise way, and helps create more accurate models and simulations, optimizing the design of objects that interact with fluids [4].

Laminar flow refers to a smooth and orderly flow, in which fluid particles move in parallel layers with no mixing between them. This type of flow is characterized by a predictable and steady motion, in which the velocity and pressure of the fluid can be described by simple mathematical equations. This type of flow usually occurs at low velocities.

In contrast, turbulent flow reflects an irregular and chaotic flow, in which fluid particles move in a random and unpredictable way, with frequent mixing and eddy formation. This type of flow occurs at high velocities and is characterized by sudden changes in velocity and pressure. For this reason, it is more difficult to model mathematically.

The transition from laminar to turbulent flow depends on a number of factors, including the velocity and viscosity of the fluid, the geometry of the flow path, and the roughness of the surface of the object. When air flows over an airfoil, considering it's laminar upstream, it keeps smooth as it moves along the surface. However, as the airfoil curves and the velocity of the airfoil changes, the laminar flow may become unstable and transition to turbulent flow. This can increase the drag in the airfoil, as well as alter the lift and other aerodynamic forces.

In F1, the turbulent and disturbed air generated by a car is called "dirty air", and can have a negative impact on the aerodynamics and performance of a trailing car. The aerodynamic devices of the trailing car become disrupted in the turbulent wake, reducing the downforce and grip needed for high-speed cornering, thus making it difficult to stay close to the leading car during twisty areas. In contrast, the low-pressure area generated behind the moving vehicles can create a vacuum-like effect called "slipstream", that pulls the trailing vehicle forward, reducing its drag. This is key to overtaking in long straights, as the trailing vehicle can reach higher top speeds and overtake the leading vehicle.

2.1.5 Bernoulli's principle

The aerodynamic forces that appear due to the interaction between the airflow and the aerodynamic surface, can appear mainly due to two factors. First, the skin friction between the air and the surface contributes mainly to the generation of drag. As the air flows around the profile, it adheres to its surface, creating the aforementioned boundary layer. In this layer appear the effects of viscosity, which end up forming aerodynamic resistance or drag force [5].

The other major component that generates aerodynamic forces is the pressure distribution around the surface which is explained according to Bernoulli's principle. According to this principle, as the speed of a fluid increases, its pressure decreases, and vice versa. When air flows over an airfoil, it encounters different velocities along the upper and lower surfaces. The curved upper surface causes the air to accelerate, resulting in lower pressure compared to the flatter lower surface. This pressure difference creates lift, the upward aerodynamic force that enables flight. Additionally, the Bernoulli principle can also explain the creation of pressure drag, the other component of air resistance. The pressure difference between the front and rear of the airfoil creates a resistive force that opposes motion, known as drag. For an incompressible flow, the Bernoulli equation can be expressed as shown below:

$$\frac{v^2}{2} + gz + \frac{p}{\rho} = constant \tag{2.2}$$

in where v refers to the fluid flow speed, g refers to the acceleration due to gravity, z is the elevation of the point above a reference plane, p is the pressure at the chosen point, and ρ is the density of the fluid.

2.1.6 Venturi effect

The Venturi effect is a phenomenon that occurs when a fluid flows through a constricted section of a pipe or a duct, and it is closely related to the Bernoulli principle. In a Venturi tube, the fluid flows through a narrow section, called the throat, which is sandwiched between wider sections, called the inlet and outlet. As the fluid approaches the constriction, it is forced to accelerate due to the reduced cross-sectional area. According to the Bernoulli principle, this acceleration leads to a decrease in pressure in the narrow section of the tube [6].

The Venturi effect can be observed by comparing the pressures at different points along the Venturi tube. At the inlet, where the tube is wider, the fluid velocity is relatively slower, resulting in higher pressure. As the fluid flows through the throat, its velocity increases, causing a decrease in pressure. Finally, at the outlet, where the tube widens again, the fluid velocity slows down, leading to pressure recovery. This classical representation of the Venturi effect is shown in Figure 2.3.

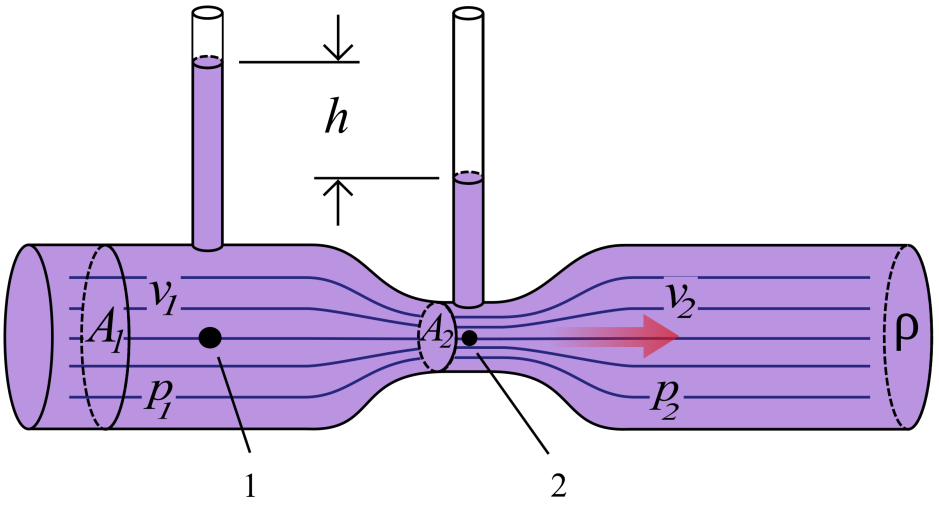

Figure 2.3: Representation of a Venturi tube. *Source: Wikipedia.*

In F1, the Venturi effect is the principle behind the ground effect, which refers to the aerodynamic phenomenon where the airflow under the car generates downforce by accelerating through a channel created between the car's underside and the track surface. The floor of an F1 car is meticulously shaped to incorporate a Venturi-like structure, featuring a curved profile, with its edges raised, which creates a narrowing channel as air flows underneath. This narrowing section increases the velocity of the airflow, resulting in a decrease in pressure according to the Bernoulli's principle.

As the high-speed airflow passes beneath the car, the Venturi-shaped floor accelerates the air, leading to lower pressure underneath the car compared to the ambient atmospheric pressure. This pressure difference creates a suction effect, effectively pulling the car closer to the ground. The intensified ground effect generated by the Venturi effect enhances the downforce produced by the car, improving its grip, stability, and overall performance.

This effect is one of the key changes introduced in the 2022 F1 season, as the ground effect had been missing since the 1980s. With the advancements in modern F1 cars, FIA designed a technical regulation that allowed teams to design a car featuring Venturi tunnels underneath the floor in a safe manner, and thus being able to simplify the rest of aerodynamic devices.

2.1.7 Streamlines, streaklines, and pathlines

Streamlines, streaklines and pathlines are field lines in a fluid flow. They only differ when the flow is not steady, when it changes over time [7].

Streamlines are imaginary lines that represent the flow direction of a fluid at a given point in space and time. These lines are drawn in such a way that they are always tangent to the velocity vector of the fluid at each point along their length.

Streaklines represent the set of points of all particles that have passed through a point in space. Unlike

streamlines, which are imaginary, streaklines show the actual path that a fluid has taken as it moves through. These paths can be visualized by injecting a small amount of dye or other tracer material into the fluid and tracking its movement over time, allowing the study of the real behavior of the fluid flow and the verification of previous simulations. F1 uses a special paint called "Flow-Viz", which is a fluorescent water-based liquid that is sprayed onto points of interest of the car before a practice session and can be seen in Figure 2.4. After the run, this paint highlights the streaklines of the fluid, which can be analyzed by the engineers to obtain real data on the behavior of the car [8].

Pathlines are the actual trajectories that individual fluid particles follow. They can be obtained by tracking down a single fluid particle as it moves through the fluid. They can be considered to be streaklines for a single particle of fluid.

Figure 2.4: Nicholas Latifi's Williams FW44 covered in Flow-Viz during pre-testing of 2022 season in Barcelona. *Source: SkySports.*

2.1.8 Vortices

In aerodynamics, a vortex refers to a rotating pattern of fluid flow, often characterized by a swirling motion. Vortices form as a result of the interaction between airflows that have differences in velocities, pressures, and directions. For instance, in a simple wing profile, there's high pressure at the bottom and low pressure at the top. At the wing tip, the high-pressure flow tends to roll up and forms a vortex [9].

Vortices offer several benefits, and play a vital role in optimizing the performance of aerodynamic elements.

One of the key vortices in F1 aerodynamics is known as the Y-250 vortex. This vortex is formed at the outer edges of the front wing endplates, which are the vertical surfaces located at the wing's outermost sections. As the high-speed airflow interacts with the endplates, it creates a pressure difference between the upper and lower surfaces, leading to the formation of the Y-250 vortex.

The Y-250 vortex is crucial for multiple reasons. Firstly, it helps in sealing the airflow beneath the car, preventing excessive air leakage and minimizing the undesirable effects of aerodynamic inefficiency. By guiding the air around the front wheels and along the car's sides, the Y-250 vortex helps to enhance the overall aerodynamic performance by reducing turbulence and improving the car's stability.

Moreover, the Y-250 vortex also plays a significant role in increasing the downforce of the car. By directing high-energy airflow towards the rear of the car, it contributes to generating additional downforce, which enhances the tire grip and improves the car's cornering capabilities, especially in high-speed turns.

The design and management of the Y-250 vortex, along with other vortices induced by the front wing, are essential factors in F1 aerodynamics. Engineers employ advanced computational fluid dynamics (CFD) simulations, wind tunnel testing, and on-track experimentation to optimize the front wing design, geometry, and operating conditions. By carefully controlling the formation and behavior of these vortices, teams can extract the maximum performance from the front wing, thereby improving the overall handling, stability, and efficiency of the Formula 1 car.

2.1.9 Navier-Stokes equations

The Navier-Stokes equations are a set of partial differential equations that describe the behavior of fluid flow, providing a mathematical framework to analyze and predict fluid motion. These equations are of fundamental importance in fluid dynamics and play a crucial role in various engineering disciplines [10]. Below are shown the equations that represent the principles of conservation of mass, momentum, and energy, respectively:

$$\frac{\partial \rho}{\partial t} + \nabla \cdot (\rho \mathbf{v}) = 0 \tag{2.3}$$

$$\frac{\partial (\rho \mathbf{v})}{\partial t} + \nabla \cdot (\rho \mathbf{v} \times \mathbf{v}) = -\nabla p + \mu \nabla^2 \mathbf{v} + \mathbf{f} \tag{2.4}$$

$$\frac{\partial (\rho E)}{\partial t} + \nabla \cdot (\rho \mathbf{v} E) = -\nabla \cdot \mathbf{q} + \nabla \cdot (\mu \nabla \mathbf{v}) + \mathbf{f} \cdot \mathbf{v} \tag{2.5}$$

The Navier-Stokes equations are essential for understanding and analyzing complex fluid flows. They allow researchers and engineers to study the characteristics of fluid motion, such as velocity, pressure, and temperature distribution. By solving these equations, it is possible to simulate and predict the behavior of fluid flows under different conditions. However, this system of equations is impossible to solve analytically, and thus to find an exact solution. For this reason, numerical methods are used to obtain an approximate solution with high accuracy.

Computational Fluid Dynamics (CFD) relies heavily on the Navier-Stokes equations for numerical simulations. CFD involves discretizing the equations and solving them using computational methods to obtain approximate solutions. CFD enables engineers to model and analyze fluid flows in a wide range of applications, including aerospace, automotive, energy, and environmental engineering.

The Navier-Stokes equations are used to study aerodynamics, such as the flow over an aircraft wing or the design of efficient wind turbines. In automotive engineering, the equations help analyze the airflow around vehicles to improve their performance and fuel efficiency. They are also employed in the design of pumps, turbines, heat exchangers, and other fluid systems. Furthermore, they have applications in understanding natural phenomena, such as ocean currents, weather patterns, and blood flow in the human body.

2.1.10 Magnus effect

The Magnus effect is a phenomenon that occurs when a spinning object moves through a fluid medium, such as air or water. When an object rotates, it creates a difference in air pressure on its opposite sides, which leads to the generation of a force perpendicular to the direction of motion and the axis of rotation. As a result, the spinning object experiences a lift or a deviation in its path, but more importantly, it increases turbulence. In F1, where the wheels are in direct contact with the flow, this effect is extremely important, and one of the causes of the turbulent wake generated by the tires.

2.2 CFD

2.2.1 Introduction to CFD

CFD is a powerful numerical tool used for simulating and analyzing fluid flow behavior in engineering and scientific applications. It has become an integral part of the design and analysis process in various industries, including aerospace, automotive, energy, and environmental engineering. It involves the use of computational methods to solve the fundamental governing equations of fluid flow, known as the Navier-Stokes equations (2.1.9). These equations describe the conservation of mass, momentum, and energy for fluid flow and provide a mathematical representation of fluid behavior. By solving these equations numerically, CFD enables the prediction and visualization of fluid flow patterns, pressure distributions, and other key parameters of interest.

The importance of CFD lies in its ability to provide insights into complex flow phenomena that are difficult or impractical to study experimentally. It allows engineers and scientists to explore and optimize designs, evaluate performance, and make informed decisions without the need for costly and time-consuming physical prototypes. With CFD, it is possible to investigate a wide range of flow scenarios, including steady or transient, laminar or turbulent, and compressible or incompressible flows.

CFD simulations are based on the discretization of the governing equations using methods that divide the computational domain into a grid or mesh of cells, enabling the representation of fluid properties at discrete locations within the domain. By solving the equations iteratively over the discretized grid, CFD calculations provide detailed information about fluid flow phenomena, such as velocity distributions, pressure gradients, and forces.

The capabilities of CFD extend beyond fluid flow analysis, as it can also be coupled with other engineering disciplines, such as heat transfer, combustion, chemical reactions, and multiphase flow, to model and analyze more complex systems. However, the main focus of this study is to analyze the behavior of a fluid flow, and therefore the explanation will focus on that branch [11].

2.2.2 CFD Workflow

A typical CFD simulation follows a systematic workflow consisting of pre-processing, solving, and post-processing stages. This workflow enables engineers and scientists to set up, solve, and analyze complex fluid flow problems

Pre-processing

In the pre-processing stage, the initial setup for the simulation is prepared before the computation commences. First, the geometry of the domain where the fluid flow analysis will take place is either created or imported, defining the relevant boundaries, surfaces, and features. Following this, the computational domain is divided into small elements or cells through mesh generation. The quality and type of the mesh have a significant impact on the accuracy and efficiency of the simulation, with a higher-quality mesh yielding more precise results but requiring greater CPU power. Once the mesh is generated, boundary conditions are established

to specify the flow conditions at the domain's boundaries, including velocity inlets, pressure outlets, and wall conditions. Lastly, material properties like density, viscosity, and thermal conductivity can be assigned, influencing the flow behavior and thermodynamic characteristics.

Solving

Once the pre-processing stage is complete, the solving stage begins, where the governing equations are numerically solved on the mesh. First, the continuous governing equations, such as the Navier-Stokes equations, are discretized using numerical methods like Finite Difference, Finite Volume, or Finite Element methods. This transforms the equations into a set of algebraic equations that can be solved on the computational grid. These equations are then solved iteratively, advancing in time or converging to a steady-state solution. Numerical algorithms like Pressure-Velocity Coupling, Implicit or Explicit schemes, and convergence criteria are employed to ensure accurate and stable solutions.

Post-processing

After obtaining the numerical solution, the post-processing stage involves analyzing and visualizing the results to gain insights into the flow behavior and draw conclusions. Data is extracted from the numerical solution, such as velocity, pressure, temperature and forces. Visualization techniques and post-processing software can be used to create graphical representations of the data extracted. This way, the result can be interpreted and analyzed to understand the flow behavior and validate the simulation against experimental data or analytical solutions.

2.2.3 Discretization methods

Discretization methods are techniques used in numerical simulations to approximate continuous mathematical equations or models. The Navier-Stokes equations, which describe the motion of a fluid flow, are generally too complex to be solved analytically, and thus finding an exact mathematical solution is not possible. Discretization methods break down these complex equations into simpler, more manageable forms that can be solved using computers. Different discretization methods have different ways of representing and solving the equations. Some common methods include Finite Difference Method (FDM), Finite Element Method (FEM), and Finite Volume Method (FVM). These methods have their own strengths and weaknesses and are suited for different types of problems and geometries.

- Finite Difference Method (FDM): This numerical technique divides the fluid domain into a grid of discrete points. Once the domain is discretized, the derivatives are approximated by comparing values of adjacent points, allowing the approximation of how the properties of the fluid change and solving the system of equations.
- Finite Element Method (FEM): This method is used to solve complex geometries or structures. The domain is divided into small elements, and the behavior of the properties is approximated within these elements using basis functions.

- Finite Volume Method (FVM): This discretization method divides the domain into small control volumes or cells. By considering the fluxes of the properties across the control volume boundaries, the net change within each volume can be determined.

2.2.4 Turbulence modeling

Turbulence models in Computational Fluid Dynamics (CFD) are mathematical equations or algorithms used to simulate the complex phenomenon of turbulence. Turbulence refers to the chaotic and unpredictable behavior of fluid flow, characterized by the presence of vortices, eddies, and fluctuations in velocity and pressure. Modeling turbulence is crucial because it plays a significant role in various engineering applications, such as aerodynamics, combustion, and heat transfer [12] [13].

- **Reynolds Average Navier Stokes (RANS):** These models are based on the concept of averaging the turbulent flow quantities over time to obtain a time-averaged description of the flow behavior. The flow variables, such as velocity and pressure, are decomposed into time-averaged mean values and fluctuating components. The fluctuating components represent the turbulent fluctuations in the flow. The main idea behind RANS models is to solve the time-averaged governing equations, which are the Reynolds-averaged Navier-Stokes equations, along with an additional equation for the turbulent viscosity or eddy viscosity. These models are highly applied for various CFD problems, due to their low hardware requirements and good convergence.
  - Spalart-Allmaras (SA): This model solves a transport equation for an eddy viscosity variable. It is known for its stability and good convergence, and it's convenient for aerodynamic flows and transonic flows over airfoils. However, its limitations include shear flows, separated flows, and decaying turbulence.
  - $\kappa - \varepsilon$: This model solves two transport equations, one for the turbulent kinetic energy (κ), which represents the energy associated with turbulent motion, and another for the turbulent dissipation rate (ε), which represents the rate at which turbulence dissipates energy. This model assumes a balance between production and dissipation of turbulence, and the eddy viscosity is estimated based on these quantities. It is a widely used model due to its good convergence rate and low computational requirements, even though it has some limitations, like flows with adverse pressure gradients or strong curvature of the flow. It performs well for external flow problems and complex geometries
  - $\kappa - \omega$: This model also solves two transport equations. It solves the same equation for the turbulent kinetic energy (κ), and another one for the specific dissipation rate (ω). This model provides improved predictions near walls and also performs better in adverse pressure gradients, as it addresses some of the limitations of the $\kappa - \varepsilon$ model near solid boundaries. This model is meant to be used for low Reynolds number problems and performs well for flows with strong curvature, internal flows, and jet flows. However, it requires more computational power than the $\kappa - \varepsilon$ model, and it is more difficult to converge.

  - $\kappa - \omega$ SST : This model is a combination of the previous two. The $\kappa - \varepsilon$ model is used in the outer region and outside of the boundary layer, while the $\kappa - \omega$ model is used in the inner boundary layer. Even though this model provides more accurate results, it is difficult to converge, which makes it less popular than its predecessors.

- **Large Eddy Simulation (LES):** This group of models decomposes the flow into two components: resolved and subgrid-scale (SGS) components. The first one represents the larger turbulent structures that are directly resolved by the numerical grid, while the SGS component represents the smaller, unresolved turbulent structures. These models require much more computational memory than the *RANS* models and therefore are less common. However, they can still be employed if required, as they captures fine-scale turbulent structures, such as in turbulent flows with complex physics, unsteady flows, and flows with large-scale vortices.

  - Smagorinsky: This model is based on the idea of eddy viscosity, which represents turbulent mixing and diffusion. It is assumed that the turbulence behaves like a sum of small whirlpools or eddies, which create a kind of "viscosity" that affects the flow. It uses a formula that relates the resolved strain rate to the eddy viscosity. This model introduces a parameter called the Smagorinsky constant, which determines the strength of the turbulent mixing. This constant is usually chosen based on empirical knowledge and calibration against experimental data.

  - Spalart-Allmaras (SA): As in the RAMS model, the LES Spalart-Allmaras model is a one-equation eddy viscosity model that simplifies the modeling process. It focuses on simulating the transport of the eddy viscosity. It is also known for its simplicity and effectiveness in simulating attached and separated flows.

- **Direct Numerical Simulation (DNS):** This method consists on the direct numerical solving of the Navier-Stokes equations, without any modeling or approximations. Using this method, all scales of turbulence, both large and small, are resolved in the simulation. This model is considered the most accurate approach for simulating turbulent flows, as it provides the most detailed results. However, DNS simulations are computationally expensive and require a high level of resources. This is due to the fact that solving all scales of turbulence demands a very fine grid and a large number of computational calculations. This model is usually limited to low Reynolds, where the viscosity of the fluid dominates the flow behavior.

2.2.5 Boundary conditions

In CFD, boundary conditions are used to specify the behavior of the fluid flow at the boundaries of the computational domain, thus defining how the fluid interacts with them, and providing essential information needed to solve the governing equations of the flow. They are essential because they simulate the real-world conditions and constraints that the fluid flow encounters in a given problem. The most important boundary conditions that are used in a CFD simulation can be classified as follows:

- Inlet Boundary Conditions: They define the properties of the fluid as it enters the computational

domain. They include parameters such as velocity, pressure, temperature, and species concentrations. Inlet conditions are often based on experimental data, physical measurements, or assumptions about the flow characteristics at the inlet.

- Outlet Boundary Conditions: Outlet boundary conditions specify the properties of the fluid as it leaves the computational domain. These conditions can include the pressure, backflow conditions, or the specification of a desired flow rate.
- Wall Boundary Conditions: These conditions specify the behavior of the fluid at solid surfaces or walls. They can include the no-slip condition, which assumes that the fluid velocity is zero at the wall, or more complex conditions such as wall roughness or heat transfer.
- Symmetry Boundary Conditions: As CFD requires high computational power and simulations can take long to complete, these conditions are applied to boundaries that possess symmetry, allowing the flow to be simulated on a smaller portion of the domain.

2.2.6 Validation and verification

Validation and verification are two important processes in CFD that aim to assess the accuracy and reliability of simulations.

Verification refers to the process of evaluating whether the numerical algorithms, equations, and models implemented in a CFD solver are implemented correctly. It focuses on assessing the accuracy and consistency of the mathematical formulations and numerical techniques used in the simulation. Verification typically involves conducting benchmark tests and comparing the results with known analytical solutions or reference data. It helps ensure that the CFD solver is functioning correctly and providing accurate solutions for idealized cases.

Validation, on the other hand, involves comparing the CFD simulation results with experimental or real-world data to assess the accuracy and reliability of the numerical model and simulation predictions. Validation aims to determine if the simulation can reproduce the observed physical phenomena and behavior of the real system being simulated. This process typically involves selecting appropriate experimental data, setting up comparable simulation scenarios, and performing a quantitative comparison between the simulation results and experimental measurements. Validation helps build confidence in the predictive capabilities of the CFD model and its suitability for real-world applications.

2.2.7 Applications and limitations

In today's world, CFD is widely used in industries such as aerospace, automotive, energy, and environmental studies. In the aerospace industry, CFD is utilized to optimize aircraft designs, analyze aerodynamics, and improve fuel efficiency. In the automotive sector, it helps design vehicles with reduced drag, enhance cooling systems, and improve overall performance. Energy companies employ CFD simulations to analyze wind turbine efficiency, optimize combustion processes, and simulate pollutant dispersion. CFD is also applied in building design to study airflow, optimize ventilation, and ensure thermal comfort. Additionally, CFD

aids in environmental studies by simulating ocean currents, analyzing pollutant dispersion, and assessing environmental impacts. With its ability to model complex fluid flow and heat transfer phenomena, CFD has become an indispensable tool in modern engineering and scientific research, enabling improved designs, increased efficiency, and informed decision-making.

However, it also has certain limitations that should be taken into consideration. One major limitation is the requirement for significant computational resources. CFD simulations can be computationally demanding, requiring high-performance computing systems and substantial processing time. This can limit the size and complexity of the problems that can be effectively solved using this method. Another limitation is the reliance on accurate and validated models. The accuracy of CFD results heavily depends on the quality of the chosen turbulence models, boundary conditions, and physical properties of the materials being simulated. Careful model selection and validation against experimental data are crucial to ensure reliable results. Additionally, CFD simulations involve numerous assumptions and simplifications. The accuracy of the results is influenced by factors such as grid resolution, numerical schemes, and convergence criteria. These approximations can introduce errors and uncertainties, particularly in capturing complex flow phenomena or near-wall effects.

2.3 Aerodynamics of F1

Over the past several decades, F1 has been at the forefront of aerodynamic development and innovation in motorsports. With each generation of F1 vehicles, engineers have pushed the boundaries of what is possible in the quest for maximizing speed and performance. From the first years of the sport with no aerodynamic devices to the highly complex designs of today, the evolution of aerodynamics in F1 is a fascinating journey of innovation and advancement. While every season there are small changes that slightly modify the cars, this section focuses on the biggest aerodynamic innovations and changes in F1 history [14] [15].

2.3.1 1946 - First F1 cars

Even though the first F1 World Championship season commenced on May 13, 1950, it was in 1946 when the first races took place. The cars of this era were built using mostly pre-war technology and were often modified from pre-existing designs. The chassis were constructed from tubular steel frames, and the suspension components were made from leaf springs and solid axles, making them quite rigid. Engines were mostly taken from mass-produced road automobiles and significantly modified to provide more power. Aerodynamics were not a design priority in this period, and the cars had simple bodywork with no aerodynamic devices.

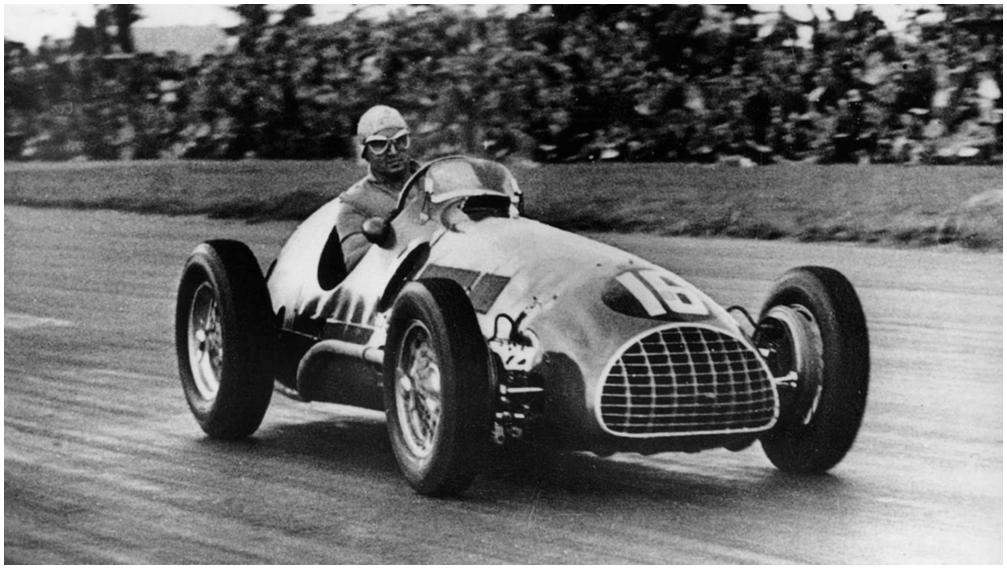

Figure 2.5: Ferrari's 125 F1 car for the 1950 F1 season. *Source: Ferrari.*

2.3.2 1959 - Rear-engine layout

The concept of the rear-engine layout was not a new idea when it was introduced into Formula 1. Auto Union had already been using this layout in the 1930s for their Grand Prix racing cars. However, it wasn't until 1959, when Cooper Car Company introduced the Cooper T51 with a rear-mid engine layout, that the concept really took off in Formula 1. The benefits of this layout were numerous, including weight reduction, increased agility, and greater efficiency. From an aerodynamic point of view, the new engine layout allowed for a smaller frontal area, reducing the car's drag. This car took its first win in the United States Grand Prix at Sebring, in the hands of Jake Brabham, and shortly after that, the other teams started adopting this

layout due to the proven improvement. By 1961, the regulations had changed, making the use of rear-engine layouts mandatory in Formula 1, but at that point, the entire grid had already swapped to rear-mounted propulsion.

Figure 2.6: Jake Brabham's Cooper T51 Climax race-winning car. *Source: Wouter Melissen.*

2.3.3 1962 - Monocoque chassis

In 1962, Team Lotus introduced the monocoque chassis to the F1 world, a design innovation that was inspired by the Lotus Elite sports car. This innovation saw the replacement of the previously used tubular spaceframe with a single aluminum shell structure that acted as both the body and the chassis of the car, bringing numerous benefits to the F1 cars. Firstly, it resulted in a significant weight reduction, thereby making the cars more agile and efficient. Secondly, the increased rigidity allowed for a reduction in the suspension stiffness, which resulted in improved handling and increased traction. Additionally, the reduced frontal area of the monocoque structure led to a reduction in drag. The adoption of this new design in F1 was so successful that Jim Clark won the 1963 championship with the car. Consequently, it became a standard design in Formula 1 cars.

2.3.4 1968 - Front and rear wings

Aerodynamic wings have become an integral part of modern Formula One cars, but this hasn't always been the case. In fact, it wasn't until 1968 that front and rear wings were first introduced in F1 by Team Lotus in their Lotus 49B for the Monaco Grand Prix. The inspiration for the wings came from the Chaparral 2E and 2F, sports cars built by Chevrolet that featured innovative aerodynamic features. The Chaparral cars were first created in 1966 and competed in the Can-Am series in North America. The principle behind the front and rear wings is to generate downforce, which helps increase grip and improve handling. Brabham and

Ferrari followed Lotus's lead and added front wings to their cars at the Belgian Grand Prix later that year, which had a significant impact on the cars' performance. However, the first wings were not without their risks, and there were several accidents due to front wings collapsing at high speeds, which led to regulations being changed for safety reasons, introducing minimum strength and dimensional requirements.

(a)

(b)

Figure 2.7: (a) Graham Hill's Lotus 49B in the Monaco Grand Prix, 1968; (b) 1969 Spanish Grand Prix grid, composed of soon-to-be banned, high-wing F1 cars. *Source: F1-photos.com.*

2.3.5 1977 - Ground effect

Ground effect was a revolutionary aerodynamic concept introduced by Team Lotus in 1977 with their Type 78 racer. The car had inverted wings inside the sidepods, creating two venturi tunnels and generating downforce over the entire underside of the car. This design was a significant departure from the conventional front and rear wing design, and it gave the car a radical increase in downforce. The downforce was generated by the low-pressure area created under the car's floor, which was sealed off by the side skirts. The team won the 1978 championship with their successor, the Type 79. However, Williams introduced a new design in 1979, the FW07, which overtook Lotus in the championship standings. The key to their success was the use of a longer and flatter underbody, which generated more downforce. The ground effect concept was dangerous, as the side skirts could break off and cause the car to become unstable. Therefore, the FIA introduced a ground clearance rule in 1981 and later mandated a flat bottom for all F1 cars to improve safety.

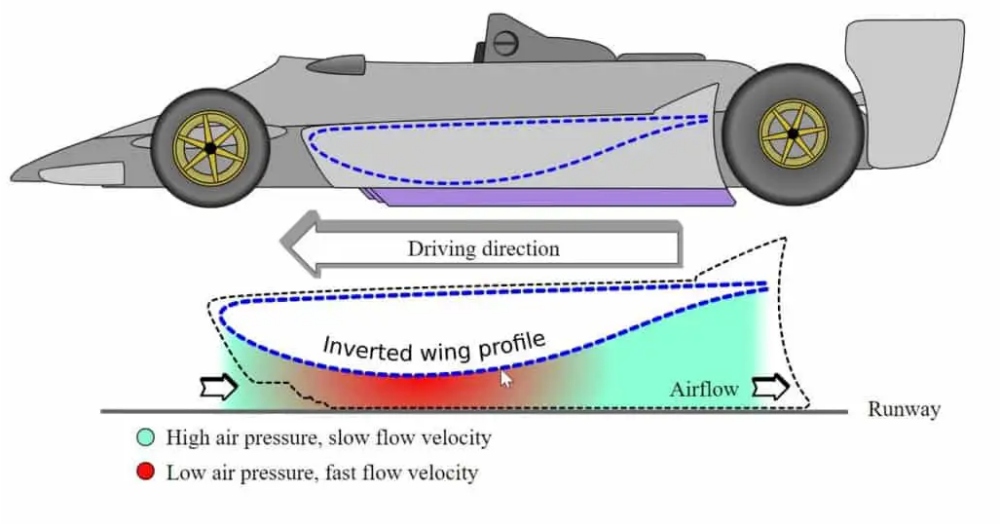

Figure 2.8: Schema of the Venturi tunnel design of the 1977 F1 cars' floor. *Source: F1technical.com.*

2.3.6 1978 - The 'fan car'

The 'fan car' was a concept introduced in F1 by the Brabham Team in 1978. The car's unique feature was a large fan mounted on the rear that drew air from under the car and created a suction effect, effectively creating a partial vacuum that greatly increased the car's downforce. This innovation resulted in the car's impressive performance during its debut race at the Swedish Grand Prix, which it won. However, Brabham team boss Bernie Ecclestone withdrew the car after only one race, operating in the best interest of the championship.

2.3.7 1981 - Carbon fiber monocoque chassis

The introduction of carbon fiber monocoque was a significant step forward in F1. The technology was first introduced by McLaren in 1981 with the MP4/1 car driven by John Watson and Andrea de Cesaris. This construction technique, used lightweight and strong carbon fiber composite material, allowing for the creation of a lighter and stiffer chassis compared to the conventional aluminum spaceframe construction. The reduction in weight and increase in rigidity allowed for improved handling and aerodynamic performance. With this car, McLaren won two races in the 1981 season. Other teams quickly followed suit, and by the mid-1980s, carbon fiber monocoques had become the standard in F1. This construction technique revolutionized F1 car design and paved the way for further aerodynamic developments.

Figure 2.9: John Watson's Mclaren MP4/1 in the 1981 Hockenheim Grand Prix. *Source: Mylifeatspeed.com.*

2.3.8 1985 - Aerodynamic appendages

Bargeboards are a type of aerodynamic device used in Formula 1 cars to control and direct airflow around the sides of the vehicle. They are typically positioned just behind the front wheels and run along the side of the car toward the rear. Bargeboards are used to improve the car's handling, stability, and overall performance by reducing drag and increasing downforce.

In 1985, the Lotus 97T and McLaren MP4/2B were the first cars to introduce a similar concept to bargeboards, with devices positioned behind the front wheels. Although the concept was dropped, the function of managing the tires was replaced by front wing endplates and footplate extensions, which worked to control the airflow around the tires and reduce drag. After the tragic events of the 1994 Imola race, where Ayrton Senna and Roland Ratzenberger were killed, a regulation change was introduced, adding an exclusion zone around the front tires. This change led to the introduction of bargeboards in the Williams FW16B later that season, which replaced the front wing extensions. Bargeboards had two main effects: forward bargeboards influenced the front tire wake more directly, while rearward bargeboards had more benefits for the underbody. In the mid-2000s, F1 cars had both types, and the forward bargeboard was renamed the turning vane. Since then, bargeboards have been a crucial part of the aerodynamics of an F1 car, until the 2022 season when they were removed due to new regulations.

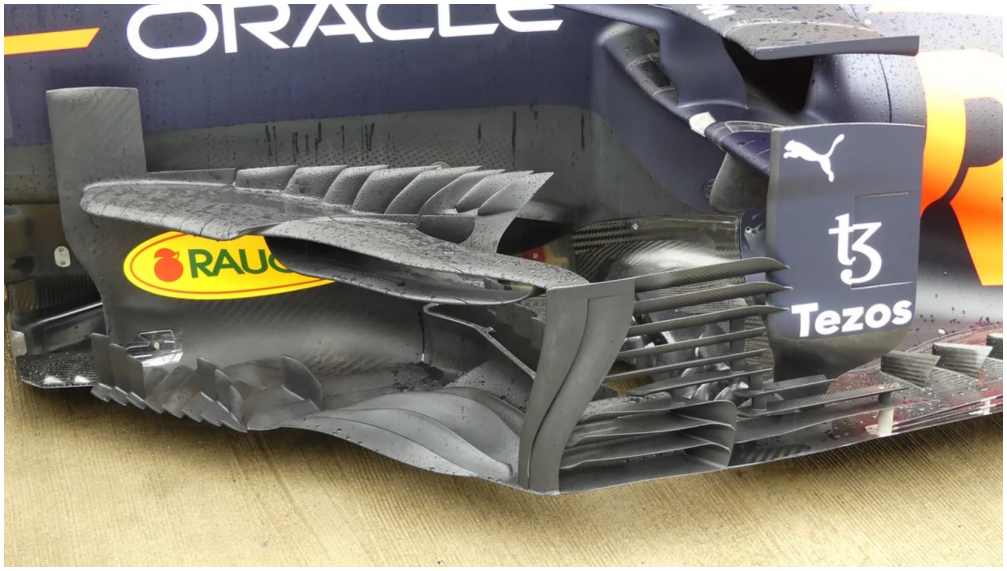

Figure 2.10: Redbull's RB16B bargeboards. *Source: Auto motor und sport.*

2.3.9 Double Diffuser - 2009

The double diffuser refers to a specific aerodynamic design feature that was introduced in F1 by Brawn GP in 2009. It involves utilizing a double-decker or multi-element diffuser at the rear of the car to generate increased downforce and improve overall aerodynamic performance. This aerodynamic advancement was met with controversy and debate. It allowed teams that had incorporated this design feature to gain a significant advantage in terms of rear-end aerodynamics and overall grip. The concept exploited a loophole in the regulations at the time, as teams interpreted the rules differently regarding the legality of such a design. The emergent team Brawn GP, which introduced this revolutionary concept, won both the Constructors' and Drivers' championships that year. Eventually, the double diffuser design was deemed legal, as the teams using it successfully argued that their interpretation of the regulations complied with the rules. However, it prompted changes to the regulations in subsequent years to prevent similar loopholes and ensure a more level playing field among the teams.

2.3.10 Blown Diffuser - 2010

Although the blown diffuser had been used throughout the 80s and 90s, it wasn't until 2010 when Redbull reintroduced it that it revolutionized aerodynamics. The blown diffuser works by utilizing the hot exhaust gases exiting the engine to create an area of low pressure above the diffuser. By carefully channeling the exhaust flow, teams can increase the efficiency of the diffuser, generating more downforce and improving overall grip. This team, combined this concept with the double diffuser introduced by Brawn GP the previous year, and ended up winning both Constructors' and Drivers' championships, and continued to do so for the following 3 years. Through those years, the FIA implemented various changes in the regulations to ban this concept.

2.3.11 F-duct - 2010

During the same season, the McLaren F1 team introduced a new concept, which was named by the paddock "F-duct", as its position in the car met the letter 'F' in the Vodafone sponsor logo. This innovation involved a duct system that channeled air from the car's cockpit to a slot on the rear wing endplate. The driver could control the airflow by covering or uncovering a small hole with their hand while driving. When the hole was covered, the airflow through the duct was disrupted, causing the rear wing to stall. This reduced downforce and drag on the straight sections of the track, allowing for higher top speeds. The following year, for the 2011 season, the regulations were revised, specifically targeting the use of such driver-controlled aerodynamic systems, resulting in the F-duct being banned.

2.3.12 Drag Reduction System (DRS) - 2011

The Drag Reduction System (DRS) was introduced in Formula 1 in 2011 as a means to increase overtaking opportunities during races. DRS is a driver-operated aerodynamic device that allows the rear wing of the car to be adjusted during specific parts of the race. When a pursuing driver is within one second of the car ahead, and at designated zones on the track, they are permitted to activate the DRS, which temporarily alters the rear wing's angle of attack. By reducing the wing's drag, the DRS enables the chasing driver to achieve higher straight-line speeds, facilitating easier overtaking maneuvers. The introduction of DRS aimed to enhance the excitement and competitiveness of racing by providing a strategic advantage to drivers attempting to pass their rivals on the track.

Figure 2.11: Redbull's RB7 DRS system. *Source: Gil Abrantes.*

2.3.13 2014 - Hybrid V6

In 2014, F1 introduced one of the biggest technical regulation changes at the time, where they introduced hybrid power units, specifically the V6 turbocharged engine. This change aimed to improve the efficiency and sustainability of the cars while maintaining competitive performance. From an aerodynamic perspective, the most notable alteration was the introduction of a narrower rear wing with a shallower angle of attack. This change was made to reduce the overall downforce generated by the rear wing, as the increased power and torque from the new power units rendered excessive downforce unnecessary. The reduced downforce resulted in lower drag and allowed the cars to achieve higher top speeds on the straights.

Another important change was the implementation of a lower and narrower nose cone, also known as the "dropped nose", introduced to enhance safety and reduce the risk of cars launching into the air in the event of a collision. The new nose design, combined with revised front wing dimensions, affected the airflow patterns around the front of the car, influencing the overall aerodynamic performance.

Additionally, the exhaust system was modified, with restrictions placed on the positioning and direction of the exhaust outlets. This change aimed to limit the aerodynamic benefits derived from exhaust gases interacting with the rear wing, known as exhaust blowing.

2.3.14 2019 - Front wing simplification

The regulations implemented for the 2019 season aimed to reduce the complexity and intricacy of the front-wing design. The width of the front wing was increased, and the number of elements, flaps, and wing profiles was significantly reduced compared to previous seasons. The goal was to minimize the aerodynamic turbulence created by the front wing and its sensitivity to the wake of the preceding car. The 2019 front wing regulations were part of a broader package of aerodynamic changes aimed at improving the quality of racing. More simplifications occurred in the subsequent years, leading to the regulation change in 2022.

2.3.15 2022 - Aerodynamic simplification and return of ground effect

Originally planned for 2021 but postponed to 2022 due to the global COVID-19 pandemic, the highly anticipated regulation changes introduced in the 2022 season aimed to bring about significant modifications to various aspects of Formula 1 car design. With a focus on enhancing the racing spectacle and improving the on-track action, these changes encompassed aerodynamics, chassis, and tires [16].

One of the primary areas of alteration involved the aerodynamics of the cars. The regulations sought to reshape the bodywork and simplify the aerodynamic elements to reduce the disruptive effects of airflow and encourage closer racing. These modifications included a reduction in the complexity of both the front and rear wings, aiming to minimize the generation of turbulence-inducing vortices. By simplifying the bargeboards, the regulations aimed to reduce their impact on airflow and improve the stability of the wake behind the cars. Another notable change was implemented in the floor design, which was completely redesigned, introducing the famous ground effect, explained previously in section 2.1.6.

In addition to the aerodynamic adjustments, the 2022 regulations also introduced changes to the tires. One significant alteration involved increasing their size, making them both wider and taller compared to previous seasons. This change was mainly motivated by the unification of F1 tire technologies with street tires, in order to save on development and take advantage of the data extracted from this competition.

By introducing these regulation changes, Formula 1 aimed to create a more thrilling and competitive on-track experience for both drivers and fans. The modifications to the aerodynamics, chassis, and tires were carefully crafted to promote closer racing, encourage overtaking, and reduce the impact of disrupted airflow. While originally planned for 2021, the decision to postpone the changes to 2022 allowed for more comprehensive development and testing, ensuring a smoother transition to the new regulations and the potential for even more exhilarating Formula 1 action.

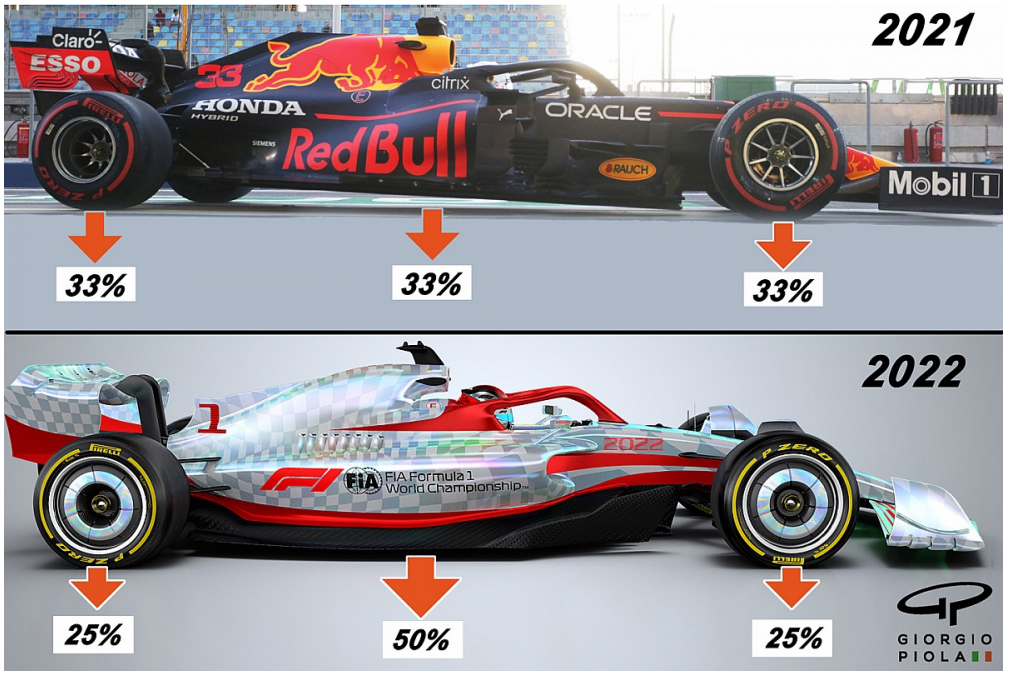

Figure 2.12: Comparison between the downforce generation of the 2021 and 2022 F1 cars. *Source: Giorgio Piola.*

Chapter 3

Front wing analysis

3.1 Front wing exploded view

In F1, the front wing plays a crucial role in shaping the aerodynamics of the car. As the first element to slice through the air, it is imperative for the front wing to operate as efficiently as possible. By carefully shaping the wing and incorporating various elements, engineers strive to reduce the drag generated by the car, allowing it to slice through the air with minimal resistance.

However, the front wing's significance extends beyond drag reduction. Its primary objective is to generate downforce for the front axis of the car, increasing the tire's grip and enhancing the car's stability during high-speed cornering. This downforce ensures that the front tires maintain optimal contact with the track, enabling the driver to have better control and more precise steering.

Another crucial role of the front wing is to redirect the airflow around the car. By carefully manipulating the flow, the wing maximizes the performance of other aerodynamic elements, such as the floor, diffuser, and rear wing. These elements work in tandem to create a well-balanced aerodynamic package, enhancing the overall performance and handling of the car. Moreover, the front wing helps in reducing flow interaction with non-aerodynamic elements, particularly the tires. By diverting the airflow away from the tires, the wing reduces the disruption caused by their rotation, minimizing turbulence and drag. This allows the other aerodynamic components to operate more efficiently, contributing to overall speed and performance.

Over the years, front wings have undergone significant evolution since their introduction in 1968. Today, they have become far more intricate and sophisticated, comprising numerous intricate elements designed to optimize aerodynamic performance. These advancements in front wing design reflect the continuous pursuit of engineers to extract every possible advantage from aerodynamics, pushing the boundaries of performance in F1.

3.1.1 Main plane

The main plane of an F1 front wing is a prominent element that spans the full width of the car's front end. It serves as the foundation of the front wing assembly and plays a vital role in generating downforce and managing the airflow around the car.

It is a wide, flat surface located at the forefront of the wing. The upper surface of the main plane is typically curved, while the lower surface is relatively flatter. This asymmetrical shape helps to create a pressure differential between the upper and lower surfaces of the wing, generating downforce.

Additionally, the main plane is often equipped with flaps along its trailing edge, which can be adjusted, allowing teams to fine-tune the aerodynamic balance and performance of the front wing. By altering the angle or configuration of the flaps, teams can modify the airflow patterns and optimize downforce levels to suit different track conditions or driver preferences. The main plane also holds the other components of the front wing, such as endplates, winglets, and canards, to shape and guide the airflow. For this reason, it is a key part of the front wing, as it puts together the rest of the elements and holds the structural integrity of the wing.

3.1.2 Flaps

Flaps in an F1 front wing are adjustable sections located on the trailing edge of the main plane. They are usually positioned in a staggered or tiered arrangement, with multiple flaps per side. The number of flaps can vary between seasons due to changes in regulations, this being 4 flaps in the 2021 season, and 3 flaps in the 2022 season. One of the key advantages of flaps is their adjustability, which allows teams to modify the angle and configuration of the flaps, adapting the front wing to different tracks. This can be done during the free practice sessions, during which teams can test different setups, or even during pitstops, to adapt the car based on changing track conditions, tire wear, or the driver's feedback.

The first function of the flaps is the generation of downforce for the front axis of the car. By modifying the angle of the flaps, teams can adjust the amount of downforce produced by the front wing. Finding the right balance is crucial because excessive downforce can result in increased drag, limiting straight-line speed, while insufficient downforce can lead to reduced grip and compromised cornering performance. Additionally, flaps contribute to redirecting the airflow around the car.

One key aspect of flaps is the generation of the Y-250 vortex. This refers to a specific vortex that is generated in the area around the 'Y-250' mark on the wing, which is located around 250 millimeters from the centerline of the car, where the end of the flaps is. This vortex, generated by the mix of high and low-pressure airflow, passes between the front tires and the chassis, sealing the airflow that goes through the bargeboards and underbody of the car. This way, these aerodynamic elements are less affected by the turbulent wake generated by the front tires.

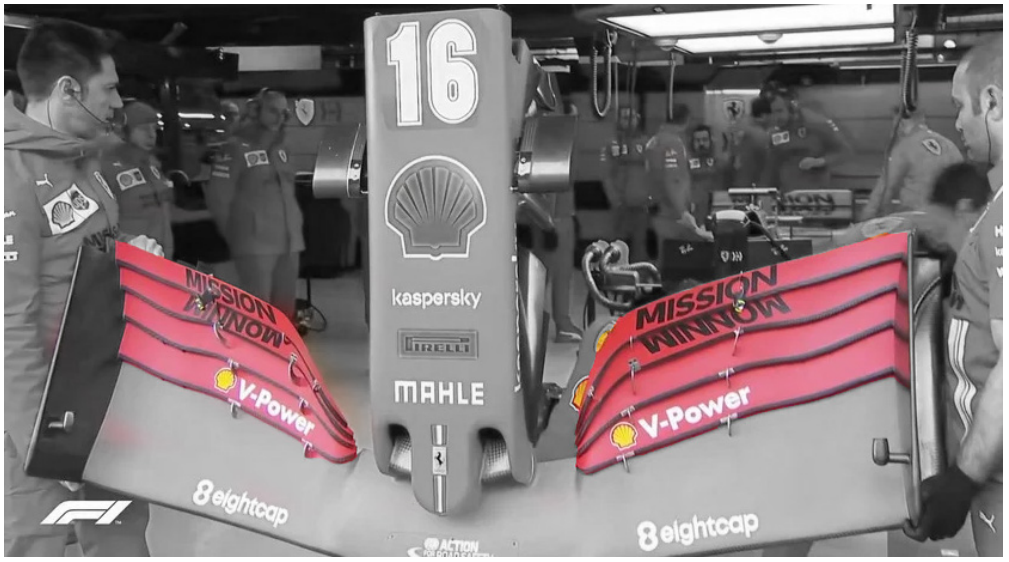

Figure 3.1: Flaps of the 2021 SF1000's front wing. *Source: Scuderiafans.com.*

However, the change in regulations for the 2022 F1 season has meant a redesign of the front wings, forcing the flaps to be in contact with the nose of the vehicle, thus eliminating the Y-250 vortex, and thus reducing wake turbulence, generated by the single-seaters.

3.1.3 Endplates

While teams strive to generate the Y-250 vortex in the inner part of the front wing to harness its aerodynamic benefits, they strategically position endplates on the exterior edges of the wing to mitigate turbulence and enhance overall performance. The endplates, which are vertical plates, serve as a crucial component in controlling the airflow dynamics.

Endplates are designed to prevent the mixing of high-pressure and low-pressure airflows. By having a flat and vertical shape, they act as barriers, effectively separating the two distinct airflow regions. This segregation helps to maintain the integrity of the airflow, preventing unwanted turbulence and disruptions that could negatively affect the aerodynamic performance of the car.

To further optimize the effectiveness of the endplates, they are often designed with a small curvature that extends outward. This curvature plays a vital role in redirecting the airflow away from the tires. By guiding the airflow outwards, the endplates effectively create a path that diverts the airstream, helping to reduce the interference and drag caused by the rotating tires. This redirection not only improves the efficiency of the aerodynamic package but also contributes to enhancing the overall stability and handling of the car.

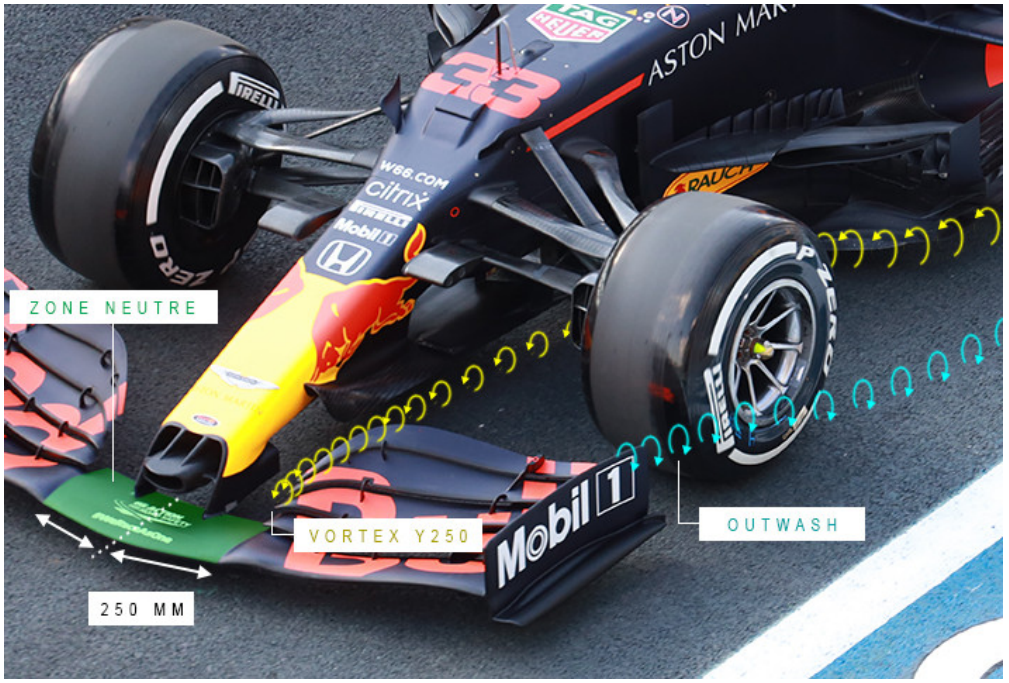

Figure 3.2: Vortex and outwash generation on an F1 front wing. *Source: autojournal.fr.*

3.1.4 Strakes

Strakes in an F1 front wing are small, vertically-oriented wing-like structures attached to the main plane of the front wing. They help improve aerodynamic performance by enhancing downforce, directing airflow, managing wake, and controlling flow separation. They contribute to the overall grip and stability of the car, reduce turbulence from the front tires, and optimize the adherence of airflow to the car's surface. Strakes' design and positioning can vary among teams and are adjusted to maximize aerodynamic efficiency within the regulations. These aerodynamic elements were present during the 2021 season but were removed for the 2022 season after the regulation changes.

3.1.5 Footplates

Footplates are wing-shaped elements attached to the bottom of the section of the endplates. They assist the endplates in managing the airflow around the front tires, by directing it toward the outside of the car. These elements were present until the 2021 season, but were removed for the 2022 season due to the regulation changes.

3.1.6 Diveplanes

Diveplanes are small, horizontal winglets that are typically mounted on the outer edges of the front wing endplates. They are angled diagonally or vertically and help manage the airflow around the front tires. Diveplanes contribute to reducing turbulence, improving aerodynamic efficiency, and enhancing downforce generation and stability. These elements were not present in the 2021 season but after the regulation changes, they were introduced for the 2022 season.

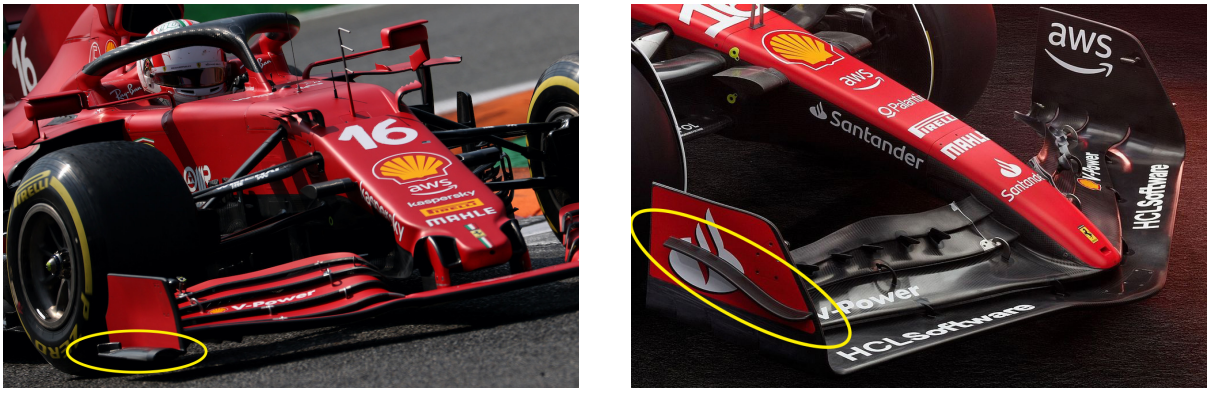

(a) (b)

Figure 3.3: (a) Footplate of the Ferrari SF21; (b) Diveplane of the Ferrari F1-75. *Source: scuderiafans.com.*

3.2 2021 and 2022 front wing visual comparison

As anticipated in this report, the 2022 season underwent one of the biggest technical regulation changes in F1 history. The main objective of this change is the simplification of the aerodynamics of the vehicles and the reduction of the turbulent wake that they generate. Bargeboards were completely removed, and the front and rear wings were simplified. To make up for this downforce reduction, ground effect was brought back, which had not been seen in F1 since the 1980s.

Figure 3.4: Comparison between the 2022 Mclaren MCL36 and 2021 Mclaren MCL35M *Source: motorsport.com.*

As it can be seen in Figure 3.4, and as detailed in both technical regulations [17] [18], both front wings have the same exact maximum width, being this 2000 mm.

Visually we can see big differences between the 2021 and 2022 designs. First, and one of the most important changes, we can see how the front wing flaps in 2021 ended 250mm from the plane of symmetry of the vehicle, causing the famous Y-250 vortex. However, from the year 2022, the profiles of the wing must reach the nose of the vehicle, and therefore, this vortex and its effects are completely eliminated. The main reason for this change is that the Y-250 vortex was used to redirect airflow between the front wings and outwards the bodywork, but since the addition of the ground effect, it's of interest to let as much air through the car's floor as possible.

Another change that we can see at a glance is the simplification of the endplates. In 2021, the profiles intersected perpendicularly with the endplate, which was a vertical plate. These intersections meant a great loss of efficiency, because due to the pressure differentials unwanted vorticity was generated, which meant an increase in drag. In 2022, the endplates have been redesigned, now being created from the curvature of the profiles themselves. In this way, it is much simpler to control the pressure gradients generated at the tips of the wing. This new endplate is also bigger, which helps to reduce the vorticity as well.

Taking a look at the additional elements, the 2021 front wing included a footplate, attached at the lower part of the endplate. However, this element was replaced in 2022 by a diveplane. Although both elements serve the same purpose, optimizing and redirecting the airflow, diveplanes can be seen as small wings that help increase downforce, and thus increase grip. On the other hand, footplates help control the airflow at the wing tip and reduce drag. Also, the 2022 front wing removed the strakes that were present in the previous season were removed.

Finally, and despite not being part of the front wing, a very important change for the 2022 season is the introduction of front wheel covers. As mentioned above, the purpose of the front wing is not only the generation of downforce, but it also plays a key role in redirecting the airflow toward the rest of the vehicle's elements. Tires are one of the elements that generate most of the drag, so it's important to redirect the air around them. Additionally, they also generate a very large turbulent wake, so the main reason for adding these wheel covers is to reduce the turbulent wake they generate, by detaching the airflow in a more smooth way and thus reducing the Magnus effect 2.1.10. It is also important to note that the tires also vary between these two seasons, as they increased from a maximum diameter of 670 mm for dry tires and 680 mm for wet tires in 2021, to a maximum diameter of 725 mm for dry tires and 735 mm for wet tires. This increase in size is important, as it leads to an increase in the resistance they generate, making it even more difficult to redirect the airflow. The wheel rim diameter also grew from 13 inches to 18 inches, but it doesn't affect this study, as the tire effect is only evaluated from a frontal perspective.

Chapter 4

Design of the front wings

The main objective of this chapter is the design and modeling of the two front wings corresponding to the 2022 and 2021 F1 seasons. Due to the high confidentiality on the part of the F1 teams, it is very difficult to find a faithful 3D model, and only fan-made models are available. For this reason, the following criteria will be followed when modeling:

- The design will not be created from scratch. It will be based on the technical regulations relating to each season, which specify the reference volumes of each element of the wing, and the maximum and minimum dimensions that it can have. Based on these dimensions, a simplified base is created, where the aerodynamic elements corresponding to each season are added later.
- For the design of the aerodynamic elements, already created 3D models will be taken, because both the profiles used and the curvature of the elements are unknown to us. From designs that resemble real wings, elements such as flaps, endplates, and others will be taken and adapted to the previously created design in order to meet the dimensions specified in the technical regulations.
- Once the design is finalized, a validation of the dimensions obtained is carried out using the reference volumes of the F1 technical regulation. In this way, it is possible to verify that all the elements introduced in the previous step, which are not designed by us but only adapted, comply with the regulation.

It is important to clarify that these designs cannot be considered optimal, as it can only be ensured that they comply with the technical regulations of each season. By not being able to confirm the aerodynamic configurations of the wings, a numerical comparison can lead to equivocal conclusions, because the same wing can generate different values of aerodynamic forces depending on the circuit. For this reason, in the study only a study of the behavior of the airflow and how it is redirected by the different elements of the wing will be carried out..

As stated in the requirements, the 3D modeling is done using *Solidworks*, which is a CAD software that

we license through the UPC software agreements. It is also the only CAD software used during the degree, making it the most well-known application for us.

4.1 2021 CAD Design

To model the 2021 F1 front wing, the *FIA 2021 Formula 1 Technical Regulations* [17] have been followed. In this regulation, the dimensions of the front wing are defined in Article 3.3, and can be seen in Figures 4.1 and 4.2.

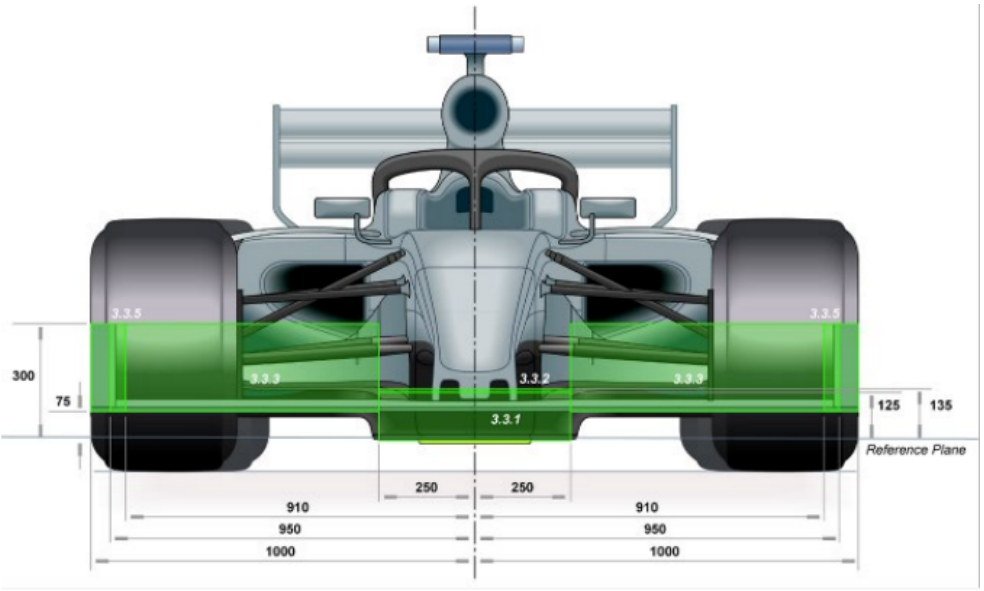

Figure 4.1: Frontal view of the 2021 front wing dimensions in mm. *Source: FIA 2021 F1 Technical Regulations.*

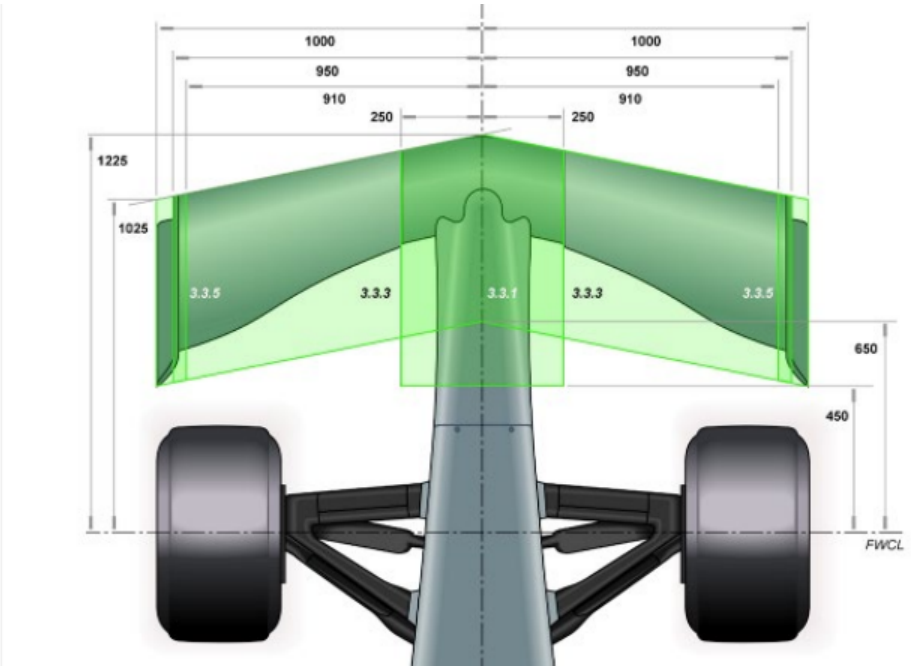

Figure 4.2: Top view of the 2021 front wing dimensions in mm. *Source: FIA 2021 F1 Technical Regulations.*

In addition to the reference dimensions given above, a CAD model of a 2021 front wing has been downloaded from [19]. This model, despite not meeting the standard dimensions, has flaps that seem reliable, which is why it was selected to carry out the study. Combining these two inputs, the model shown in Figure 4.3 is created:

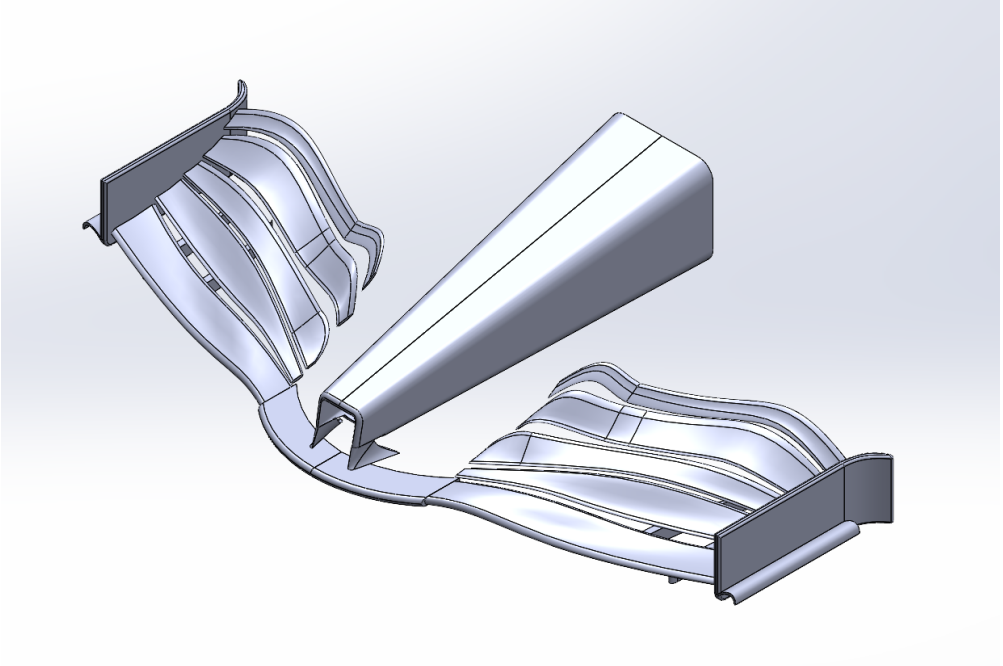

Figure 4.3: Isometric view of the 2021 front wing design. *Source: Own Work.*

In Appendix A.1, the ortographic projections of the 3D model can be seen.

The nose of the car has not been one of the focuses when modeling, so it has been created with a very simple design. This is because the aim of the project is only to analyze the front spoiler, and therefore the fine tunning of the nose is out of scope. However, the fact that in the 2022 season, the flaps connect to the nose of the vehicle means that this must be included, even if it is done in a simplified way. For this reason, and to maintain balance in the comparison, it has also been added to the 2021 design.

The flaps, as mentioned previously, have been adapted from the profiles obtained from the downloaded 3D model. Other elements such as the endplates, footplates and strakes have been created in a very simplified form, and following the proportions extracted from the CAD.

Once the design is finished, its dimensions are validated, ensuring compliance with the technical regulations shown in Figures 4.1 and 4.2. The verification of the reference volumes is done by comparing the actual size of the design with the reference volumes given in the technical regulations. This can be seen in Figures 4.4 and 4.5.

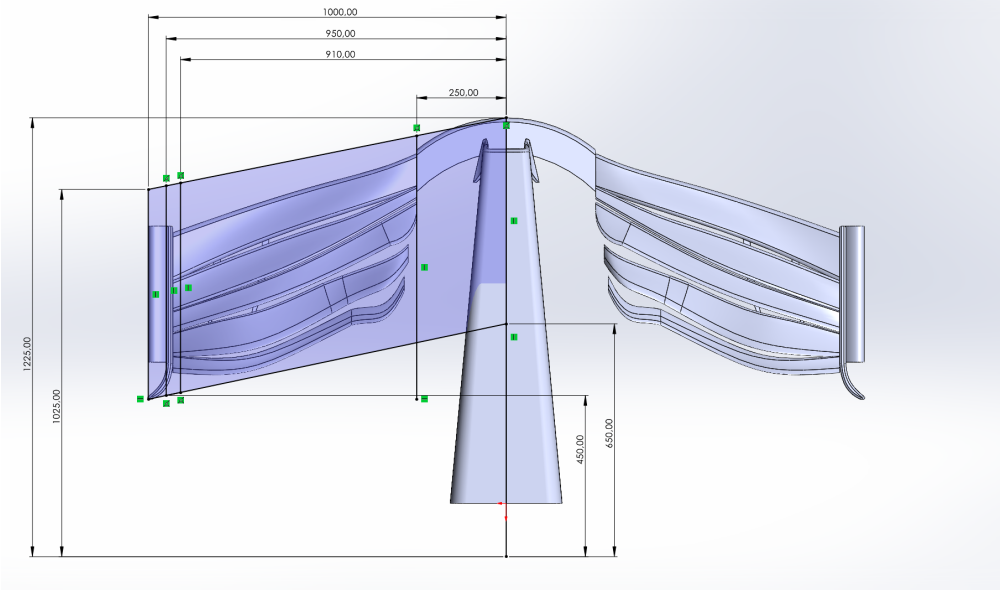

Figure 4.4: Verification of the compliance of the design with the reference dimensions from an upper view, dimensions are given in mm. *Source: Own Work.*

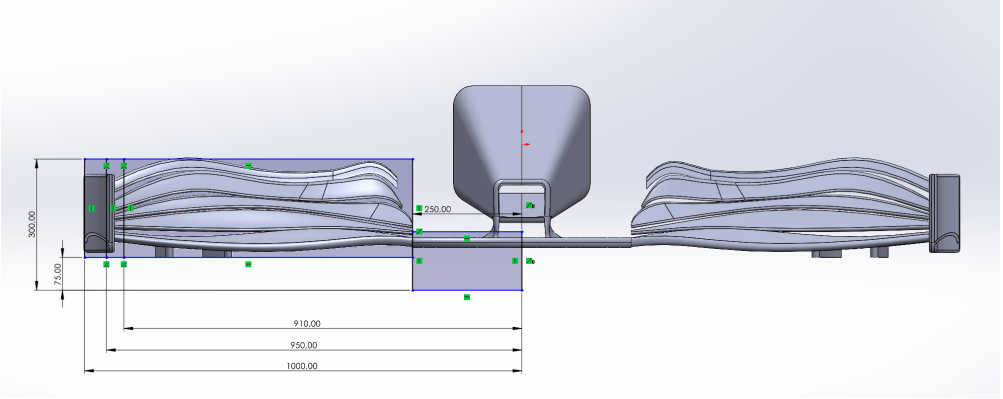

Figure 4.5: Verification of the compliance of the design with the reference dimensions from a frontal view, dimensions are given in mm. *Source: Own Work.*

As the study focuses on the behavior of the airflow through the wing and its redirection, it has been considered to add an F1 tire to the CFD analysis. In this way, it will be possible to check the effectiveness of the wing in redirecting the air around the front wheel, which is one of its main functions.

To do this, a 2022 wheel model has been taken from [20], and adapted to the dimensions of the 2021 season. In Figure 4.6 you can see the isometric view of the spoiler and wheel assembly. Additionally, the orthographic projections are included in Appendix A.2.

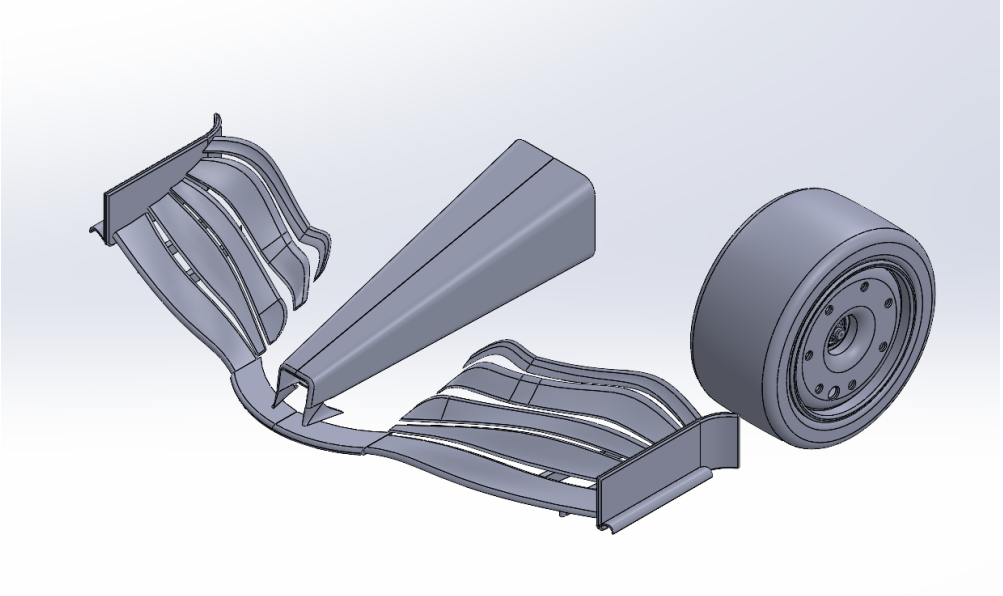

Figure 4.6: Isometric view of the 2021 front wing and tire assembly. *Source: Own Work.*

It should be mentioned that only one tire has been added to one side of the wing, because, in order to reduce the computational cost of the simulation, and since it is a symmetrical model, the CFD analysis will be performed only using a half of the design.

4.2 2022 CAD Design

For the design of the 2022 F1 front wing, a similar approach is taken. The *FIA 2022 Techincal Regulations* [18] have been followed, in where the dimensions of the front wing are given by reference volumes, defined in Article 2.10, and can be seen in Figure 4.7

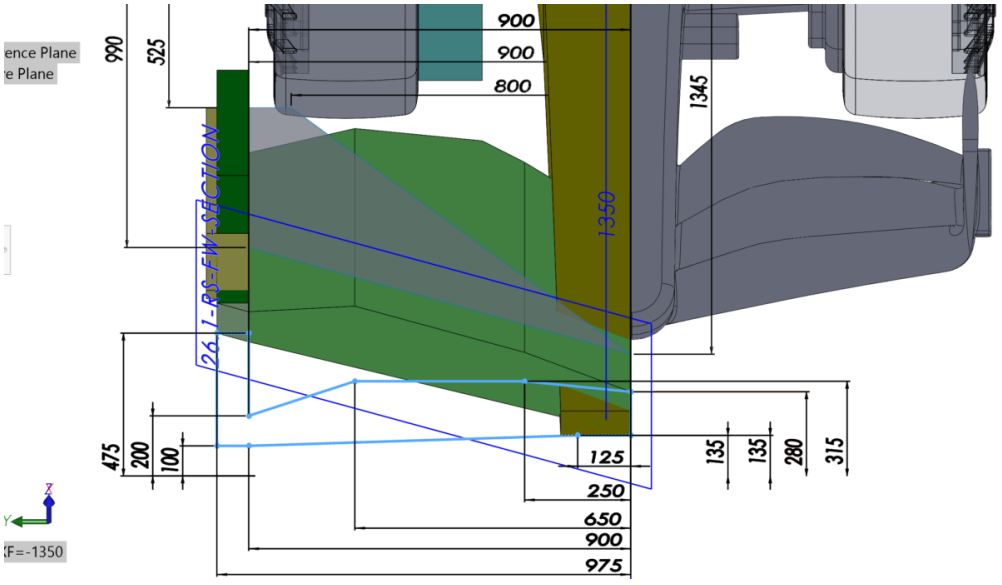

Figure 4.7: Top view of the 2022 front wing dimensions *Source: Michael Masdea.*

Following the same procedure as in the 2021 design, a reliable-looking 3D model has been downloaded [20]. From here, the combination of the reference dimensions, and the profiles of the downloaded model, the wing design shown in Figure 4.8.

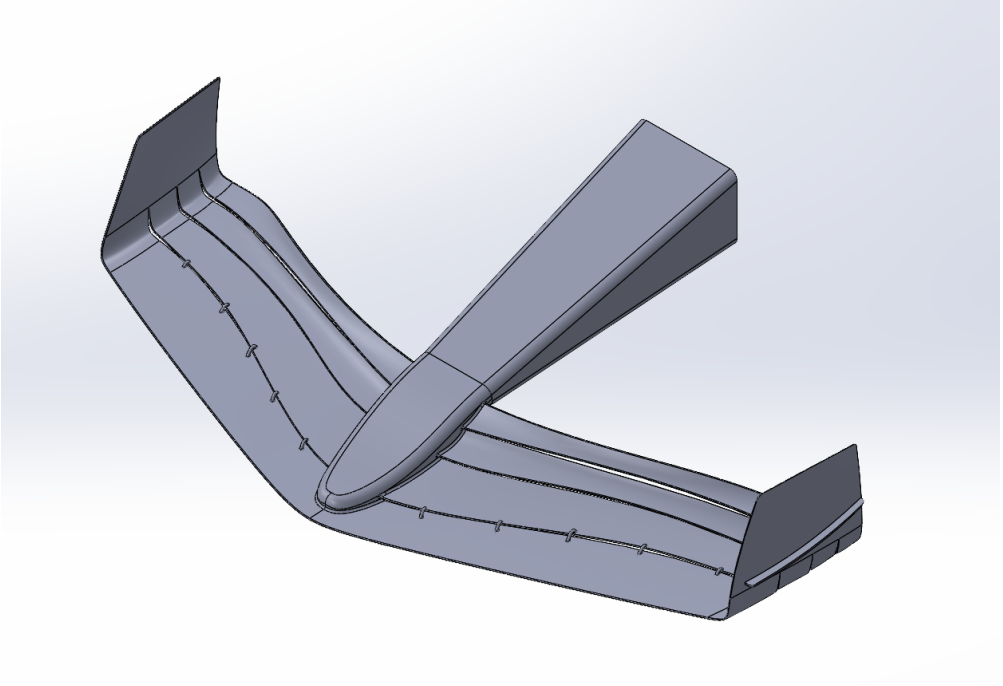

Figure 4.8: Isometric view of the 2022 front wing design. *Source: Own Work.*

As we can see in the design, and more specifically in the front view available in Appendix A.3, the flaps have a rather reduced angle of attack, compared to the 2021 model. This may be due to the two downloaded models corresponding to different configurations, the 2021 being a configuration with more aerodynamic load, and the 2022 a configuration with less load. For this reason, and as mentioned earlier, the downforce and drag comparison would be less reliable and therefore is not conducted in this study.

Next, the verification of the reference volumes given by the technical regulations is made. As done for the 2021 model, the 2022 design's dimensions are compared to the reference volumes given in Figure 4.7. To ensure compliance, all elements of the design must fit inside the blue reference volumes seen in Figures 4.9 and 4.10.

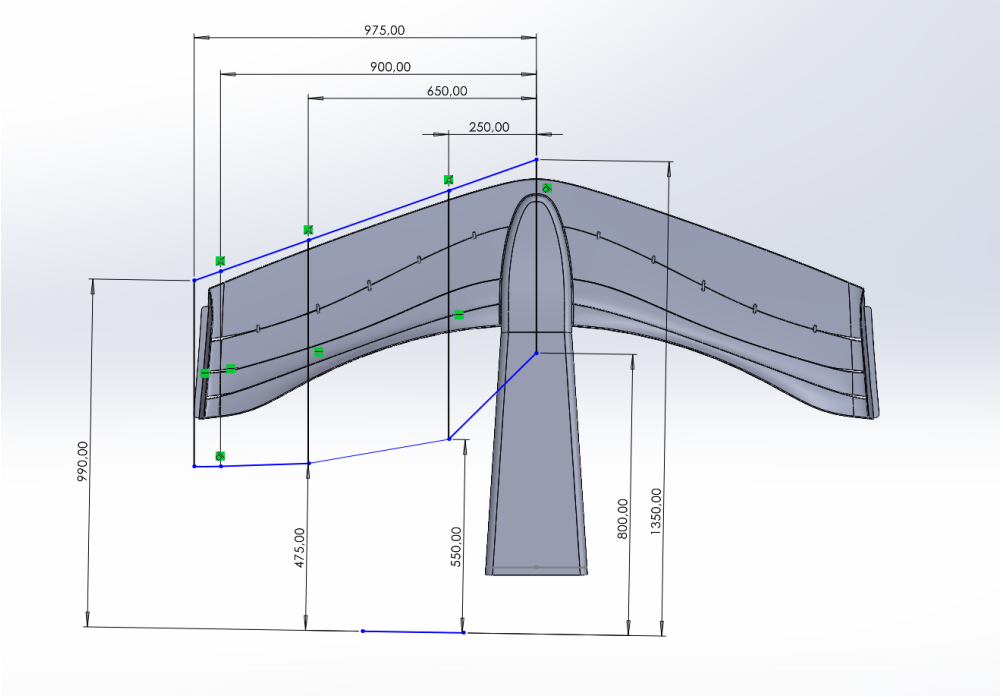

Figure 4.9: Verification of the compliance of the design of the 2022 front wing with the reference dimensions from a top view, dimensions are given in mm. *Source: Own Work.*

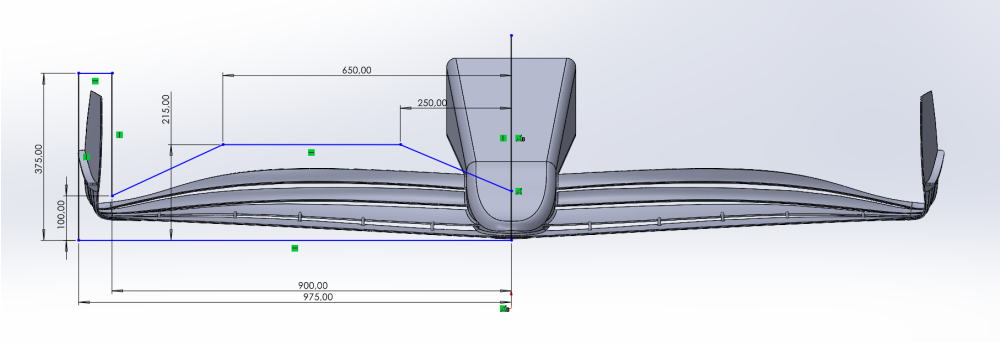

Figure 4.10: Verification of the compliance of the design of the 2022 front wing with the reference dimensions from a front view, dimensions are given in mm. *Source: Own Work.*

Although the model falls within the established reference volumes, it can be seen how there is some margin to

occupy all of the permitted dimensions. This fact does not mean that the design of the spoiler is not correct, but it reinforces the theory that it is a low downforce wing.

Finally, and as done with the 2021 design, a tire is added to the model in order to be able to evaluate the wing's performance in redirecting the airflow around the tire. This wheel model has also been obtained from [20], and corresponds to the regulation tire for 2022. This comes with a cover for the tire, which was also introduced in the same season.

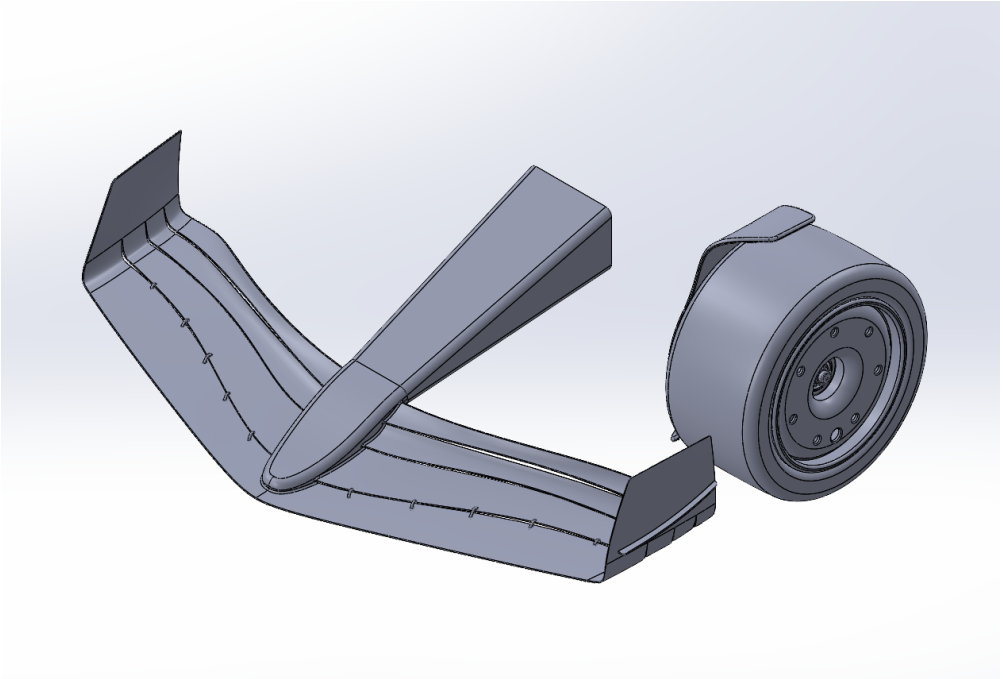

Figure 4.11: Isometric view of the 2022 front wing and tire assembly. *Source: Own Work.*

Chapter 5

CFD Simulations

In this section, the CFD simulations are conducted. As stated previously, both the 2021 and 2022 models are simulated with and without the wheel attachment. This way, the effect of the tire can be seen, and both wings can be compared in terms of flow redirection.

The simulations to be conducted are as follows:

Simulation 1	2021 F1 Front wing
Simulation 2	2021 F1 Front wing + Tire
Simulation 3	2022 F1 Front wing
Simulation 4	2022 F1 Front wing + Tire + Wheel cover

Table 5.1: List of the CFD simulations to be performed. *Source: Own Work*

5.1 Software selection

One of the requirements of the project is the realization of the CFD simulations using open-source software. Based on this, any software that requires some kind of subscription or payment in order to use it is discarded. This requirement is imposed in order to make the project accessible, as many CFD simulation programs can cost thousands of euros for an annual subscription.

Among the programs considered to carry out the simulations, Autodesk CFD, Ansys Fluent Student, OpenFOAM and Simscale can be found, among others.

Firstly, Autodesk CFD is not a free program, but thanks to UPC software agreements, students are licensed and can use it for free. This program, despite having integrations with Solidworks for the import of geometries, was quickly discarded, mainly due to the high hardware requirements to be able to perform both meshing and simulations.

Next, Ansys Fluent Student was also tested, the free version of the popular CFD simulation software, considered one of the leading software in computational fluid dynamics. However, this was discarded for the same reason as the Autodesk CFD, because with the locally available hardware, the meshing of half of the

wing with an acceptable quality elapsed for days. Additionally, the number of elements in the free version of this program is limited to 512k elements, and due to the characteristics and dimensions of the models to be simulated, this did not allow using a mesh with sufficient quality to perform the simulations.

Due to hardware limitations, other programs such as OpenFOAM were quickly discarded, and the focus was placed on the Simscale software. This program, also open source, uses computational resources in the cloud, allowing users to perform complex simulations using external hardware. In this way, larger and higher-quality simulations can be performed in less time. Additionally, this program has previously been used in subjects of the career, so there is a certain familiarity, which facilitates the process.

The free version of this program offers up to a total of 10 successful simulations, and up to 3000 computational hours, which correspond to the performance measure used by the program, to evaluate how much resources each simulation consumes.

5.2 Simulation set up

Once the software is selected, and the models of the wings are designed, the simulation setup can begin.

The first step is to import the geometry into the simulation software, Simscale in this case. As the geometry is imported, it is divided in two by the plane of symmetry, because as mentioned before, the simulations will be done using only one half of the design. Once the division has been carried out, the next step is the definition of the volume of fluid to be analyzed. In CFD simulations, it is the air that must be simulated, not the geometry of the wing, and for this reason, a new geometry must be defined around the front wing. This can be done in the CAD editor available in Simscale, using the *External Flow* option. This volume is created around the geometry, and subsequently, the geometry of the aileron is deleted, leaving only the volume of air around it.

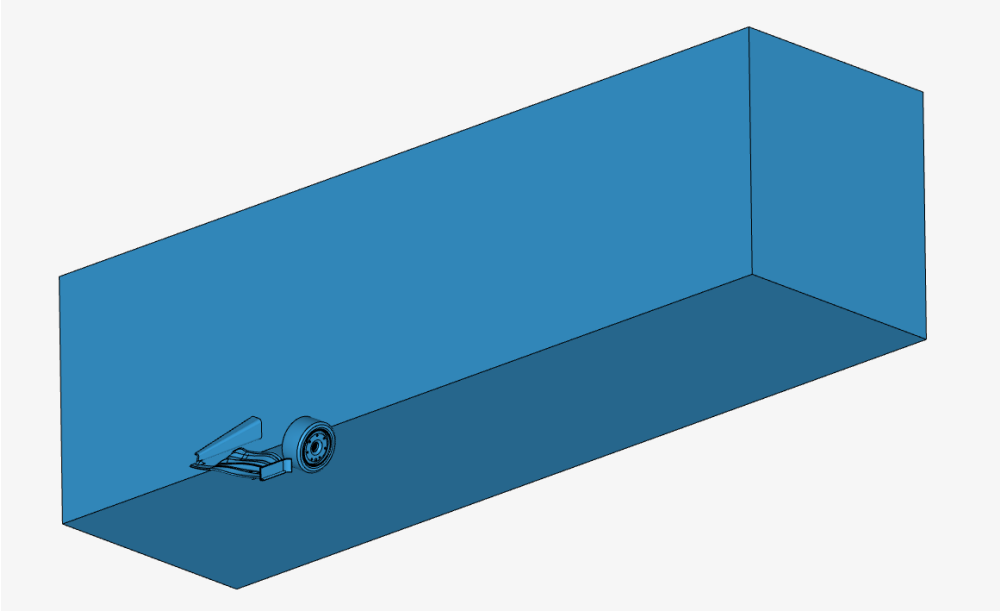

Figure 5.1: Isometric view of the flow region around the 2021 front wing and tire model. *Source: Own Work.*

The region is set up from the symmetry plane, and the contact patch of the tire, and from there it's extended about 3 meters wide, 3 meters high, and 10 meters long. The length is distributed asymmetrically, leaving about 7 meters behind the front wing, as it's the region where the airflow is studied.

The next step is the definition of the simulation properties. For the case study, and because F1 cars do not exceed Mach 0.3, the nature of the chosen simulation is incompressible flow. In this way, the problem is simplified and the computational requirements are lightened. As explained in Section 2.2.4, RANS models are the most used in CFD, due to their good relationship between reliability and computational requirements. Due to the use of computing power in the cloud, we can use model $\kappa - \omega\ SST$, because it is the most reliable among the RANS models, and despite requiring more hardware and being more complicated to converge, this disadvantage is compensated by the software used. Also, the simulation is set as steady-state, as the result sought does not involve time dependant variables, but seeks to obtain a converged solution.

Next, the material to be simulated is defined, in this case, air. The air properties come already been predefined by Simscale, and are as follows:

Density	1.1965 kg/m^3
Kinematic Viscosity	0.000015295 m^2/s

Table 5.2: Properties of air. *Source: Simscale*

The viscosity model used by Simscale is Newtonian, which means that the viscosity of the fluid remains constant regardless of the applied shear rate or stress.

Next, we proceed to define the boundary conditions of the problem. The boundary conditions define how the fluid interacts with the various fluid surfaces, and allows the software to solve the fluid governing equations. The applied boundary conditions are the same for all four simulations, except for the simulations where the tire is not present, where the wheel conditions are not considered. These applied control conditions can be seen in Table 5.3:

Part	**Boundary Conditions**
Flow Region Inlet	Velocity Inlet
Flow Region Outlet	Velocity Outlet
Symmetry plane	Symmetry
External Walls	Slip condition wall
Ground	Moving condition wall
Front Wing	No-slip condition wall
Wheel	Rotating condition wall
Wheel Cover	No-slip condition wall

Table 5.3: Boundary conditions applied. *Source: Simscale*

The velocity input condition is applied to the front face of the flow region and assigned a velocity of 90 m/s. This value has been chosen because current F1 cars reach this speed easily on most circuits on the calendar, and at the same time, it is a speed that ensures the simulation stays below Mach 0.3.

At the rear face of the flow region, the pressure outlet condition is imposed, where the pressure is set to 0 Pa. This condition is typically applied when the flow field is approaching a state of fully developed flow or when the downstream conditions are known or can be reasonably estimated. Next, a symmetry condition is applied at the symmetry plane of the geometry, allowing to simulate only half of the geometry, and thus reducing the computational requirements. The moving condition wall is applied to the ground of the fluid domain. Its velocity is set at 90 m/s, just as the airflow, to simulate the motion of the ground in relation to the front wing. Next, both the front wing surfaces and the wheel cover surfaces (when present) are applied with the no-slip condition, assuming that the velocity at the surface is zero. Finally, the rotating wall condition is applied to the tire surfaces. This allows to take into account the interaction between the flow and the rotation of the wheel, obtaining more accurate results. In order to apply this condition, a rotating velocity is defined, dividing the airflow velocity by the diameter of the wheel. As mentioned previously, the 2021 wheel has a diameter of 670 mm, while the 2022 wheel has a diameter of 725 mm. Using these values, rotating speeds of $\sim 125\ rad/s$ and $\sim 134\ rad/s$ respectively.

5.3 Meshing

Once the geometry is imported into the software, and the boundary conditions and properties of the fluid are applied, the fluid domain can be discretized. The number of elements, and their size, as well as the overall quality of the mesh, is directly related to the accuracy of the results. The quality of the mesh refers to how well it represents the geometry of the simulated object and how it affects the accuracy and stability of the simulation results, and it's calculated automatically by Simscale. A high-quality mesh ensures that the discretization of the geometry is done in a way that accurately captures the flow physics and minimizes numerical errors. For the mesh to be good enough, the quality value must be less than 1, with smaller values corresponding to higher quality.

Meshing can be done using different software, but in this case, the automatic mesher included in Simscale is used. It involves automatic meshing algorithms that generate a polyhedral mesh. It also incorporates adaptative mesh refinement techniques, allowing for localized mesh refinement in regions of interest based on flow gradients or other relevant parameters. This generated mesh undergoes quality control checks to ensure its integrity and reliability.

The mesh can be chosen to be coarser or finer, depending on the quality requirements for the simulation. For this case, all four meshes are defined with a parameter of 8 out of 10, with 10 being the finest, and 0 being the coarsest. Once the meshes of the four models are done, the following properties are obtained:

Properties	2021 Front wing	2021 Front wing and tire	2022 Front wing	2022 Front wing and tire
Number of faces	12693922	15244214	12509663	20868036
Number of nodes	2324089	2495276	1954370	3353091
Number of edges	8613	20594	13805	29807
Number of volumes	5414231	6679424	5542727	9197754
Overall mesh quality	0.204	0.107	0.365	0.113
Time elapsed (hours)	0.35	0.5	0.48	0.78
Core hours consumed	1.47	2.07	1.93	3.20

Table 5.4: Properties of the four meshes generated. *Source: Own Work*

Based on the properties of the mesh, some conclusions can be drawn about each mesh. First, given that the domain size is the same for all flow regions, the number of faces, nodes, edges, and volumes is directly related to the mesh detail. A higher number generally represents that the mesh is more refined and dense, allowing for more accurate simulations. From the table, it can be seen that both designs with tires have a higher number of elements compared to their non-wheeled counterpart. This is explained by the more complex geometry with a greater number of faces to mesh, resulting in a more detailed mesh. As a consequence, the meshing of models with tires also consume more computational resources, and more time. It can also be observed that both 2022 models have a more complex mesh than the 2021 models, and also consume more resources. This can be explained by the fact that the 2022 geometry has quite a bit more curvature than the 2021 model and is, therefore, more difficult to mesh correctly and requires more definition for a good rendering. Also, it must be considered that the 2022 front wing and tire design incorporates the wheel cover, which adds complexity to the mesh.

As for the overall mesh quality, all the values are acceptable as they are lower than 1. However, the meshes of the tire models have a higher quality, related to the number of elements present.

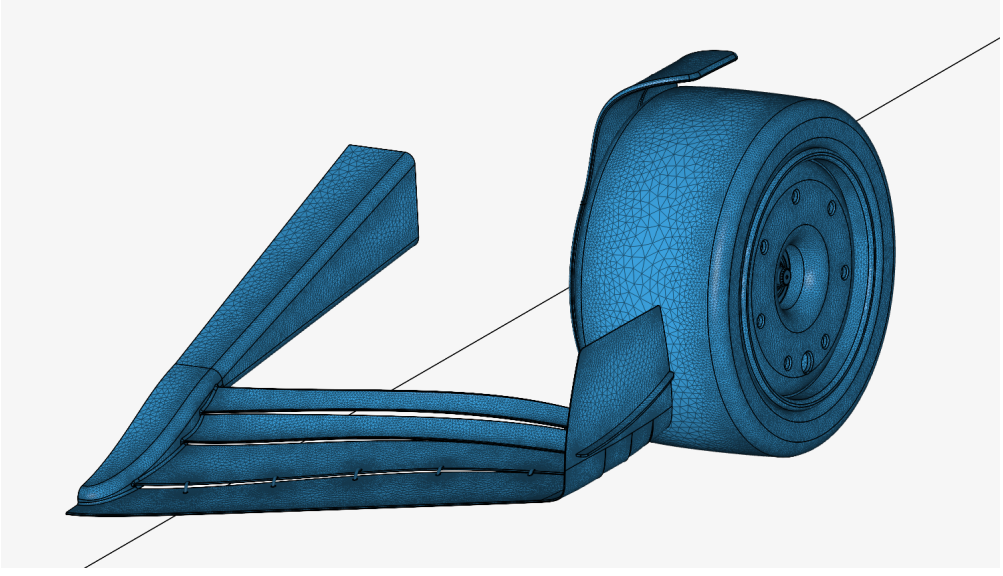

Figure 5.2: Isometric view of the mesh generated on the 2022 front wing and tire model. *Source: Own Work.*

5.4 Simulation

The final step is to proceed with the simulation. This is the step that takes the longest time to complete and requires the most computational power. In the following table, the computational cost of each simulation is shown:

	2021 Front wing	**2021 Front wing and tire**	**2022 Front wing**	**2022 Front wing and tire**
Core hours consumed	20.53	23.73	26.40	42.93
Time elapsed (hours)	1.27	1.48	1.63	2.67

Table 5.5: Resources consumed by the CFD simulations. *Source: Own Work*

As can be seen, the core hours consumed and time elapsed by the simulations are higher in the models with tires than in the models without tires. This is consistent with the mesh quality and size, discussed above. Additionally, it can also be seen how the two models of 2022 have consumed significantly more resources than those of 2021, which on the one hand can be explained by the greater definition of the meshes, but could also be due to the fact that the simulations were carried out at different times, thus being able to vary the demand of the Simscale servers, and therefore the simulation speed. Also, as mentioned in the meshing, the 2022 front wing and tire model includes a bigger tire and the addition of the wheel cover, which may add some complexity to the simulation, and combined with the other factors, may explain the increase in time and computational power used.

5.5 Convergence of the simulation

The convergence of the simulation refers to the attainment of a stable and reliable solution. It signifies that the calculated values have reached a steady state and are no longer changing significantly with further iterations or time steps. Convergence is a crucial aspect of CFD simulations as it ensures the accuracy and reliability of the results.

The residuals plot is an essential tool for analyzing the convergence of a CFD simulation. It displays the variation of the residuals, which represent the differences between the computed values and the converged values of the governing equations, as a function of the number of iterations or time steps. The residuals plot provides insights into the convergence behavior of the simulation and helps assess the reliability of the solution.

In Figures 5.3 and 5.4, the residual plots of the four simulations carried out are shown.

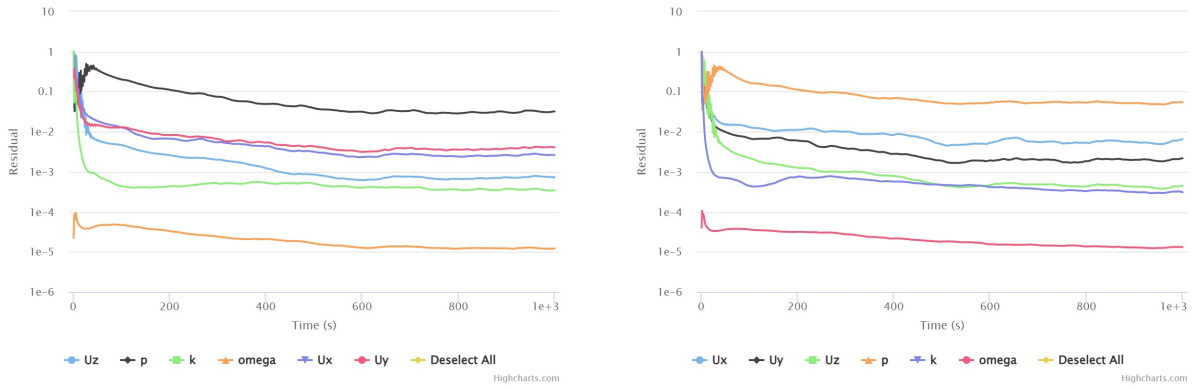

(a) (b)

Figure 5.3: Residual plots of the: (a) 2021 front wing simulation; (b) 2021 front wing and tire simulation. *Source: Own Work.*

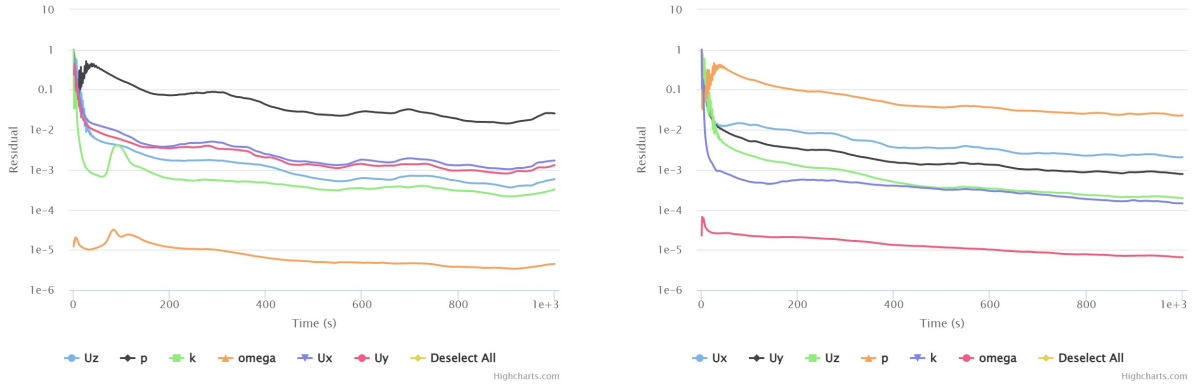

(a) (b)

Figure 5.4: Residual plots of the: (a) 2022 front wing simulation; (b) 2022 front wing and tire simulation. *Source: Own Work.*

Analyzing the four residual plots, it can be seen that all parameters end up stabilizing, with a relatively low residual value of less than $1e-2$. However, the pressure is the only parameter that stabilizes at a higher residual value, of just under 0.1. This could suggest that the simulation is converging well in most aspects, but the pressure field in the simulation is more sensitive to convergence challenges compared to the other parameters. As the pressure is exhibiting reasonable stabilizing trends, and the overall simulation convergence is consistent, the simulations can be considered acceptable considering the purpose of this study, and continue with the analysis of the results.

5.6 Analysis of the results

In this section, the results obtained in the four simulations are analyzed, and the corresponding comparisons between both years are done. Only some images are shown in this section, and the complete views of every simulation are included in Appendix C.

5.6.1 2021 front wing simulation

In the following Figures, the results of the 2021 front wing simulation are shown:

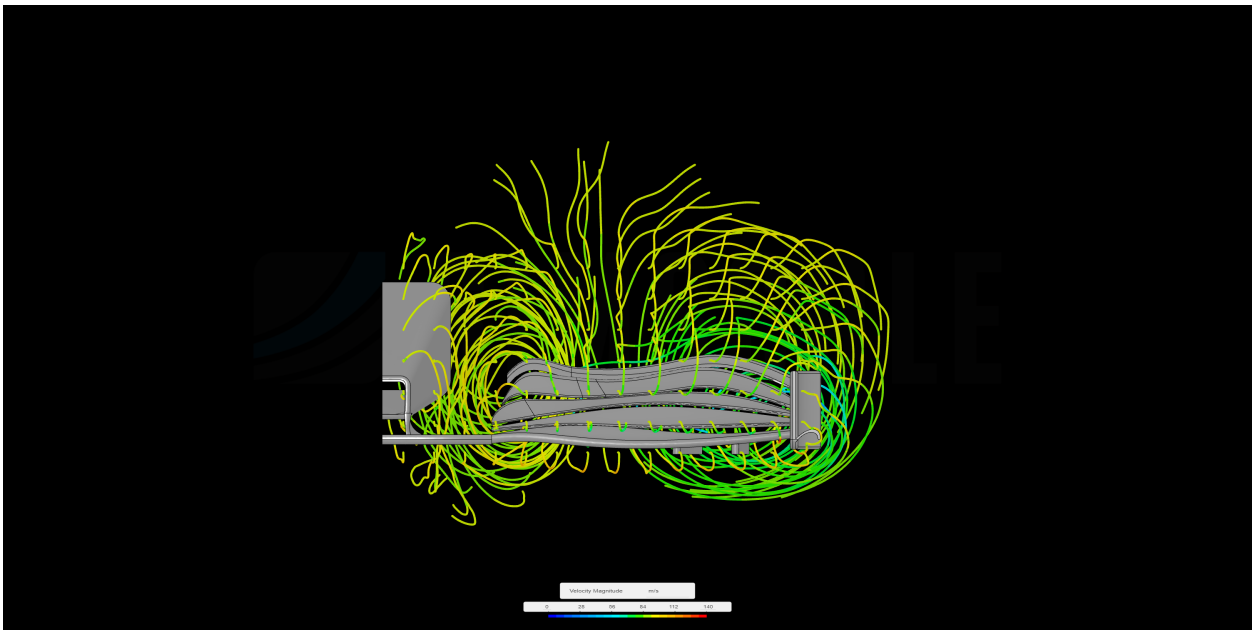

Figure 5.5: Front view of the streamlines in the 2021 front wing simulation. *Source: Own Work.*

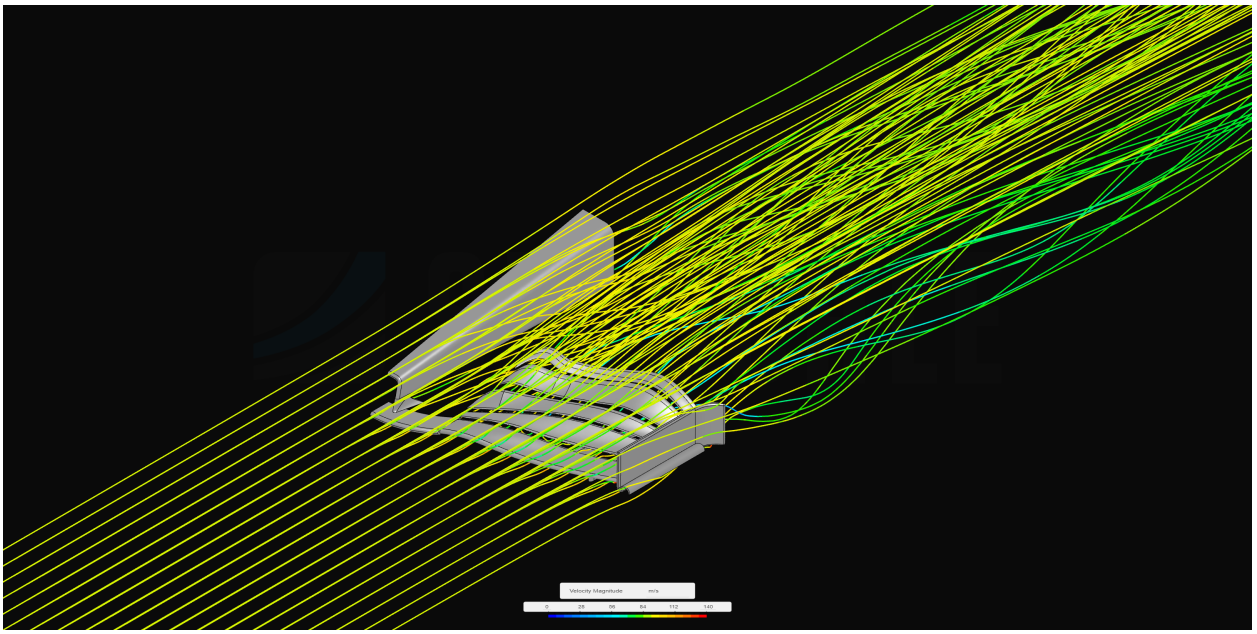

Figure 5.6: Isometric view of the streamlines in the 2021 front wing simulation. *Source: Own Work.*

By analyzing the streamlines you can observe the behavior of the fluid particles as they move through the domain. In Figure 5.5 we can clearly see the two vortices that form in the spoiler of the 2021 season. First, on the outer part of the wing, we find the vortex generated in the endplate, which generates an outwash that redirects the flow of air towards the outside of the vehicle, in order to avoid the front tires, because they are the least aerodynamic element of the car. This outward effect is increased by the outward curvature of the

endplate itself and is also increased by the footplate.

The other vortex that is generated occurs on the inside of the flaps, more specifically 250mm from the plane of symmetry of the vehicle, and corresponds to the famous Y-250 vortex. This vortex is generated by the mixing of the low-pressure and high-pressure flows and is used to redirect the airflow between the front tires and the chassis towards the bargeboards.

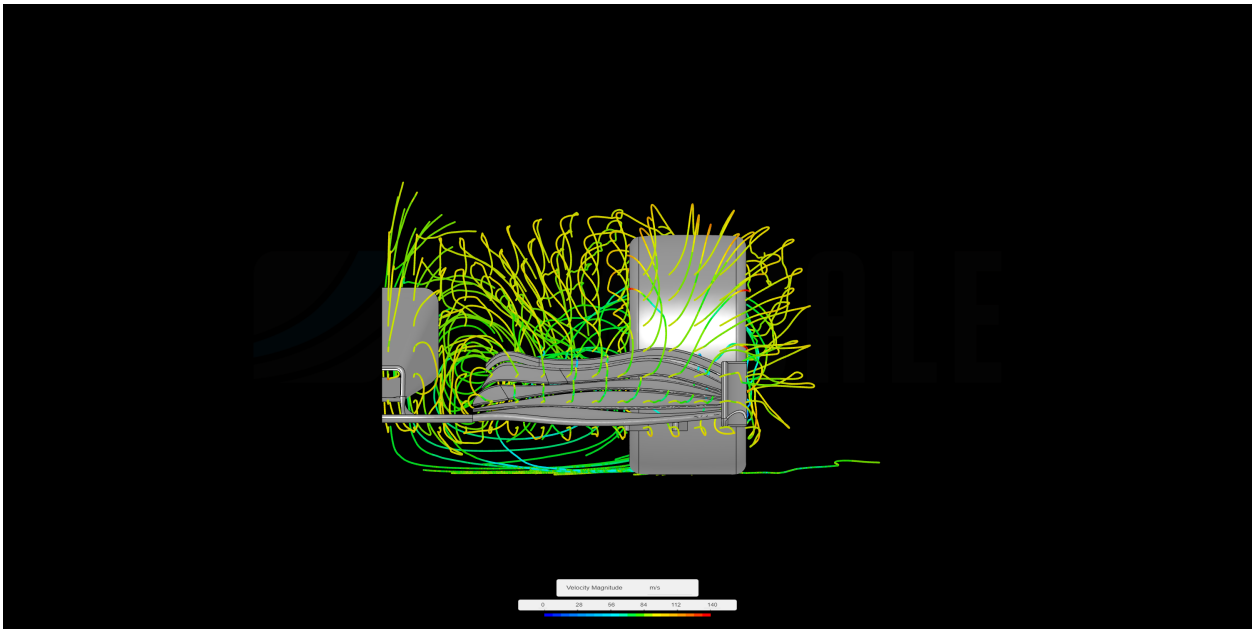

Figure 5.7: Front view of the streamlines in the 2021 front wing and tire simulation. *Source: Own Work.*

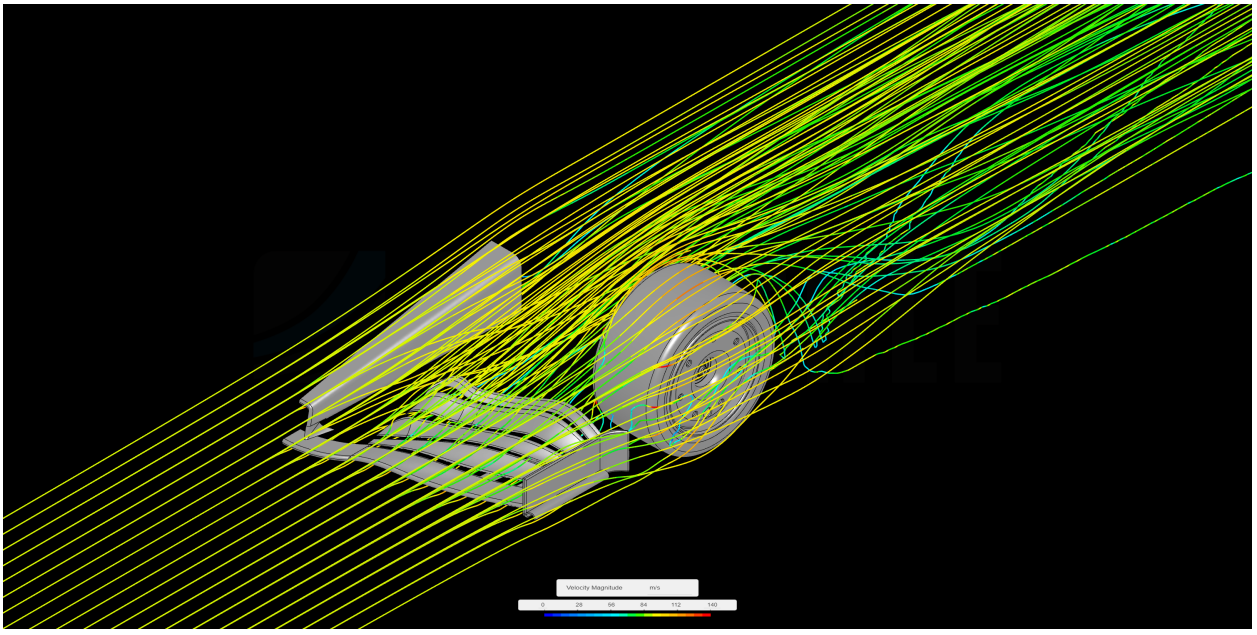

Figure 5.8: Isometric view of the streamlines in the 2021 front wing and tire simulation. *Source: Own Work.*

When the tire is added to the simulation, it can be seen that the Y-250 vortex is not affected by its presence, and it continues to appear as in the previous simulation. However, the outwash that appeared on the endplates

is affected by the presence of the wheel, reducing it significantly. Nevertheless, it does still exist, and serves its purpose of redirecting the flow outwards to reduce the drag generated by the front tires.

Additionally, it can be seen how the front tire generates turbulence behind it, as it creates a wake region due to the separation of the airflow from the tire surface. Moreover, the rotation of the tire can induce rotational effects that result in increased vorticity. The vorticity field of the front wing without and with the tire can be seen in Figures 5.9 and 5.10:

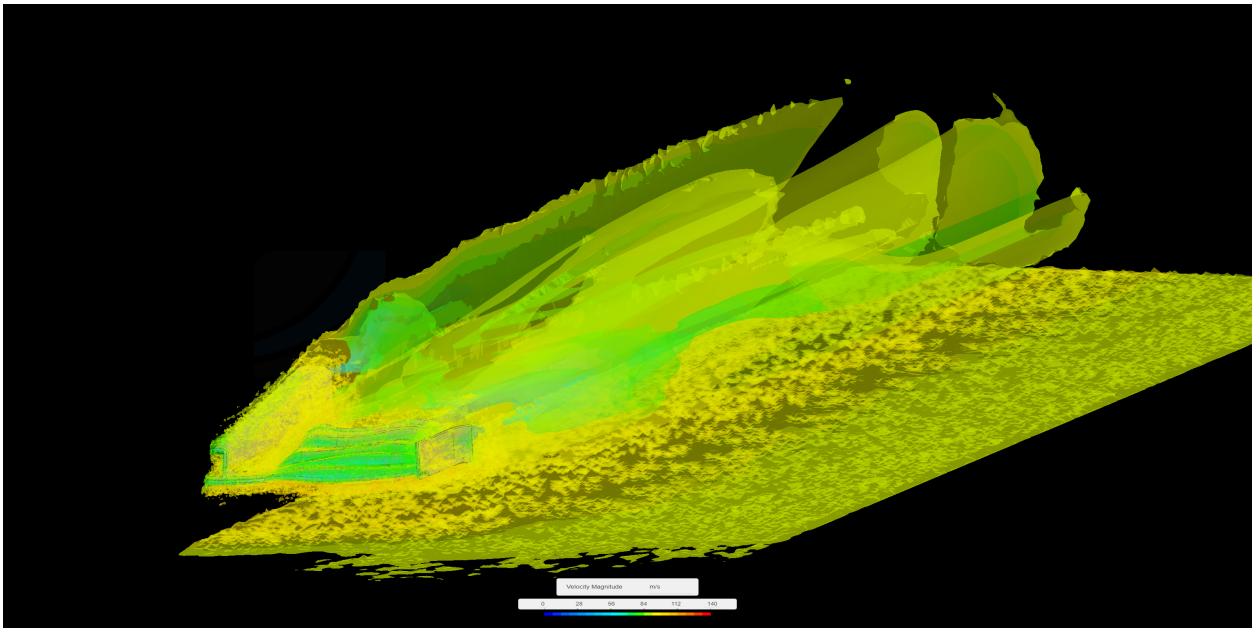

Figure 5.9: General view of the vorticity in the 2021 front wing simulation. *Source: Own Work.*

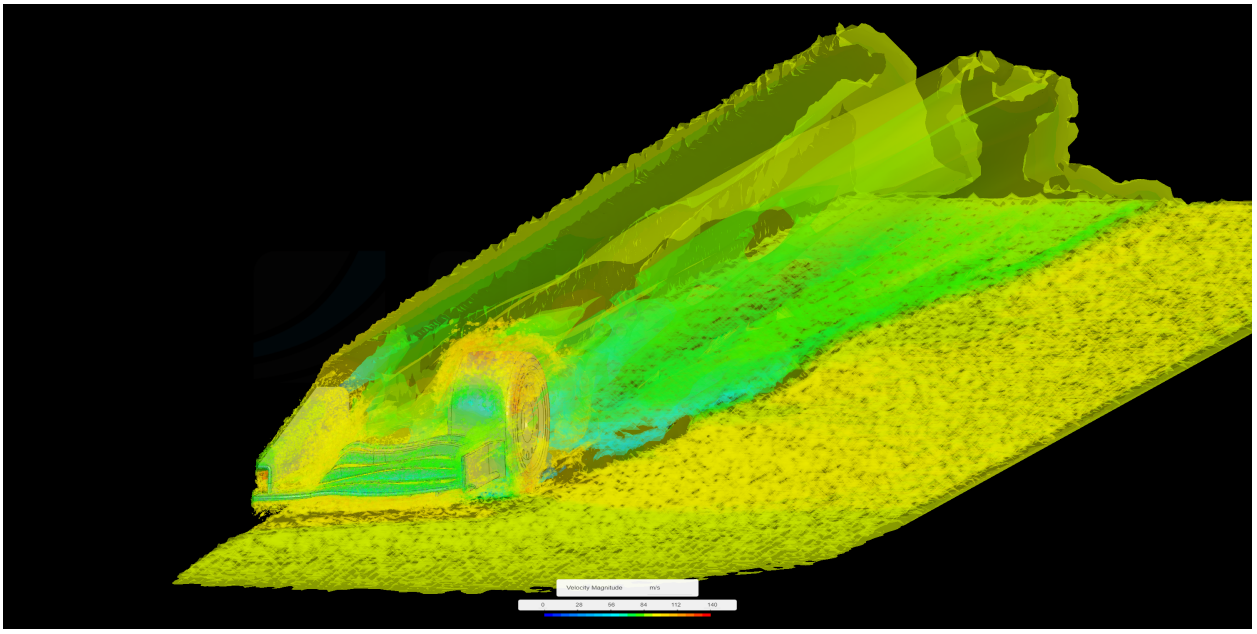

Figure 5.10: General view of the vorticity in the 2021 front wing and tire simulation. *Source: Own Work.*

In these figures, when the tire is not present in the simulation, the two primary vortices can be observed: the

Y-250 vortex and the outwash. However, when the tire is included in the simulation, the presence of the tire significantly affects the flow patterns. The vorticity increases due to the interaction of the tire with the surrounding airflow, as its shape and rotational motion introduce additional flow disturbances and complex vortical structures.

5.6.2 2021 front wing simulation

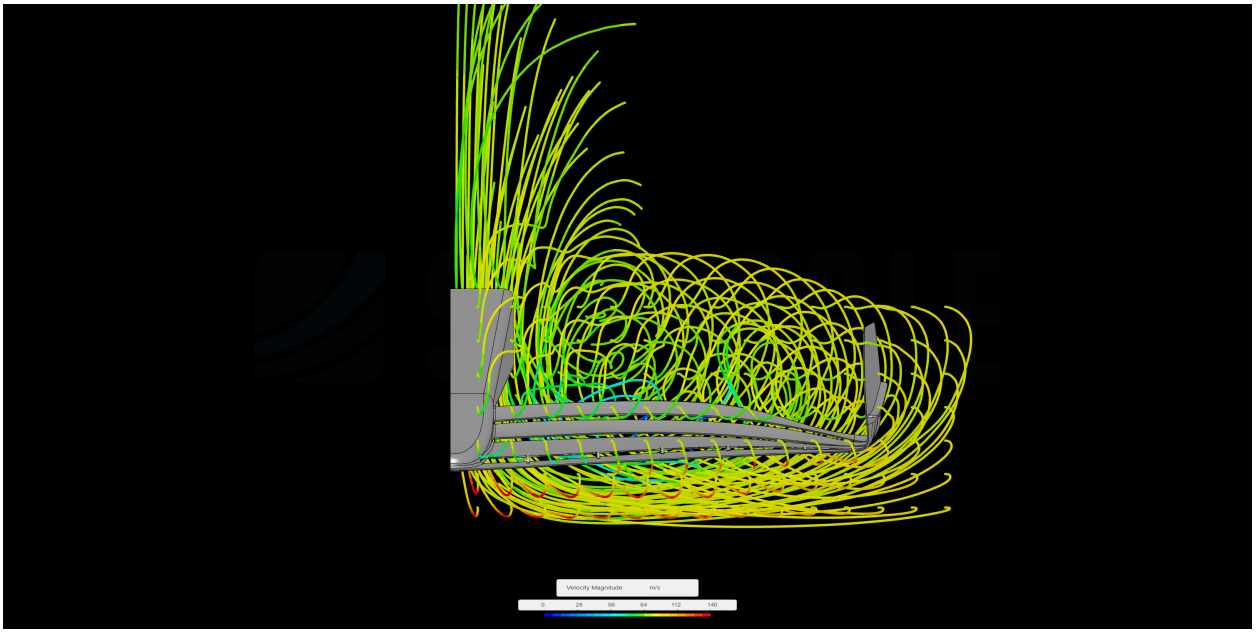

Figure 5.11: Front view of the streamlines in the 2022 front wing simulation. *Source: Own Work.*

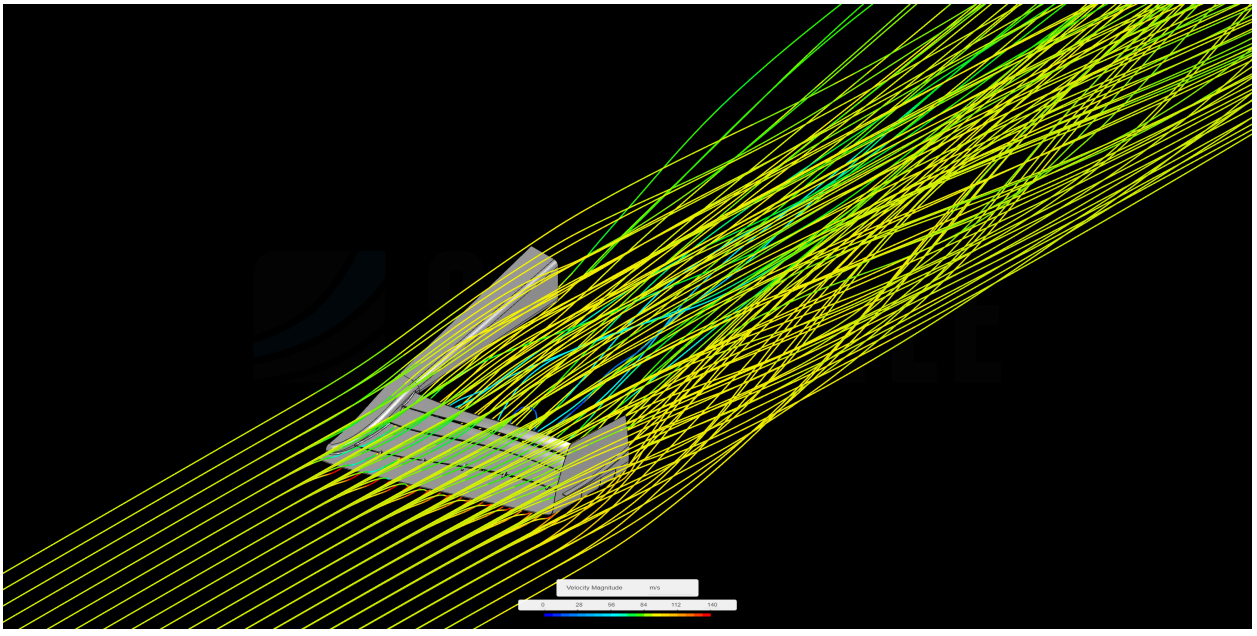

Figure 5.12: Isometric view of the streamlines in the 2022 front wing simulation. *Source: Own Work.*

Comparing the streamlines of the 2022 front wing simulation to 2021 one, several differences can be noticed. First of all, due to the flap profiles reaching the nose of the vehicle, the Y-250 vortex is completely eliminated.

This is one of the most important changes in the regulations, as the Y-250 vortex had been a key feature of front wings in recent years. However, due to its elimination, the turbulence behind the front wheel is significantly reduced.

Additionally, with the redesign of both the endplates and the flaps, a new vortex is generated throughout the whole width of the front wing, and it redirects the airflow toward the lower center of the car. This effect is sought in order to introduce as much air as possible into the car's floor, thus increasing the ground effect caused by the venturi-like design of the new floors. The new generation of F1 cars have floor inlets in the lower center of the fuselage, so this behavior of the airflow matches the objective of redirecting the flow towards this area.

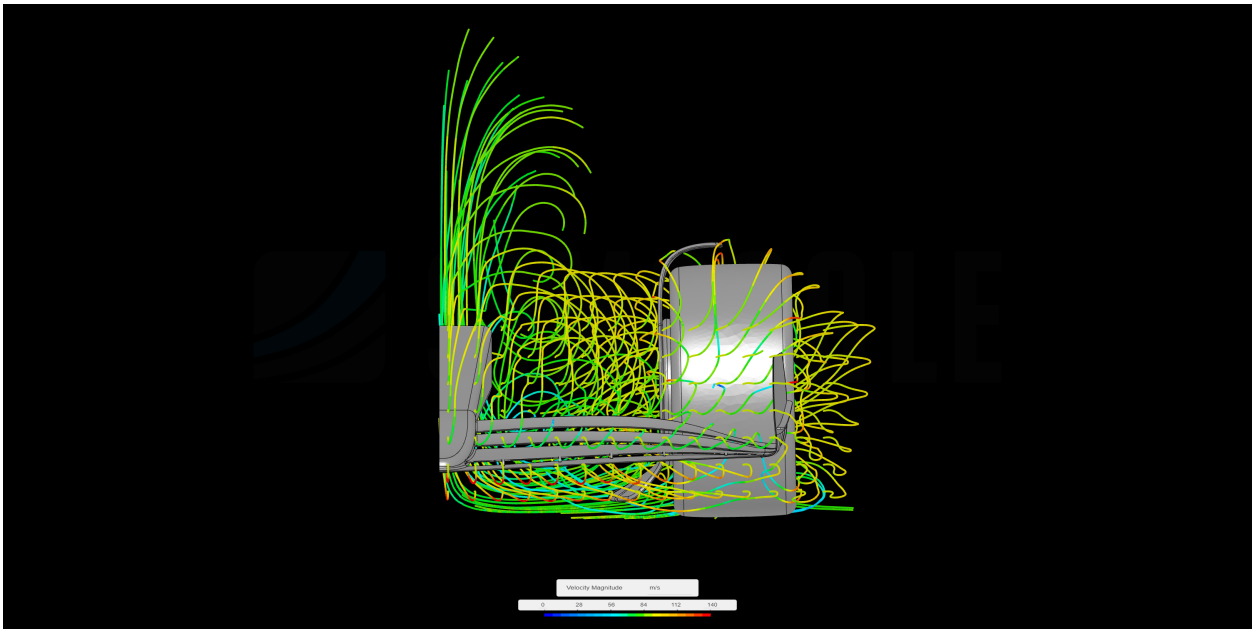

Figure 5.13: Front view of the streamlines in the 2022 front wing and tire simulation. *Source: Own Work.*

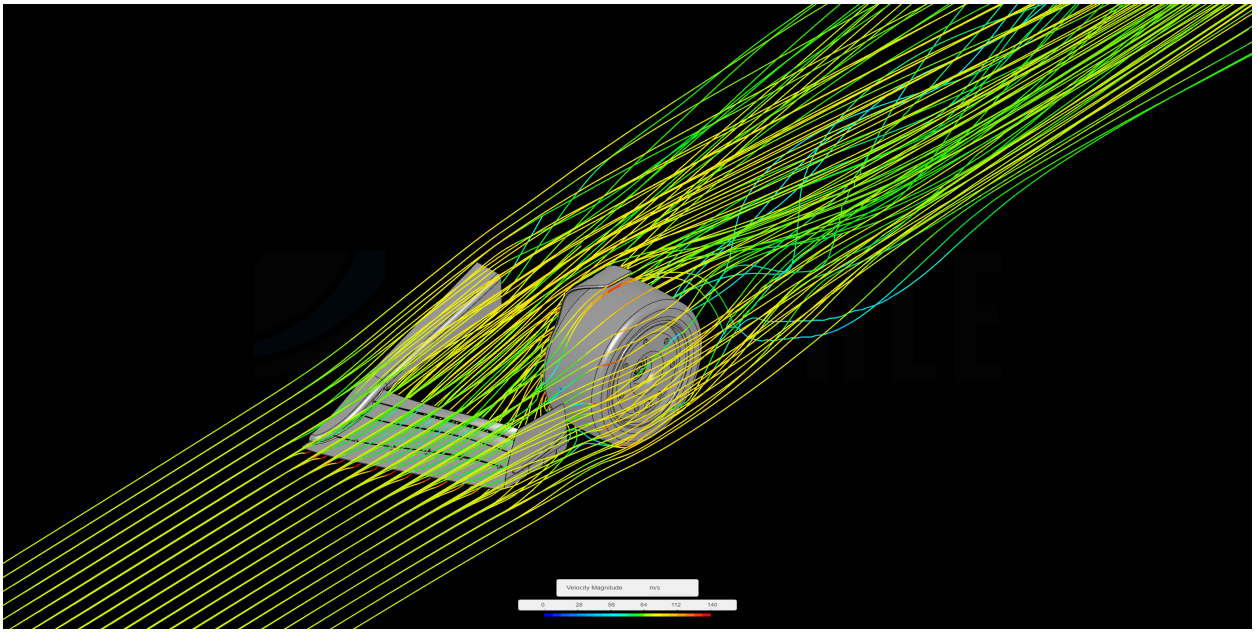

Figure 5.14: Isometric view of the streamlines in the 2022 front wing and tire simulation. *Source: Own Work.*

When the tire is introduced into the simulation, the behavior of the streamlines on the inner part of the wing doesn't get much affected. This is already seen in the 2021 simulation, in which the Y-250 vortex does not suffer any alteration due to the tire presence. However, the flow on the outer part of the wing does get affected by the tire, and the new vortex that formed throughout the wing is slightly reduced, but the overall turbulence is increased due to the tire effects.

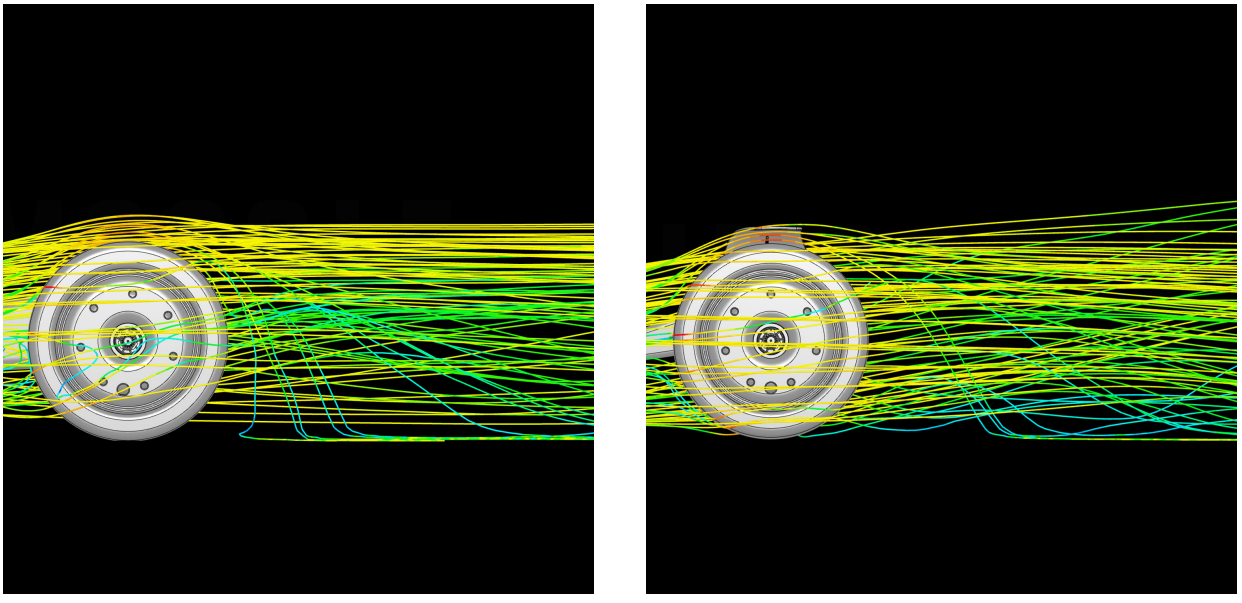

(a) (b)

Figure 5.15: (a) Profile view of the 2021 simulation with tire; (b) Profile view of the 2022 simulation with tire. *Source: Own Work.*

As for the wheel covers, when comparing the profile view of both simulations, in Figure 5.15, it can be

seen that in 2022 the air follows a smoother path around the tire, while in 2021 its rotation caused more turbulence. This is caused by the Magnus effect, as explained in Section 2.1.10, and it is proven that the wheel cover reduces this phenomenon and, consequently, the "dirty air" generated downstream.

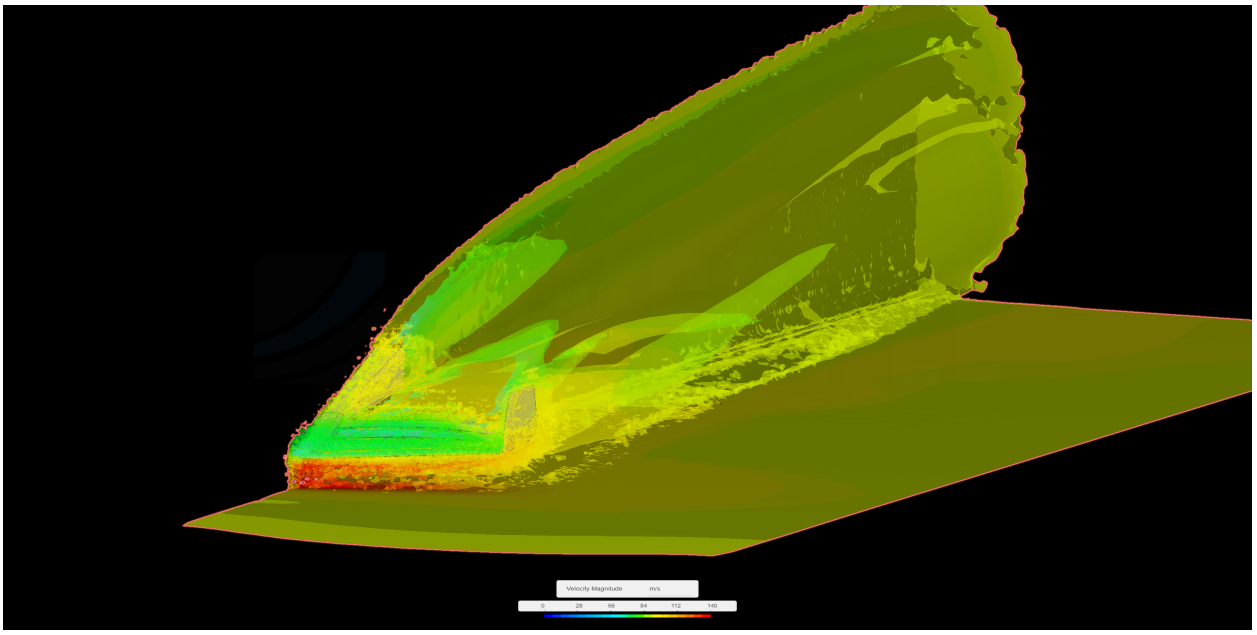

Figure 5.16: General view of the vorticity in the 2022 front wing simulation. *Source: Own Work.*

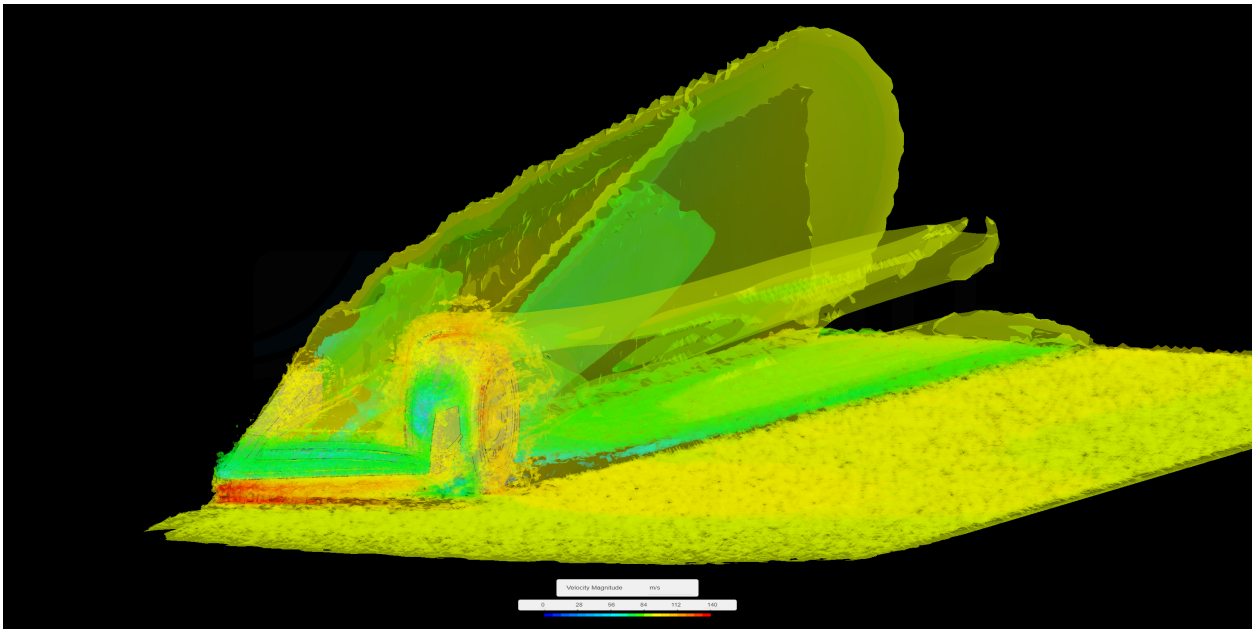

Figure 5.17: General view of the vorticity in the 2022 front wing and tire simulation. *Source: Own Work.*

Comparing both the 2021 and 2022 designs, it can be stated that the 2022 front wing design definitely generates less turbulence and successfully meets the objective of simplifying the design. Apart from that, one can observe how the two models redirect the airflow in a different manner, as the first one seeks to expel it towards the bargeboards in order to take advantage of the aerodynamic load that these elements generate,

while the second focuses more on redirecting it towards the lower center of the vehicle, where it enters the floor of the vehicle to take advantage the venturi effect and generate a large amount of aerodynamic load.

As for the dirty air generated, the 2021 wing generates two big vortices that are aimed to avoid other aerodynamic elements of the car, and thus are added to the turbulent wake of the rest of the car. In contrast, the 2022 wing generates a large vortex that aims directly at the floor inlets, and thus it doesn't add up to the rest of the turbulence generated by the car. Taking this into account, it can be said that the new design of the 2022 front wing successfully reduces the turbulent wake generated, and fulfills the purpose of the redesign.

Chapter 6

Conclusions

The main objective of this thesis was to conduct a CFD simulation comparing the aerodynamic performance and design of the 2021 and 2022 front wings of an F1 car. The implementation of the 2022 regulations brought about significant changes in the aerodynamic concept, in particular, simplifying the design of the front wing. The primary focus of the FIA was to minimize the wake turbulence generated by the complex aerodynamic components of previous years' cars, thereby promoting closer racing and overtaking. As a result, the 2022 front wing was designed with a simplified configuration, featuring three flaps and the exclusion of the Y250 vortex, leading to reduced turbulence and wake generation.

First of all, a theoretical study has been carried out on the physical phenomena that describe the aerodynamics of F1, in order to have a good understanding of how the cars work. The operation of CFD has also been studied, as how its use can help solve complex problems and analyze visually and numerically the behavior of airflow around various geometries. Finally, a walk through the history of F1 has been taken, and it is seen how the vehicles have evolved aerodynamically since the beginning of the sport, understanding the reasons for each improvement and how the aerodynamic complexity of nowadays was reached.

Then the two front wing designs have been compared visually, and the differences in design elements and philosophy have been highlighted. To validate the performance of the front wings, CAD models have been created combining the respective technical regulations of each season with already designed wings. These models have been verified to compile with the regulations, and additionally, the front tires were added to the assembly for deeper study. The design and validation of these models highlighted the massive change brought about by the new 2022 regulation and made it possible to analyze in detail the technical regulations of both years.

CFD simulations revealed remarkable findings. The front wing of 2022 demonstrated less complex behavior, effectively reducing the turbulent wake and efficiently channeling airflow away from the vehicle's tires. Additionally, it was possible to check how the different wings redirect the airflow differently, in order to take advantage of the rest of the aerodynamic elements of each vehicle, such as the bargeboards and the floor of the car. The newly introduced front tire winglets proved to reduce the Magnus effect caused by them, thus

reducing the turbulent wake generated.

In conclusion, the scope established at the beginning of the project has been achieved, and its requirements have been met. The main objective of the work was to verify how the redesign of the front wings had affected the turbulent wake generated by them, and how the change in the design philosophy has affected the airflow around them. Through different CFD analysis, it has been proved that the design of the 2022 front wing has successfully reduced the turbulent wake generated. It has also been proven that both designs redirect the flow accordingly to the design of the rest of the car, either to avoid the front tires and accentuate the effect of the bargeboards in 2021 or to introduce as much air as possible throughout the car's floor to maximize the ground effect.

6.1 Future work

Expanding on the analysis, taking it a step further involves incorporating real models of the front wings into the investigation to accurately quantify the aerodynamic forces generated. Utilizing these models provides a tangible representation of the wings' intricate design features, allowing for precise measurements and a more realistic simulation of their performance. In addition, conducting a convergence study is crucial in refining the analysis. This study involves varying the mesh resolution used in the CFD simulations to determine the optimal mesh quality for accurate and reliable results.

Moving forward, further analysis should consider the overall vehicle aerodynamics, particularly how the front wing interacts with the underbody, to validate the effectiveness of ground effect in generating downforce.

Chapter 7

Environmental impact

The totality of this study was conducted solely on computers over a duration of three months. Although computer-based simulations generally have a lower environmental footprint compared to physical testing, it is important to consider the energy consumption and associated emissions during the study.

Considering that the workload of the project is equivalent to 300h, the electricity consumption will be calculated based on this number. The power supply of the computer used allows for a maximum of 500W, when browsing the web the real consumption of the computer can be considered about 20% of the maximum. As for the 3D design periods, it will be assumed that the computer had a consumption of 70% of the maximum. As the CAD design occupied about 80 hours, the remaining 220 hours will be considered as used in the browser.

$$\text{Energy Consumed} = 70\% \cdot 500\ W \cdot (80\ \cdot 3600) + 20\% \cdot 500\ W \cdot (220\ \cdot 3600) = 129,6\ MJ$$

In addition, the energy consumed by doing the simulations on the cloud must also be considered. By adding up all the core hours consumed, including the ones consumed in canceled and trial simulations, the results shown in Table 7.1 are obtained.

	Core Hours Consumed
Mesh Generation	8.67
CFD Simulations	113.59
Trial Simulations	182.74
Total	**305**

Table 7.1: Total core hours consumed for the project. *Source: Simscale*

These core hours represent the time it would have taken to do the simulation if only one core was used. As the hardware used for the simulation can't be determined, but can be estimated to be high-end, the energy consumption for only one core of Simscale's hardware will be assumed to be the same as the consumption of personal computers when designing the CAD models. So, the final energy consumption of the project results

as:

$$\text{Energy Consumed} = 129,6\ MJ + 70\% \cdot 500\ W \cdot (305\ \cdot 3600)\text{Energy Consumed} = 513,9\ MJ$$

$$\boxed{\textbf{Energy Consumed= 142.75 kWh}}$$

Regarding CO_2 emissions, since the entire project has been solely developed by computer, only the emissions derived from the consumption of electricity need to be considered. To do this, the parameter known as "electric mix" can be used, which relates CO_2 emissions to the electricity consumed. The last available data for this indicator corresponds to 2021 and is 259 $gCO2eq/kWh$ [21]. For the case study, this data will be taken as valid to calculate the total emissions. Multiplying this value for the electricity consumption obtained above, the total carbon footprint of the project can be obtained:

$$mCO_2 = 259\ \frac{gCO_{2\ eq}}{kWh} \cdot 142.75\ kWh \Longrightarrow \boxed{\mathbf{mCO_2 = 36.97KgCO_2}}$$

To conclude this section, it can be said that the realization of this project has generated 36.97 Kg of CO_2.

Bibliography

1. BENSON, Tom. *Boundary Layer* [online]. NASA - Glenn Research Center, 2021 [visited on 2023-03-20]. Available from: https://www.grc.nasa.gov/www/k-12/BGP/boundlay.html.
2. BENSON, Tom. *Aerodynamic Forces* [online]. NASA - Glenn Research Center, 2021 [visited on 2023-03-20]. Available from: https://www.grc.nasa.gov/www/k-12/rocket/presar.html.
3. SIMSCALE. *Compressible Flow vs Incompressible Flow* [online]. Simscale, 2023 [visited on 2023-03-22]. Available from: https://www.simscale.com/docs/simwiki/cfd-computational-fluid-dynamics/compressible-flow-vs-incompressible-flow/#:~:text=Difference%5C%20between%5C%20Compressible%5C%20and%5C%20Incompressible,fluid%5C%20does%5C%20not%5C%20remain%5C%20constant.&text=On%5C%20the%5C%20other%5C%20hand%5C%2C%5C%20incompressible,of%5C%20the%5C%20fluid%5C%20remains%5C%20constant..
4. LIBRARY, Engineering. *Laminar and Turbulent Flow* [online]. Engineering Library, 2023 [visited on 2023-03-22]. Available from: https://engineeringlibrary.org/reference/laminar-and-turbulent-fluid-flow-doe-handbook.
5. UNIVERSITY, Princeton. *Bernoulli's Equation* [online]. Princeton University, 2023 [visited on 2023-03-22]. Available from: https://www.princeton.edu/~asmits/Bicycle_web/Bernoulli.html.
6. FELFÖLDI, Attila. *What is the Venturi Effect?* [online]. Simscale, 2023 [visited on 2023-03-22]. Available from: https://www.simscale.com/blog/what-is-venturi-effect/.
7. BRENNEN, Cristopher E. *Streamlines, Pathlines and Streaklines - An Internet Book on Fluid Dynamics*. CalTech University, 2006. Available also from: http://brennen.caltech.edu/fluidbook/basicfluiddynamics/massconservation/streamlines.pdf.
8. BANG, Chris Sungkyun. *Tech Explained — Flow viz* [online]. Racecar Engineering, 2018 [visited on 2023-03-20]. Available from: https://www.racecar-engineering.com/tech-explained/tech-explained-flow-viz/2.
9. MOFFATT, H. K. *A brief introduction to vortex dynamics and turbulence* [online]. University of Cambridge, 2023 [visited on 2023-03-23]. Available from: http://www.damtp.cam.ac.uk/user/hkm2/PDFs/Moffatt_2011_WorldScientific_Abitvdat_1.pdf.
10. HALL, Nancy. *Navier-Stokes Equations* [online]. NASA - Glenn Research Center, 2021 [visited on 2023-03-23]. Available from: https://www.grc.nasa.gov/www/k-12/airplane/nseqs.html.

11. RAJESH BHASKARAN, Lance Collins. *Introduction to CFD Basics* [online]. Cornell University, 2023 [visited on 2023-03-27]. Available from: https://dragonfly.tam.cornell.edu/teaching/mae5230-cfd-intro-notes.pdf.
12. SOLMAZ, Serkan. *Turbulence: Which Model Should I Select for My CFD Analysis?* [online]. Simscale, 2023 [visited on 2023-03-29]. Available from: https://www.simscale.com/blog/turbulence-cfd-analysis/.
13. IDEALSIMULATIONS. *Turbulence Models In CFD* [online]. IdealSimulations, 2023 [visited on 2023-03-29]. Available from: https://www.idealsimulations.com/resources/turbulence-models-in-cfd/#:~:text=Turbulence%5C%20models%5C%20in%5C%20Computational%5C%20Fluid,occur%5C%20in%5C%20most%5C%20engineering%5C%20applications..
14. PETE. *F1 History: The Mechanical Evolution Through The Eras Of Formula 1* [online]. Chronicle, 2023 [visited on 2023-04-02]. Available from: https://f1chronicle.com/f1-history-mechanical-evolution-through-the-eras/.
15. KEW, Matt. *The 10 biggest innovations in Formula 1 history: active suspension, halo, fan car & more* [online]. Autosport, 2022 [visited on 2023-04-02]. Available from: https://www.autosport.com/f1/news/the-10-biggest-innovations-in-formula-1-history-active-suspension-halo-fan-car-more/10125979/.
16. MARK HUGHES, Giorgio Piola. *TECH TUESDAY: How the front wing on the all-new 2022 cars has been designed to improve overtaking* [online]. F1.com, 2022 [visited on 2023-04-04]. Available from: https://www.formula1.com/en/latest/article.tech-tuesday-why-the-front-wing-will-be-a-key-technical-battleground-on-the.3Ep4LEu5mTMRkXrClOQtRg.html.
17. FIA. *2021 FORMULA 1 TECHNICAL REGULATIONS* [online]. FIA, 2020 [visited on 2023-04-06]. Available from: https://www.fia.com/sites/default/files/2021_formula_1_technical_regulations_-_iss_7_-_2020-12-16.pdf.
18. FIA. *2022 FORMULA 1 TECHNICAL REGULATIONS* [online]. FIA, 2021 [visited on 2023-04-06]. Available from: https://www.fia.com/sites/default/files/2022_formula_1_technical_regulations_-_iss_3_-_2021-02-19.pdf.
19. NIKOLAIDIS, Ioannis. *red bull RB16B front wing season 2021* [online]. GrabCAD, 2021 [visited on 2023-04-10]. Available from: https://grabcad.com/library/red-bull-rb16b-front-wing-season-2021-1.
20. BOSISIO, Riccardo. *Ferrari F1-75 2022* [online]. Sketchfab, 2022 [visited on 2023-04-25]. Available from: https://sketchfab.com/3d-models/ferrari-f1-75-2022-9c0e66050db941eeaa261f96ea13002e.
21. CATALUNYA, Generalitat de. *Factor de emisión de la energía eléctrica: el mix eléctrico* [online]. Gencat, 2023 [visited on 2023-06-21]. Available from: https://canviclimatic.gencat.cat/es/actua/factors_demissio_associats_a_lenergia/.

Appendix A

CAD otrographic projections

A.1 2021 front wing model

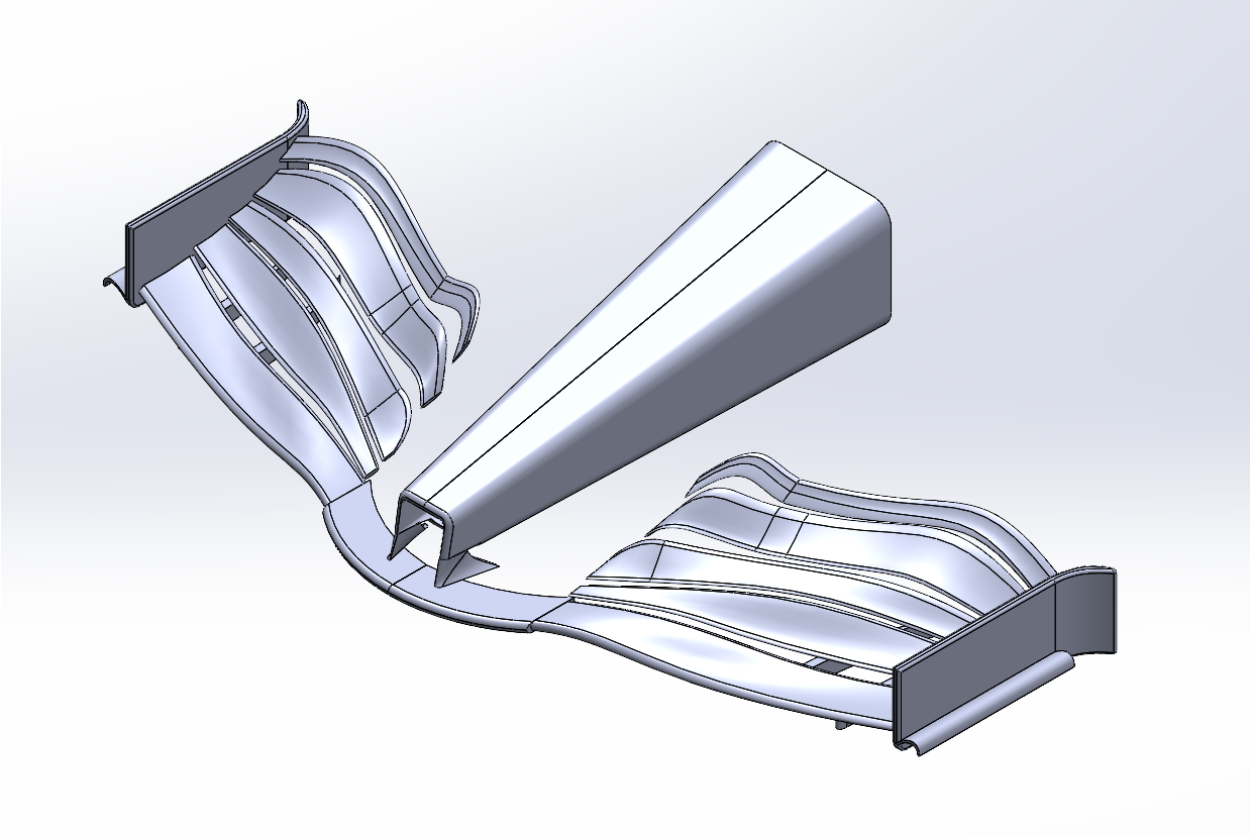

Figure A.1: Isometric view of the 2021 front wing design. *Source: Own Work.*

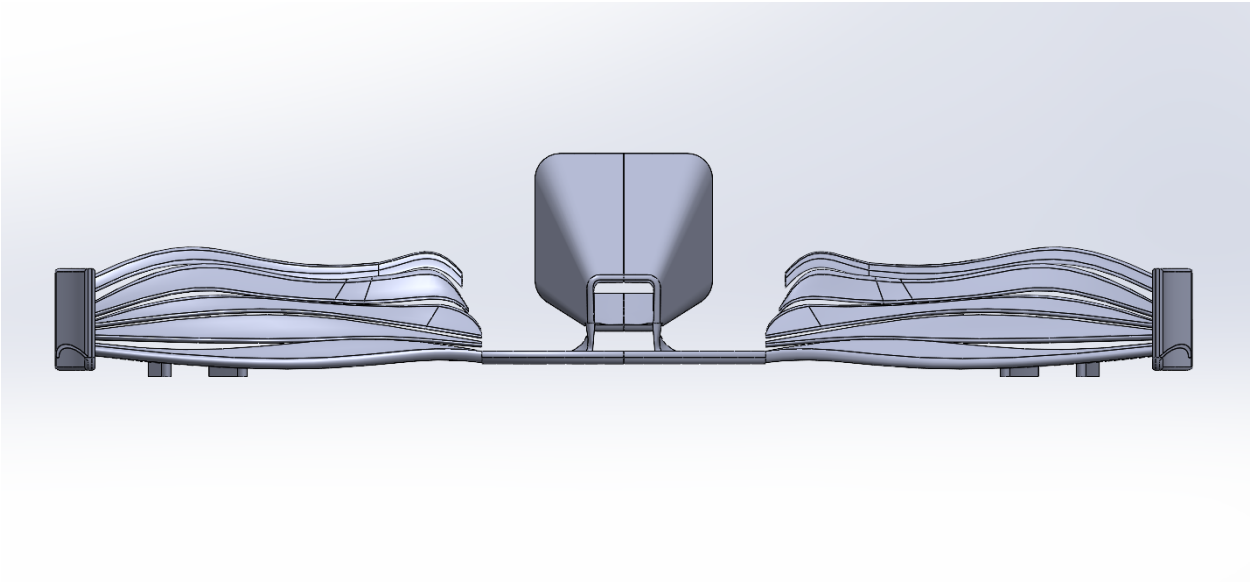

Figure A.2: Front view of the 2021 front wing design. *Source: Own Work.*

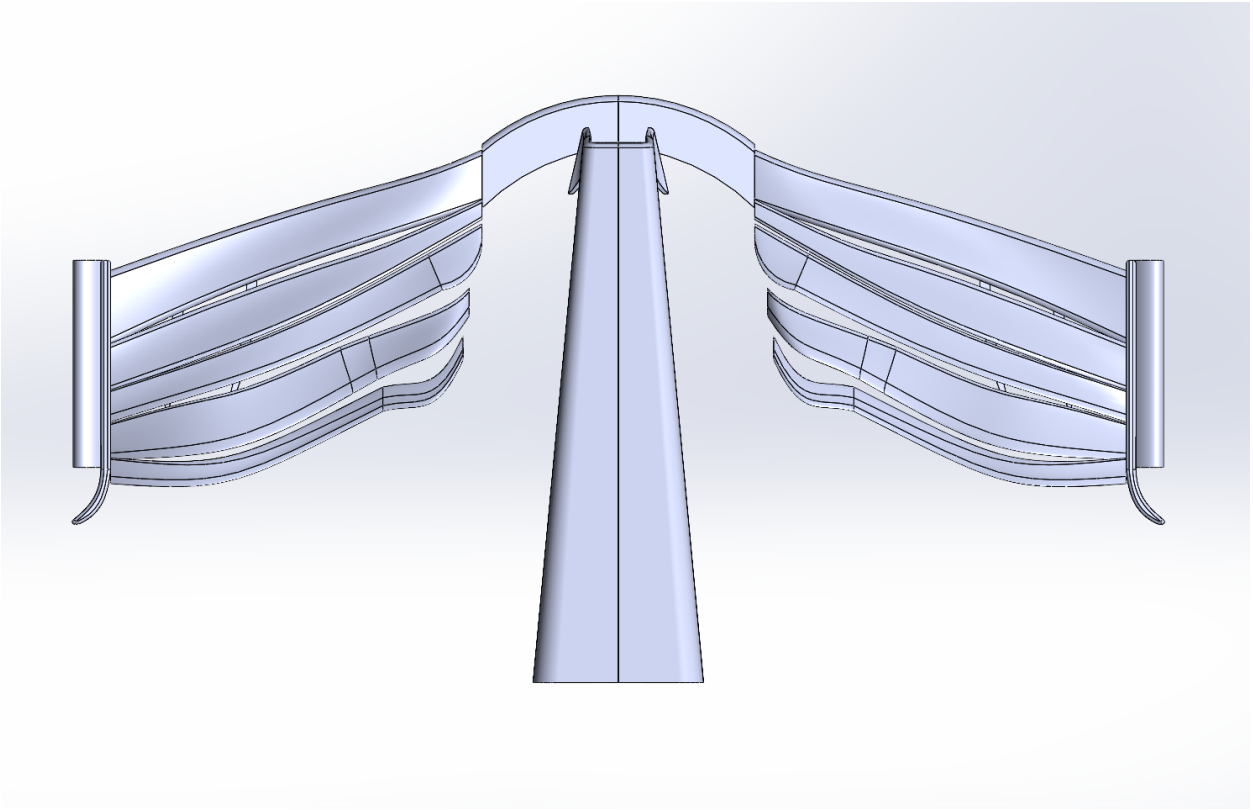

Figure A.3: Top view of the 2021 front wing design. *Source: Own Work.*

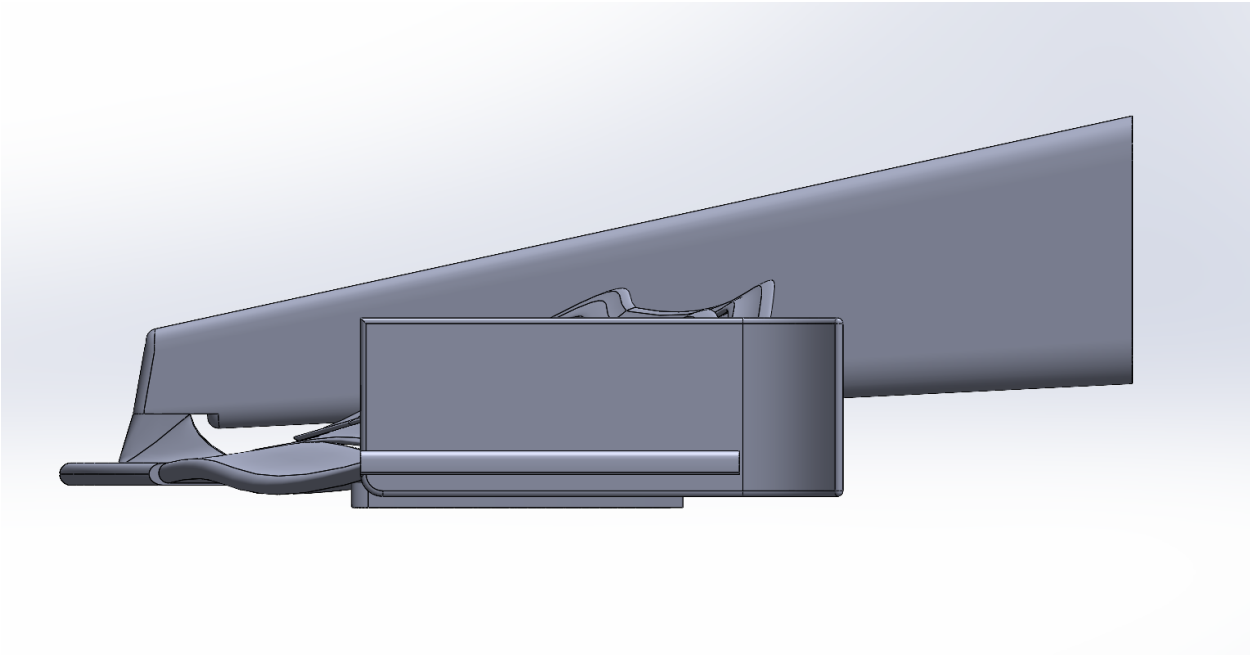

Figure A.4: Profile view of the 2021 front wing design. *Source: Own Work.*

A.2 2021 front wing and tyre model

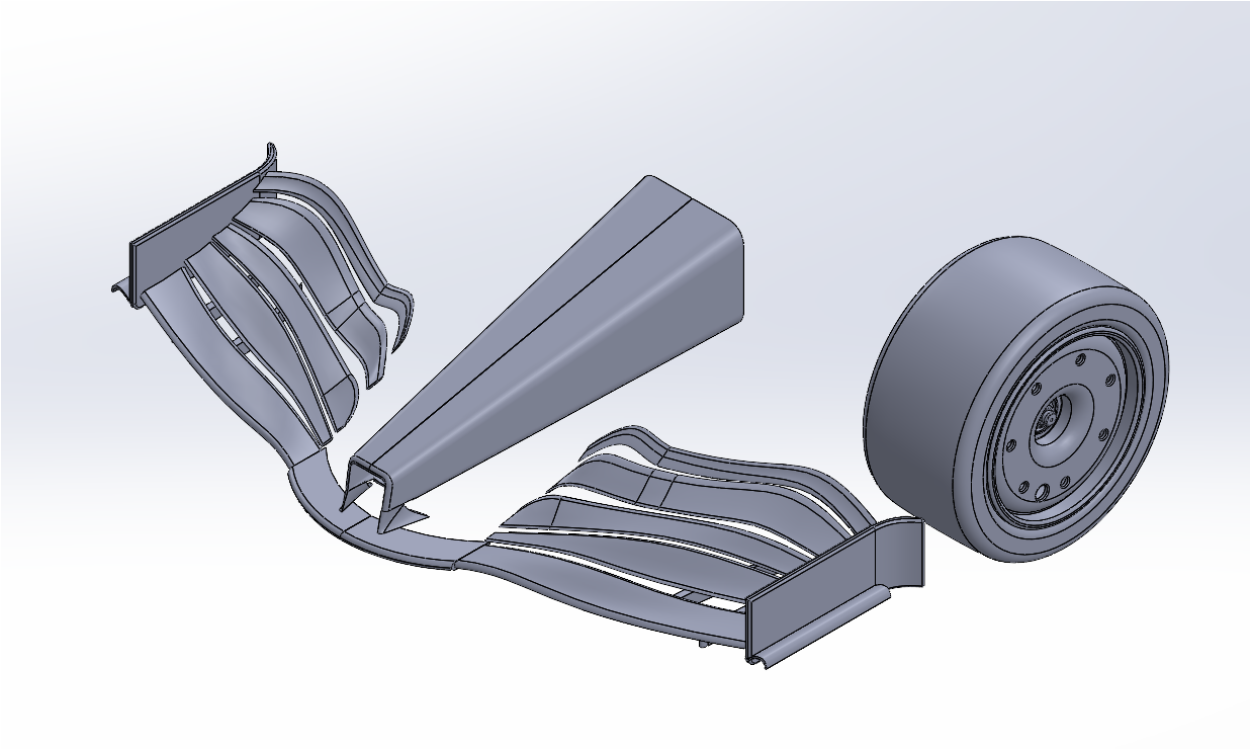

Figure A.5: Isometric view of the 2021 front wing and tire design. *Source: Own Work.*

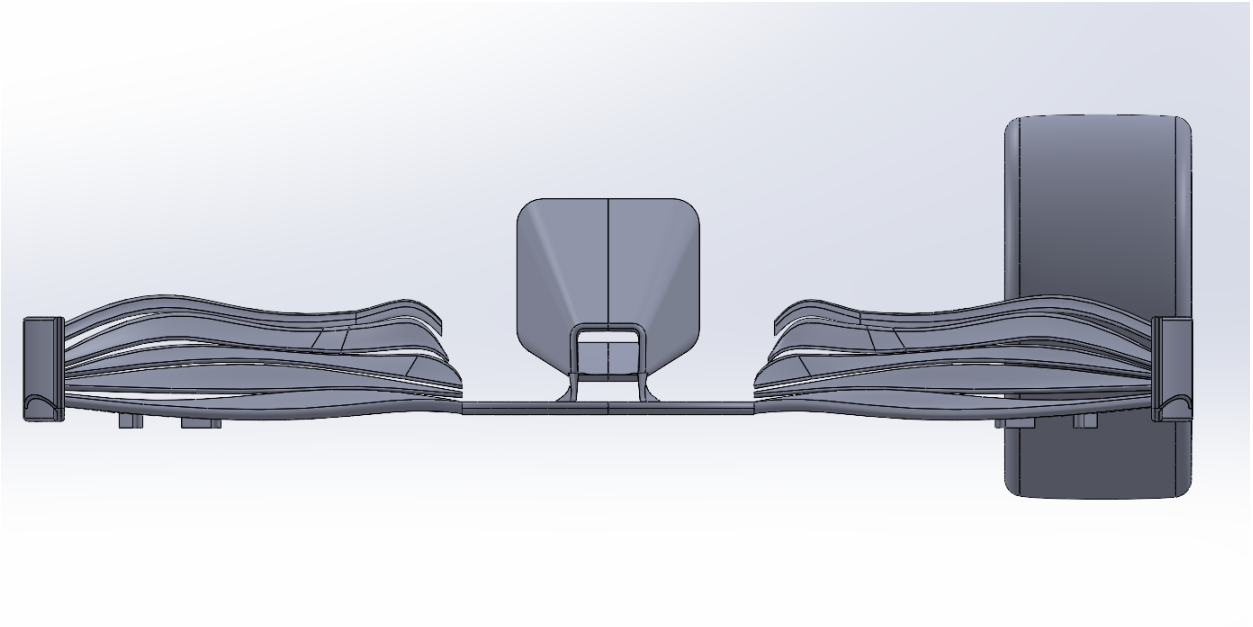

Figure A.6: Front view of the 2021 front wing and tire design. *Source: Own Work.*

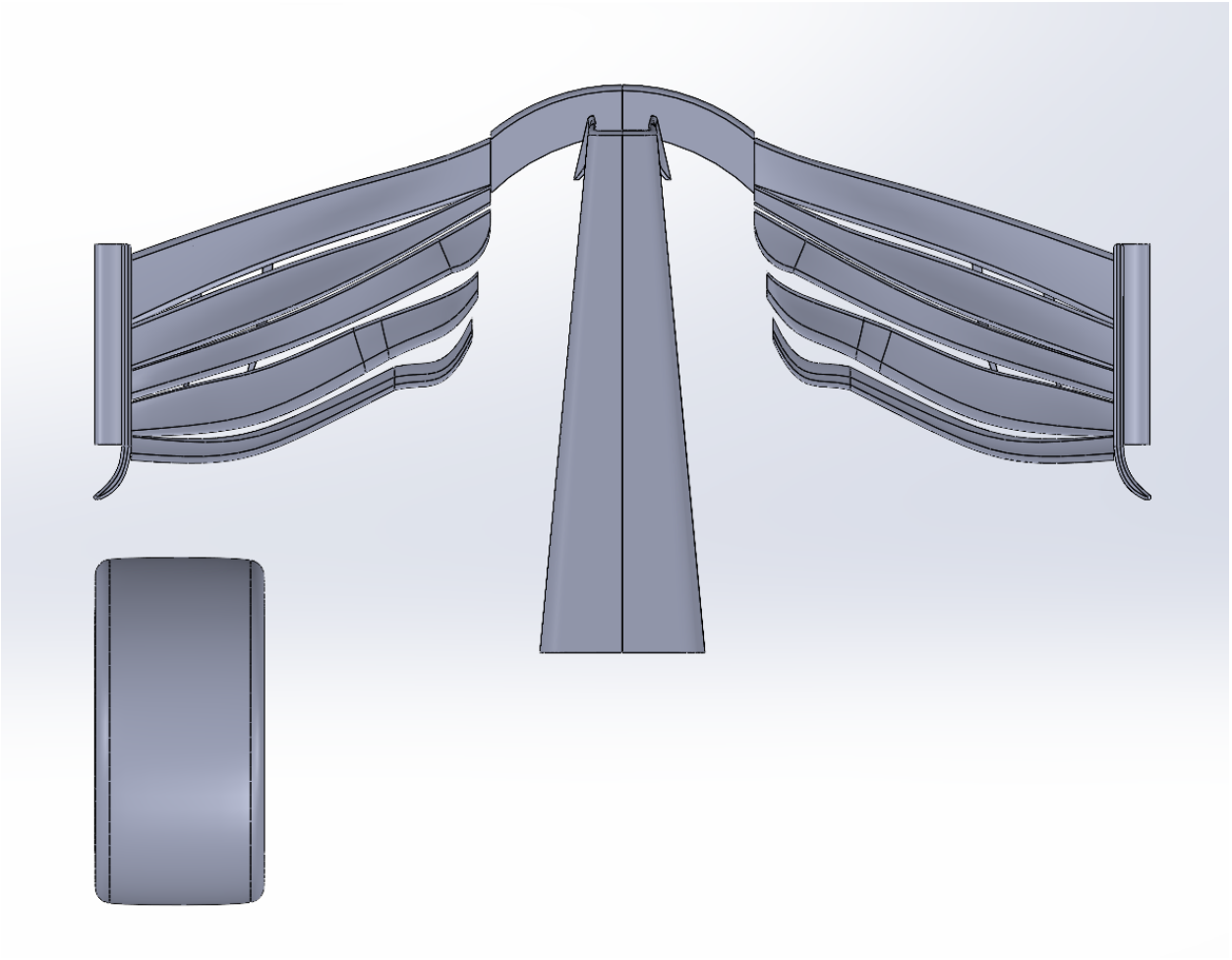

Figure A.7: Top view of the 2021 front wing and tire design. *Source: Own Work.*

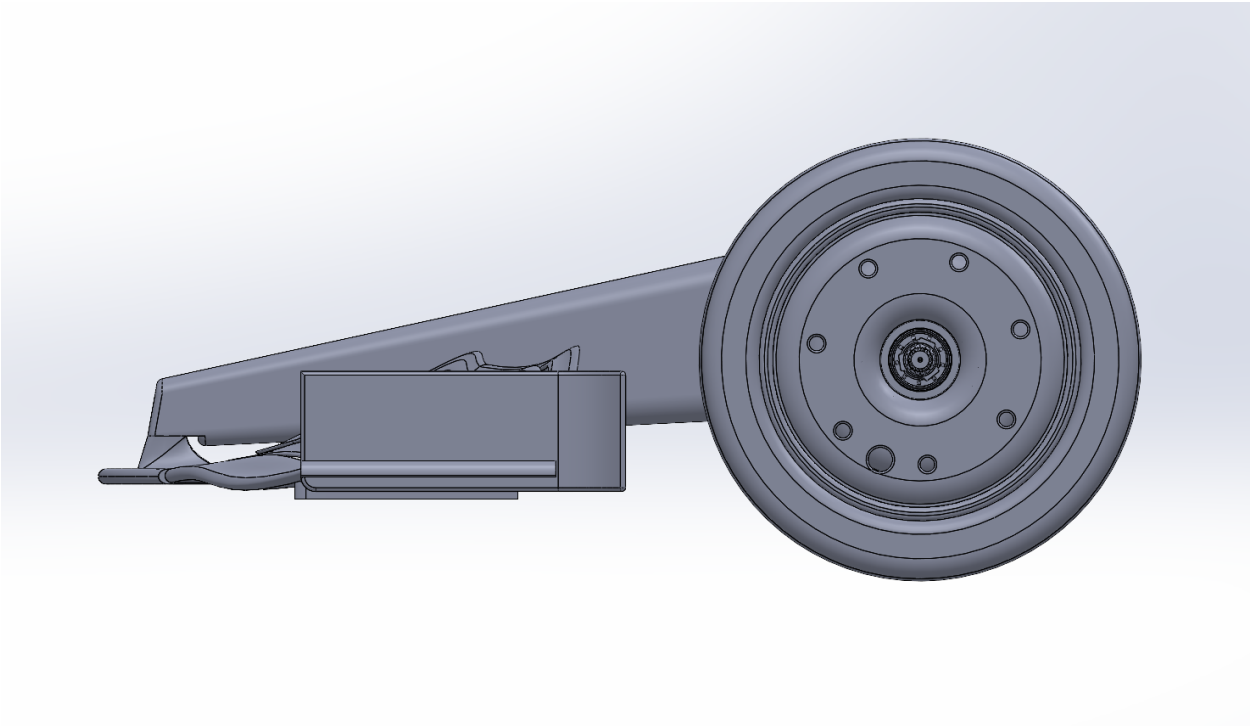

Figure A.8: Profile view of the 2021 front wing and tire design. *Source: Own Work.*

A.3 2022 front wing model

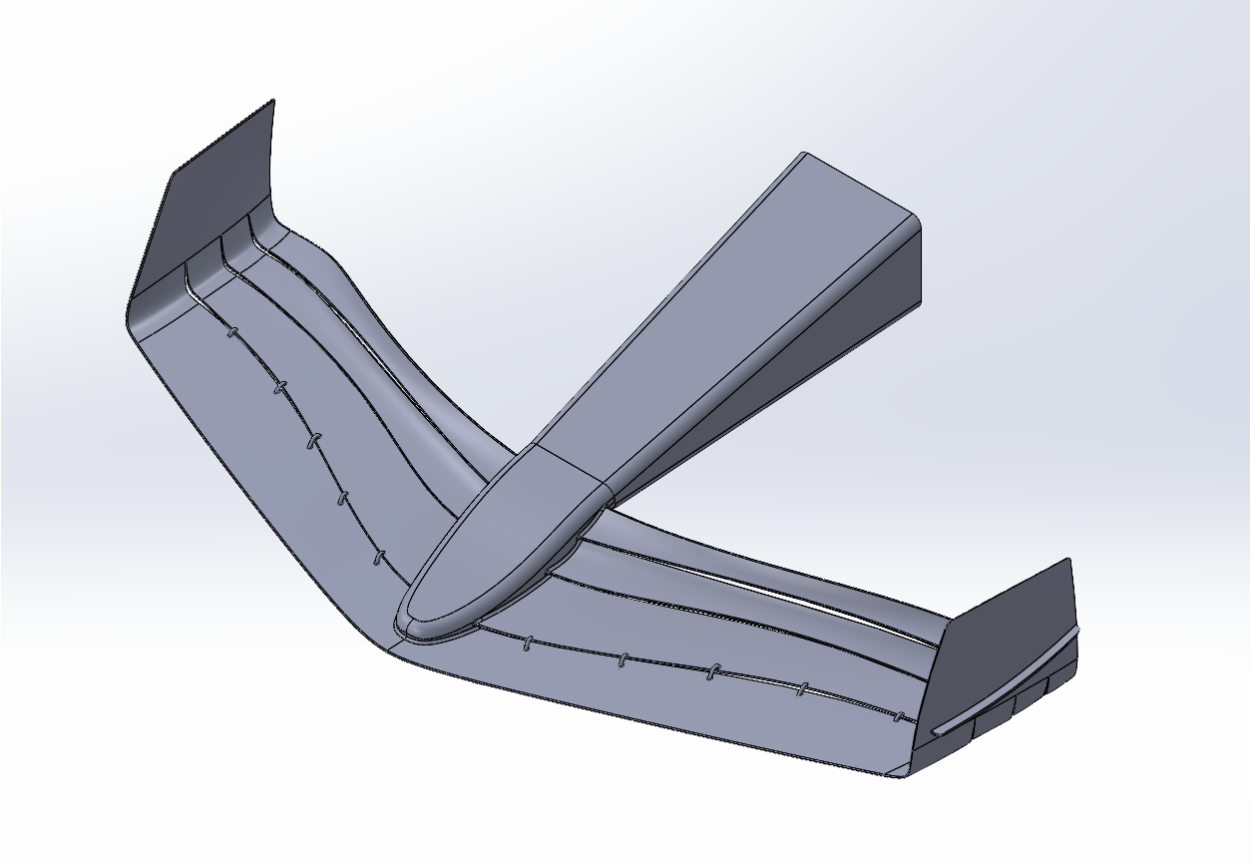

Figure A.9: Isometric view of the 2022 front wing design. *Source: Own Work.*

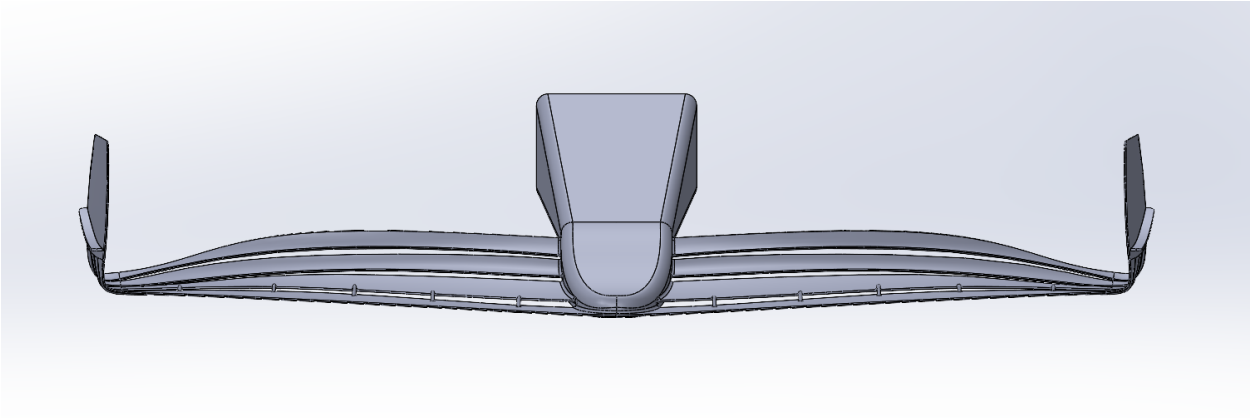

Figure A.10: Front view of the 2022 front wing design. *Source: Own Work.*

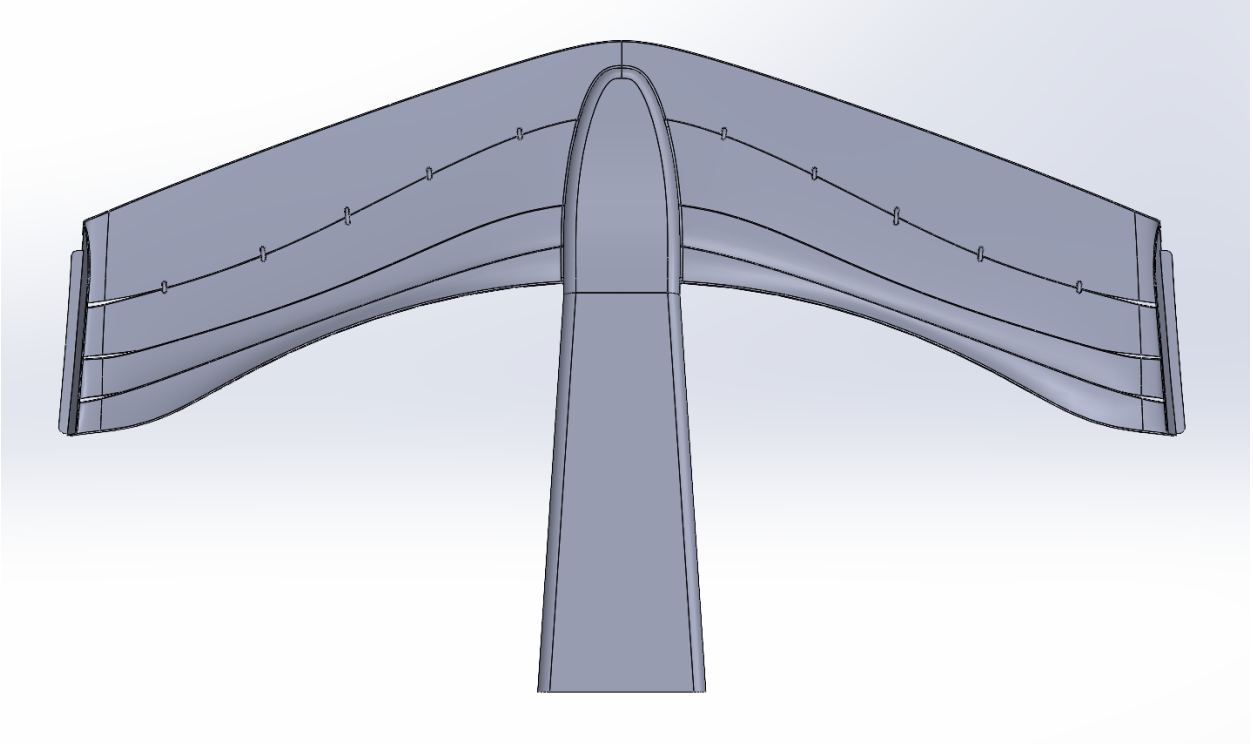

Figure A.11: Top view of the 2022 front wing design. *Source: Own Work.*

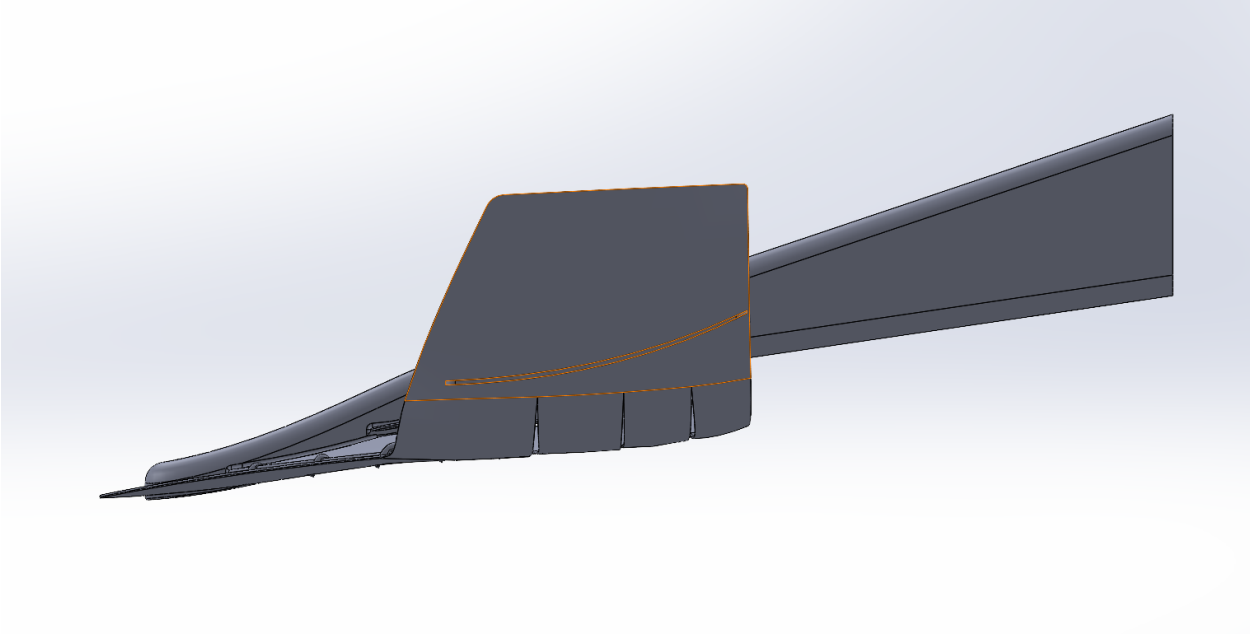

Figure A.12: Profile view of the 2022 front wing design. *Source: Own Work.*

A.4 2022 front wing and tyre model

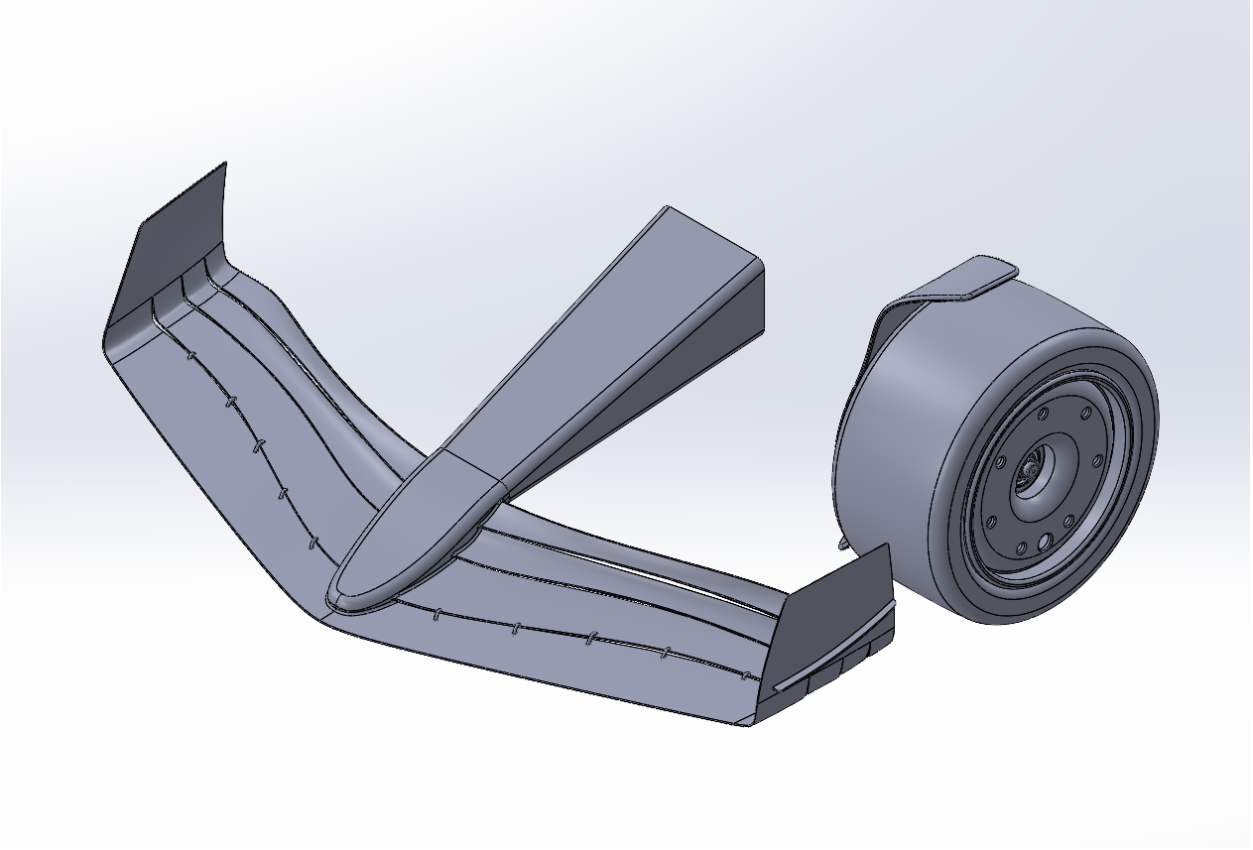

Figure A.13: Isometric view of the 2022 front wing and tire design. *Source: Own Work.*

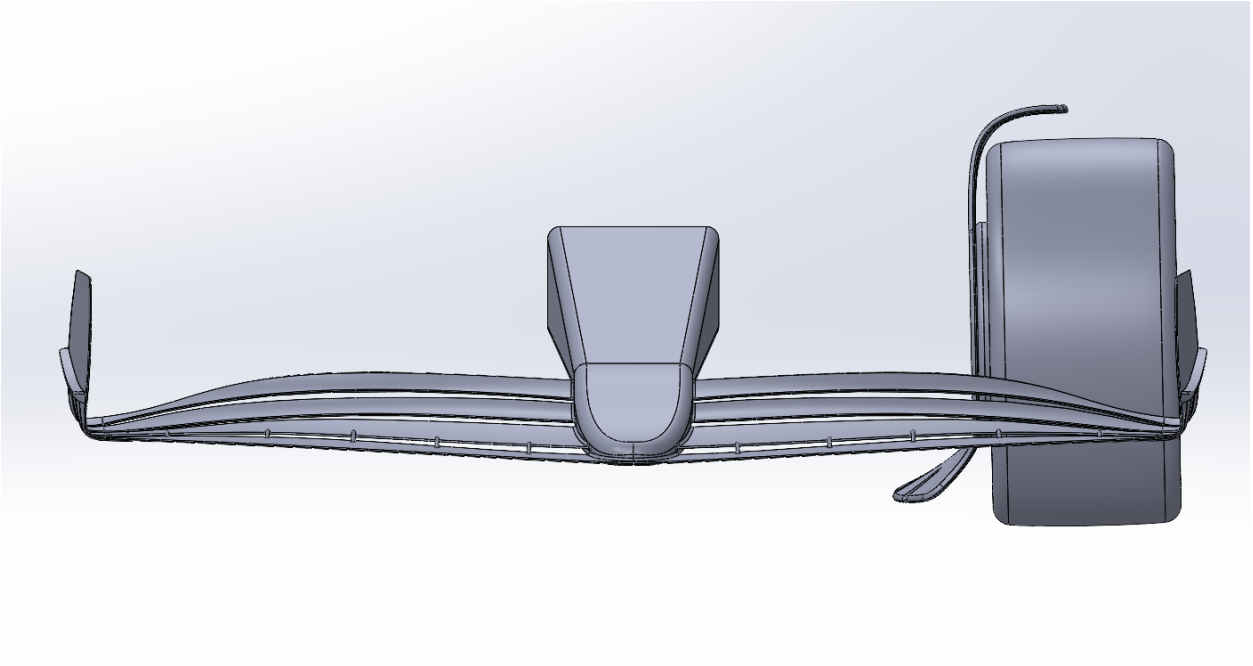

Figure A.14: Front view of the 2022 front wing and tire design. *Source: Own Work.*

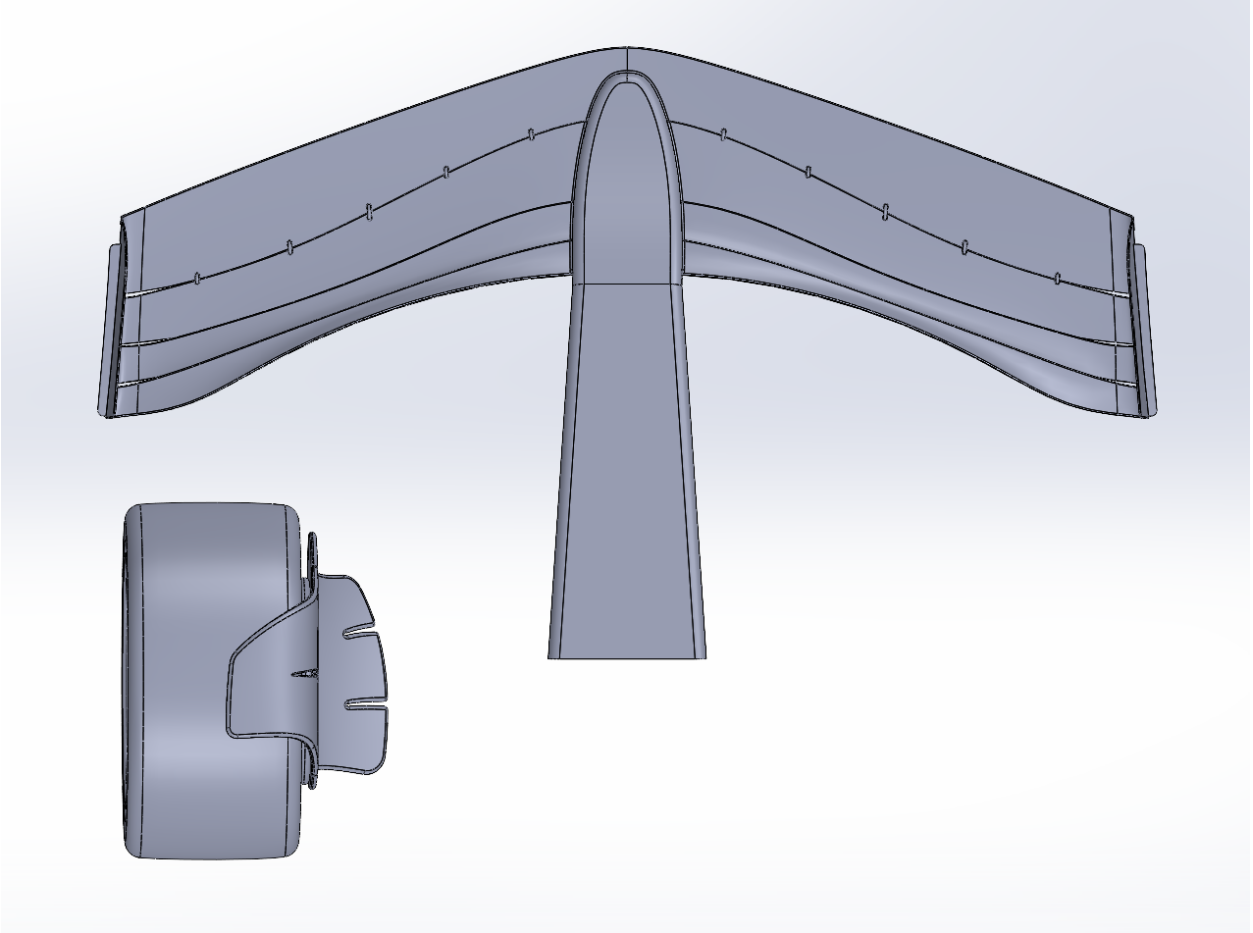

Figure A.15: Top view of the 2022 front wing and tire design. *Source: Own Work.*

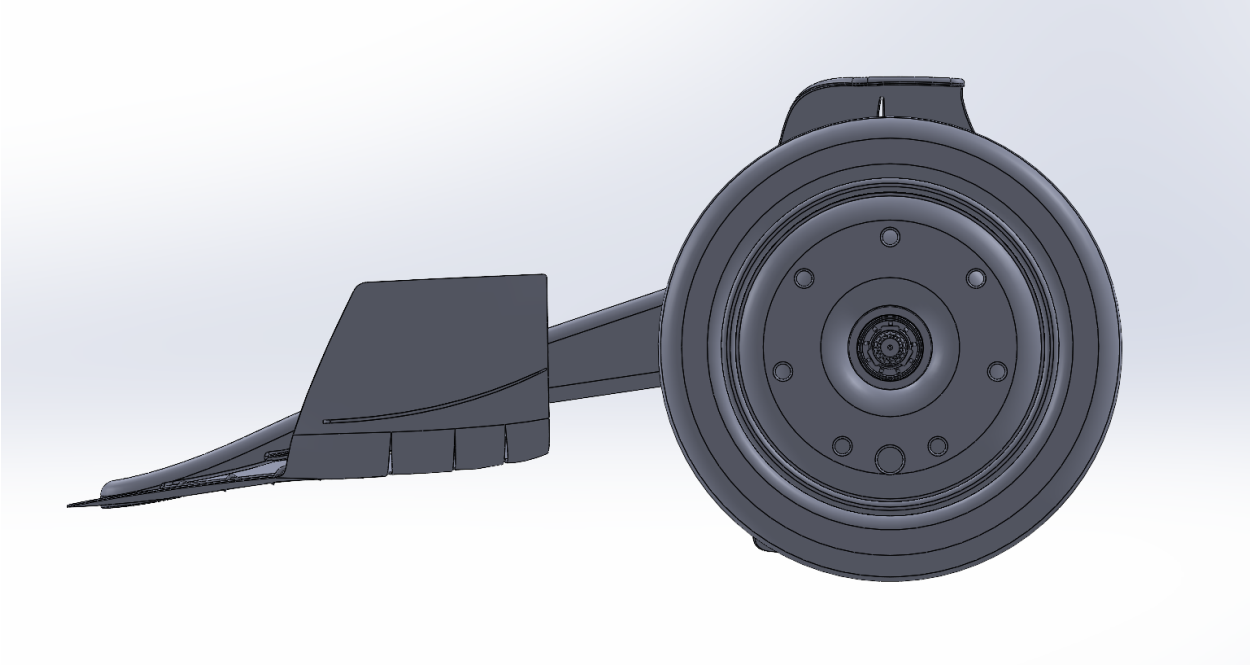

Figure A.16: Profile view of the 2022 front wing and tire design. *Source: Own Work.*

Appendix B

Meshes

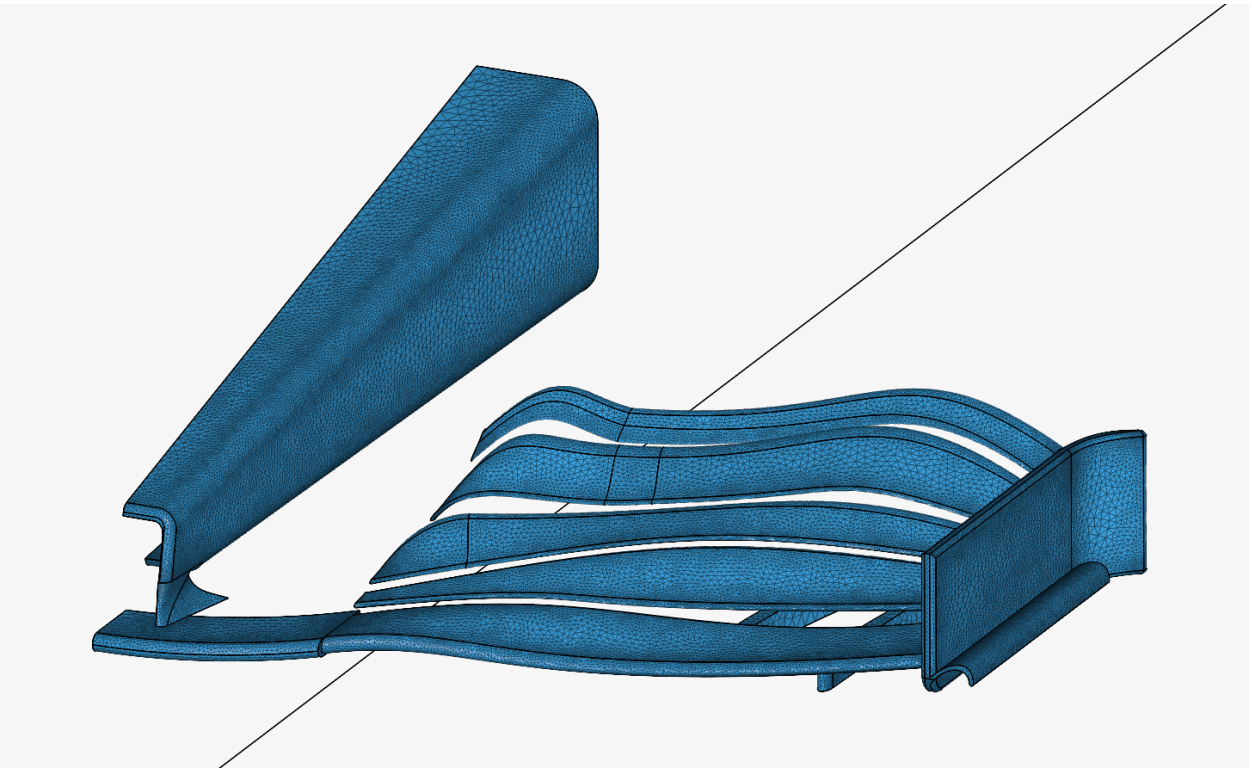

Figure B.1: Isometric view of the mesh generated in the 2021 front wing simulation. *Source: Own Work.*

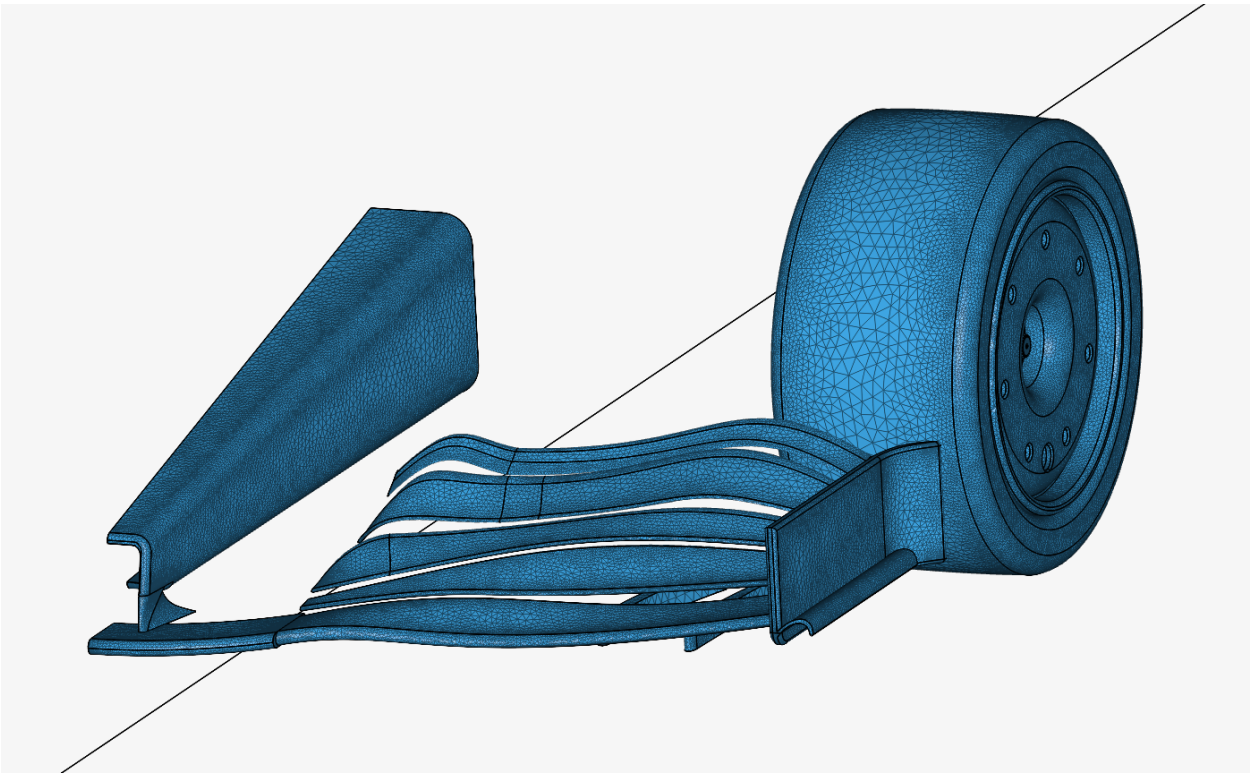

Figure B.2: Isometric view of the mesh generated in the 2021 front wing and tire simulation. *Source: Own Work.*

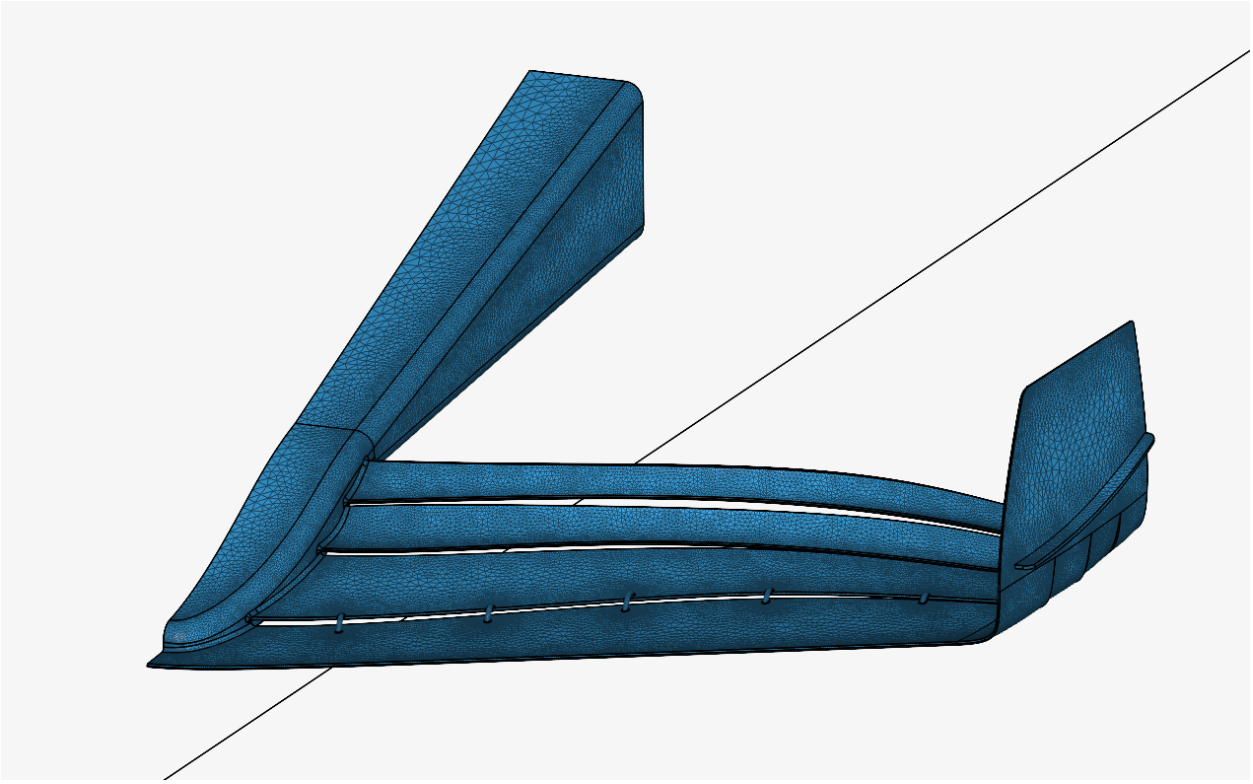

Figure B.3: Isometric view of the mesh generated in the 2022 front wing simulation. *Source: Own Work.*

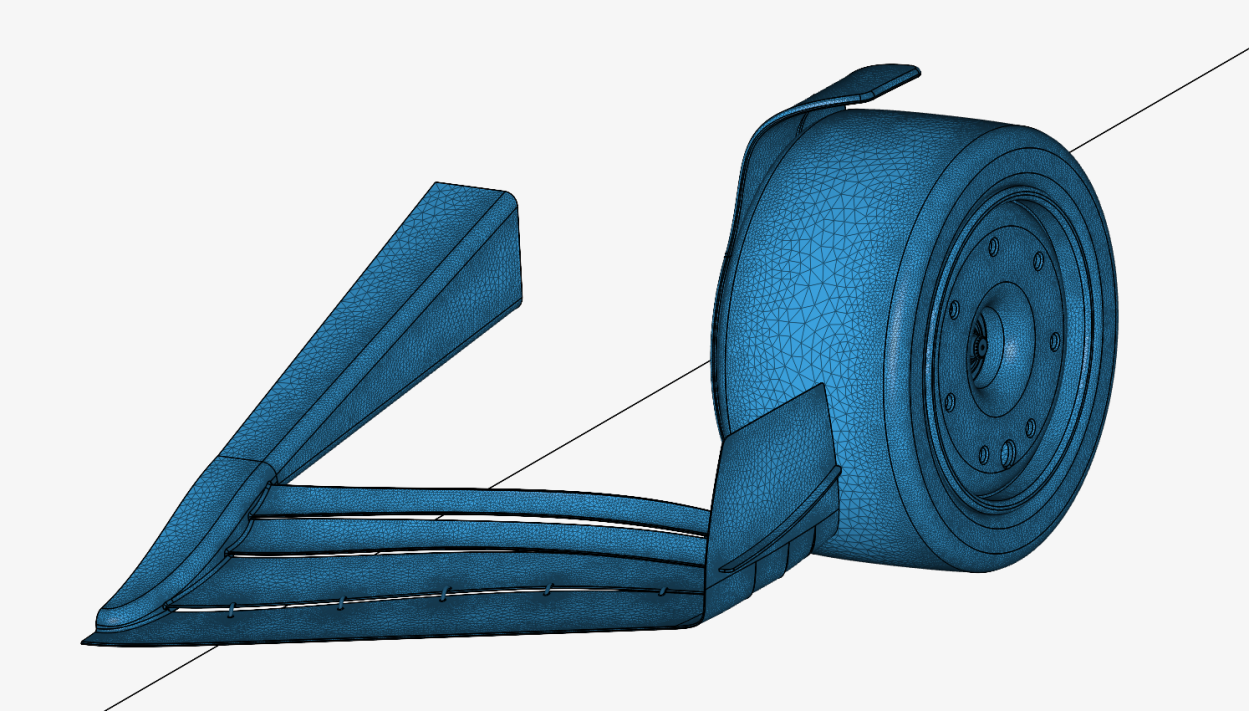

Figure B.4: Isometric view of the mesh generated in the 2022 front wing and tire simulation. *Source: Own Work.*

Appendix C

CFD simulation results

C.1 2021 front wing simulation

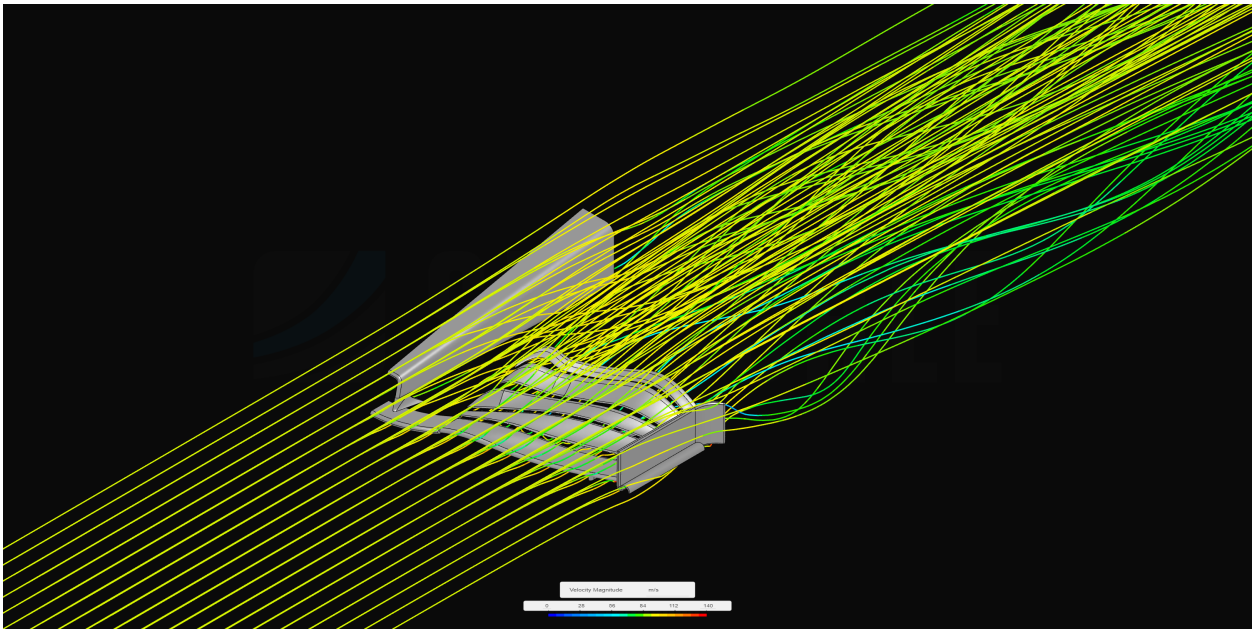

Figure C.1: Isometric view of the streamlines in the 2021 front wing simulation. *Source: Own Work.*

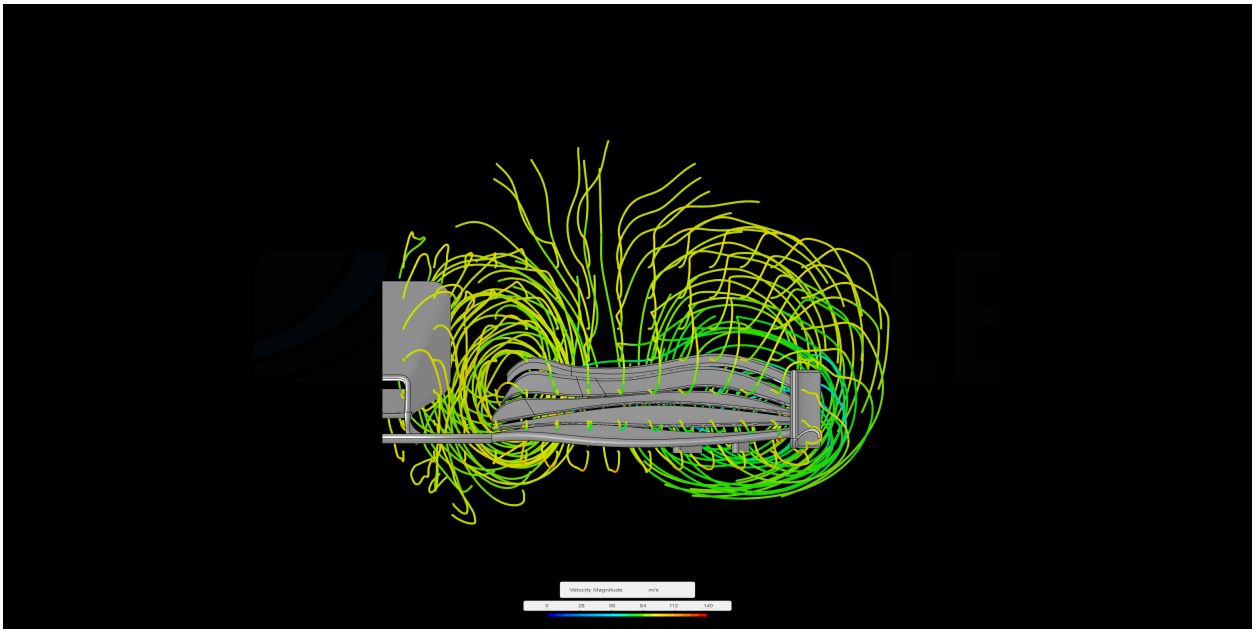

Figure C.2: Front view of the streamlines in the 2021 front wing simulation. *Source: Own Work.*

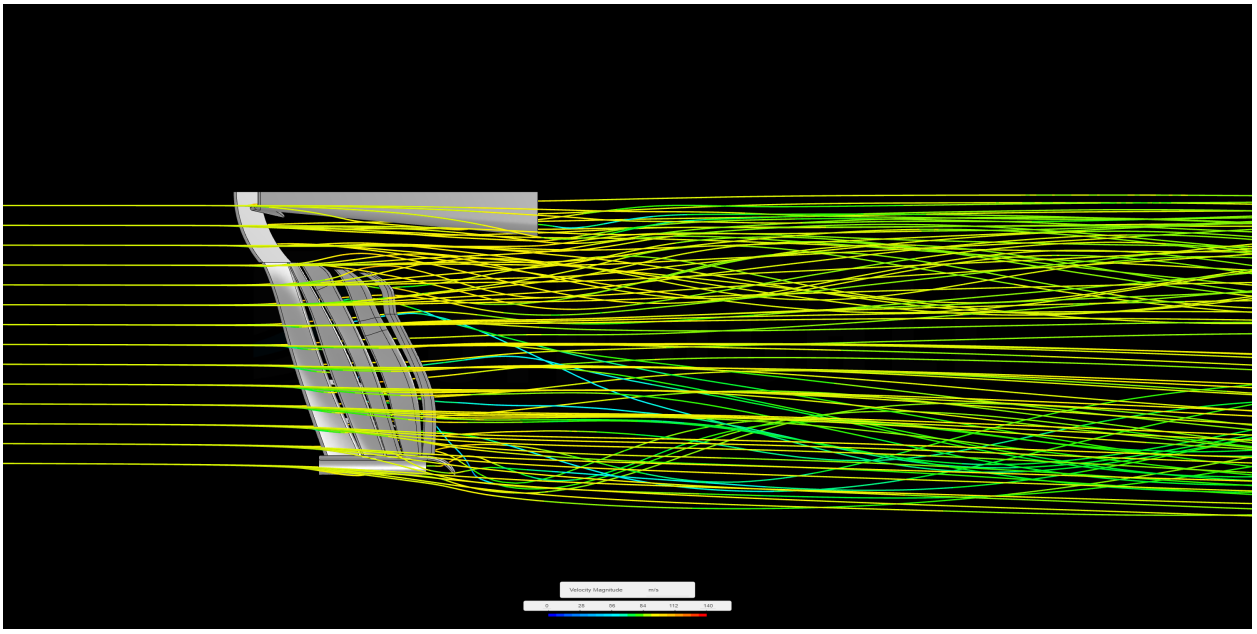

Figure C.3: Top view of the streamlines in the 2021 front wing simulation. *Source: Own Work.*

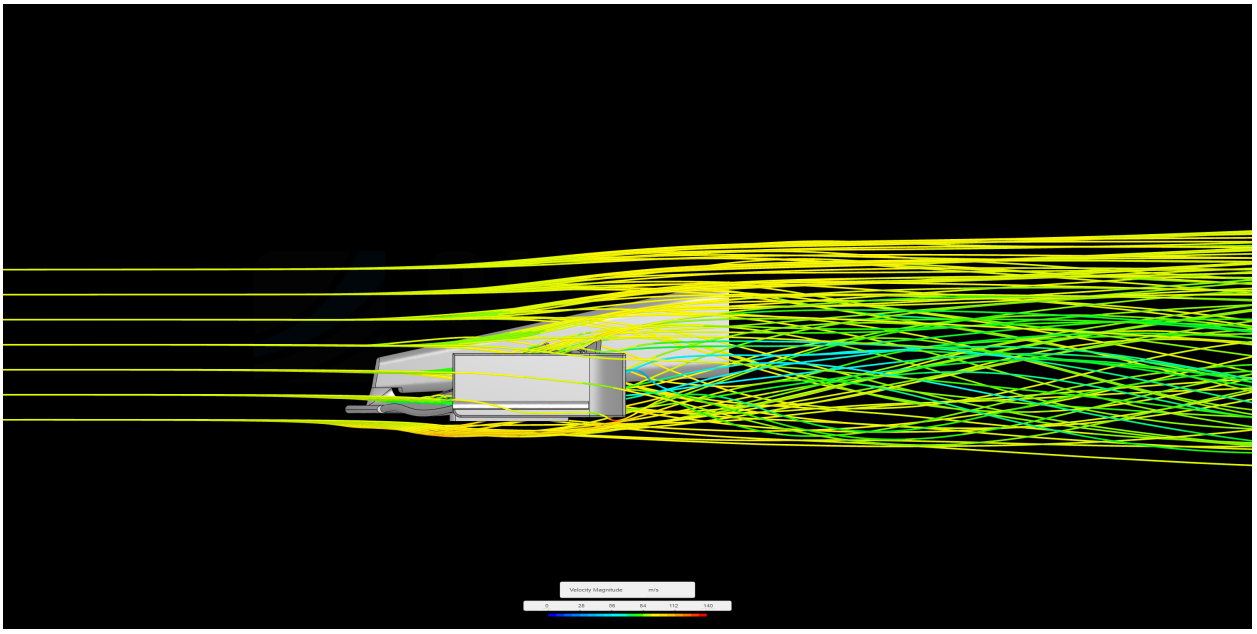

Figure C.4: Profile view of the streamlines in the 2021 front wing simulation. *Source: Own Work.*

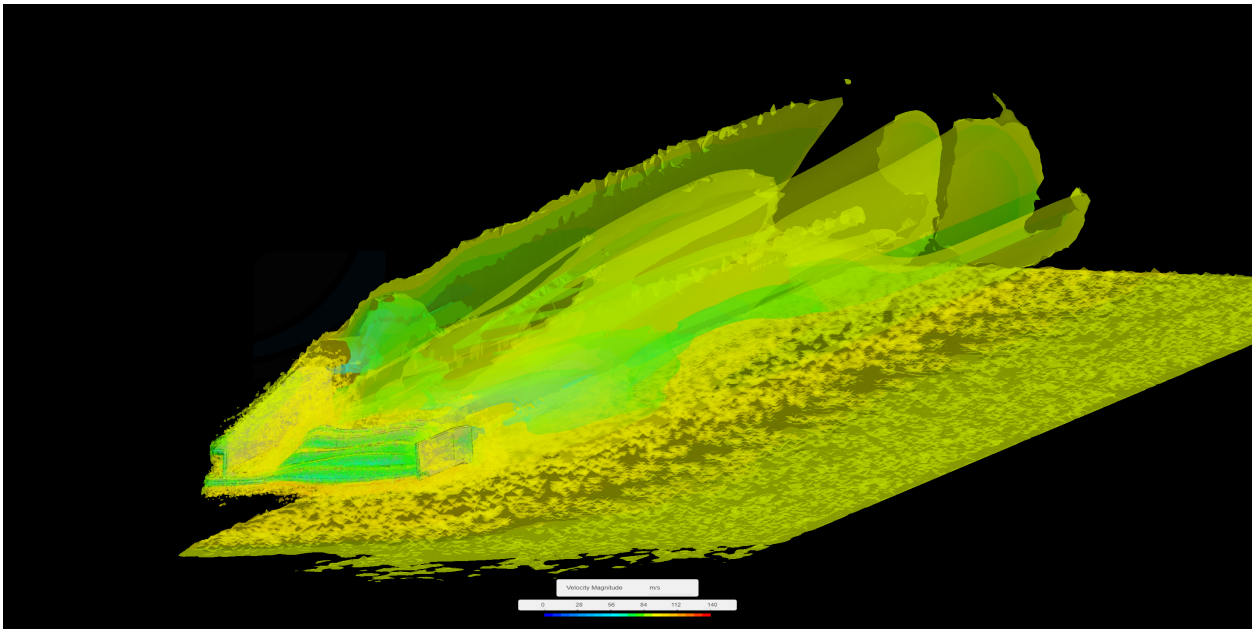

Figure C.5: General view of the vorticity in the 2021 front wing simulation. *Source: Own Work.*

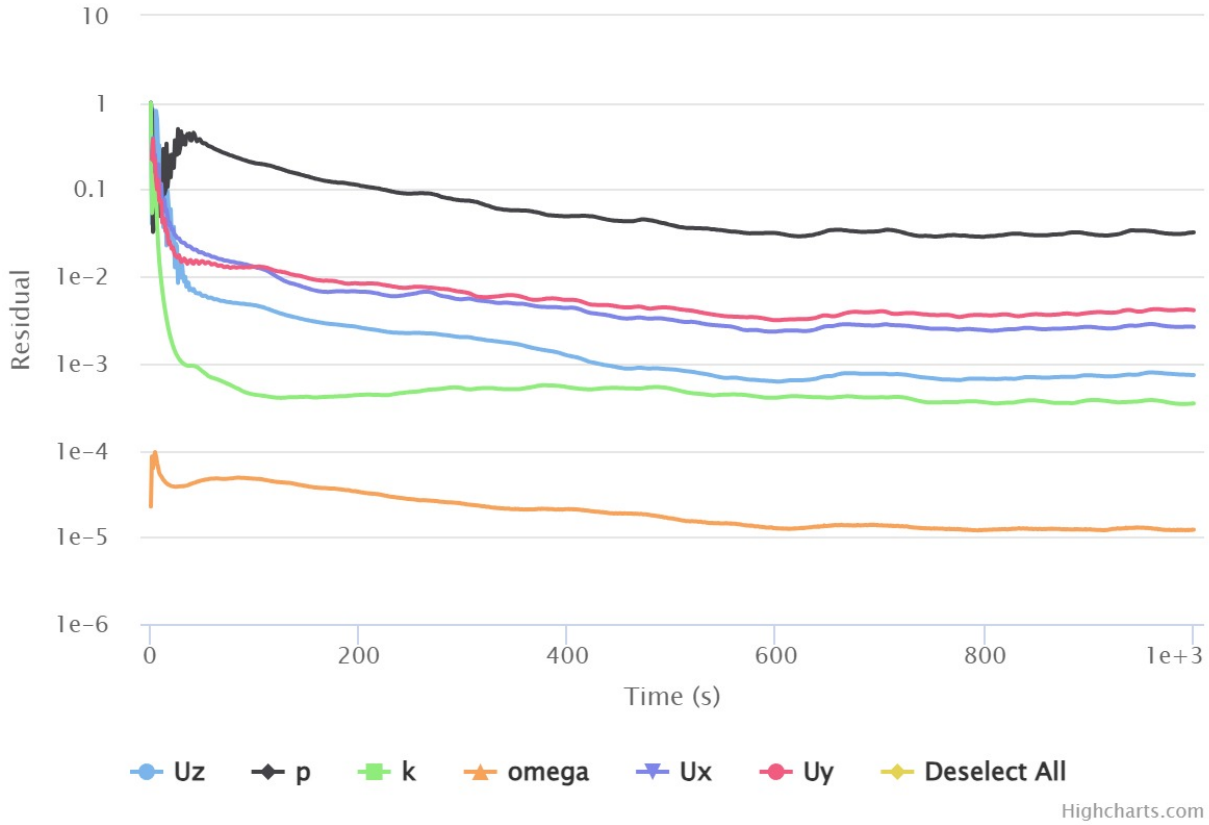

Figure C.6: Residual plots of the 2021 front wing simulation. *Source: Own Work.*

C.2 2021 front wing and tire simulation

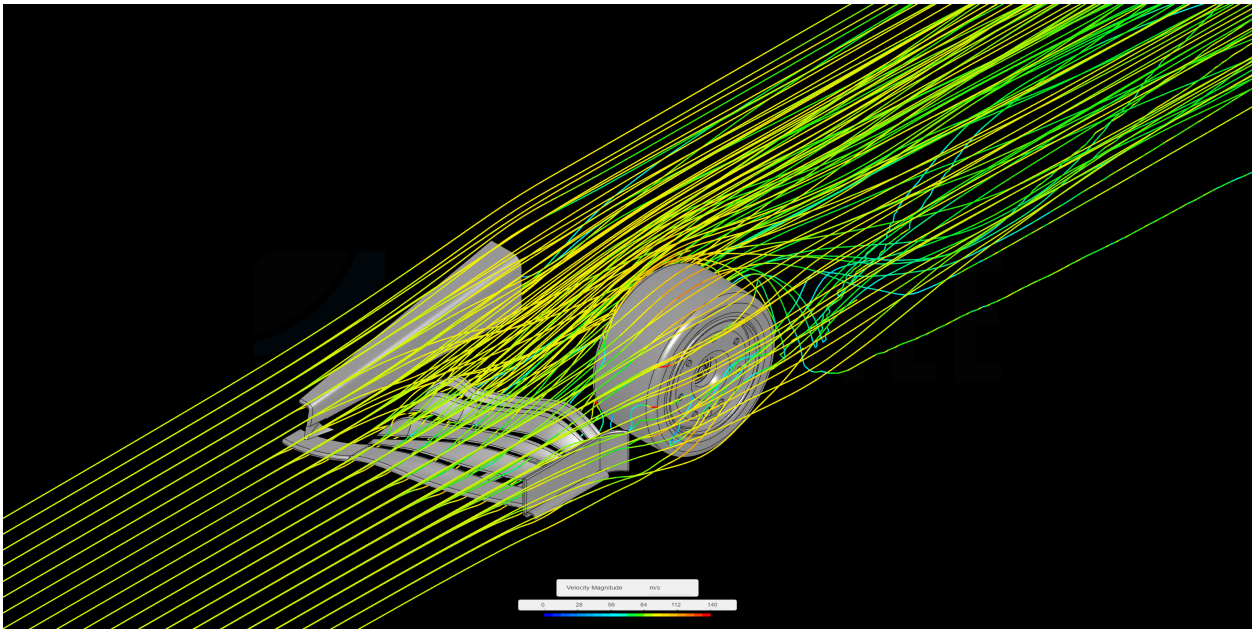

Figure C.7: Isometric view of the streamlines in the 2021 front wing and tire simulation. *Source: Own Work.*

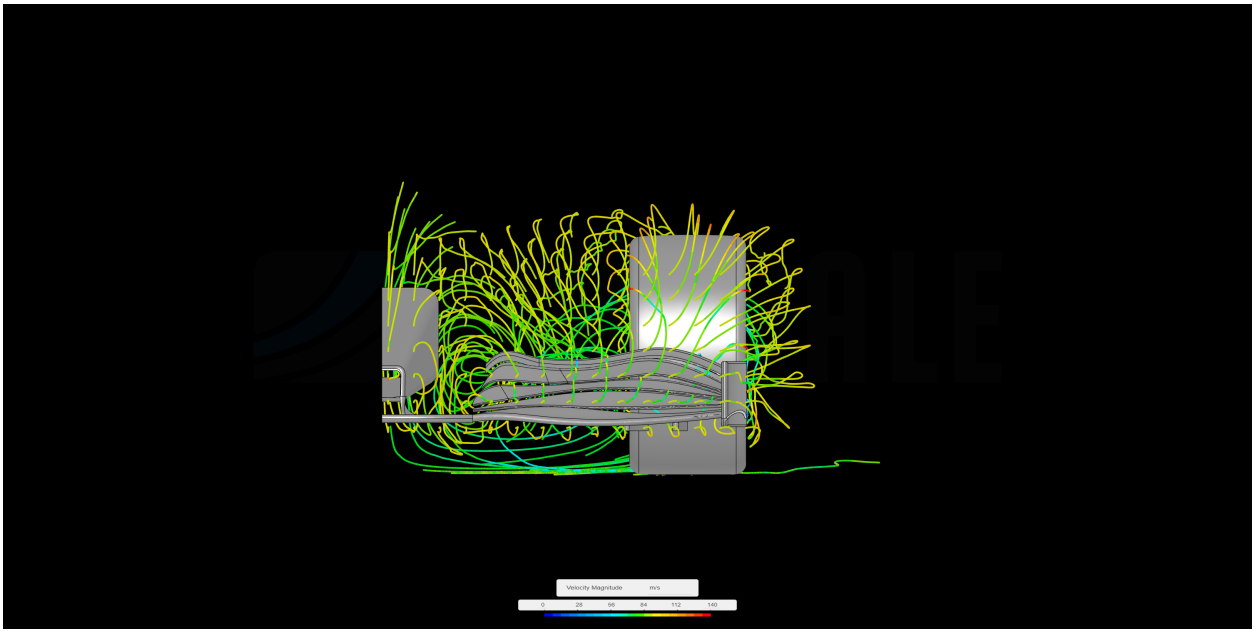

Figure C.8: Front view of the streamlines in the 2021 front wing and tire simulation. *Source: Own Work.*

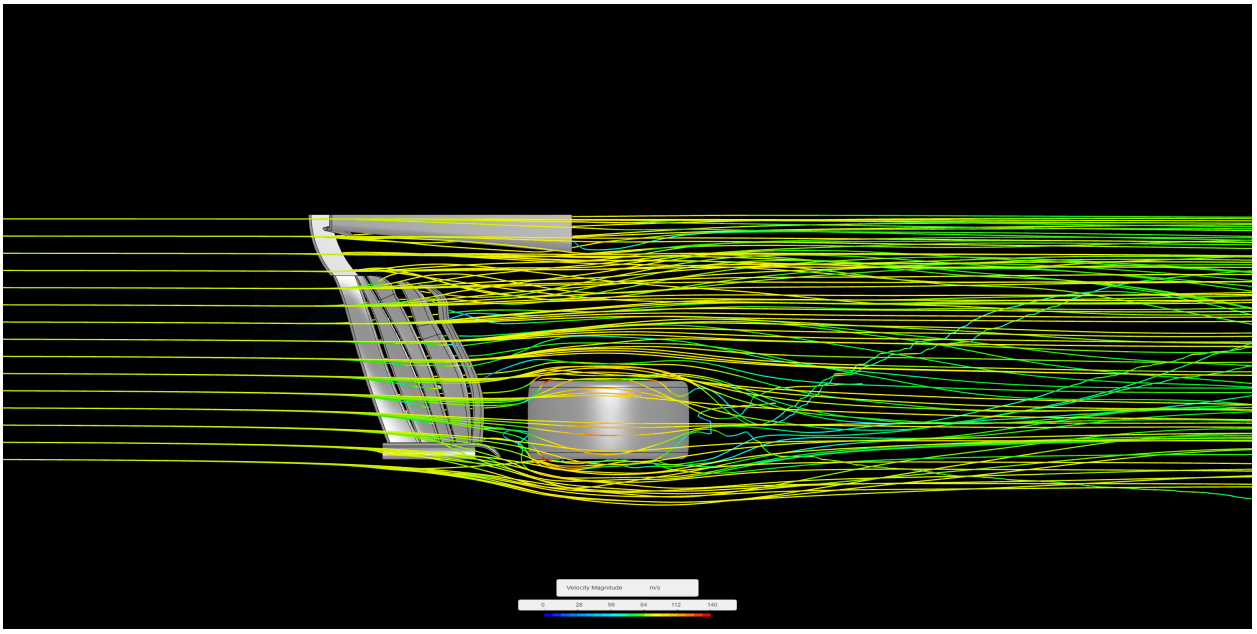

Figure C.9: Top view of the streamlines in the 2021 front wing and tire simulation. *Source: Own Work.*

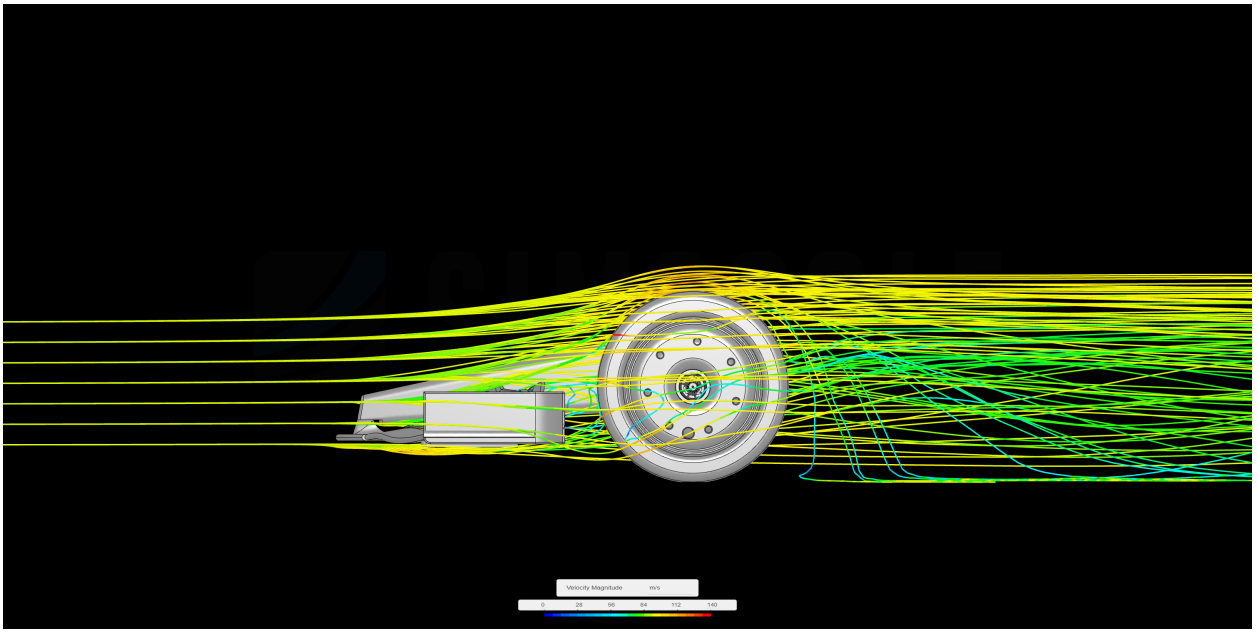

Figure C.10: Profile view of the streamlines in the 2021 front wing and tire simulation. *Source: Own Work.*

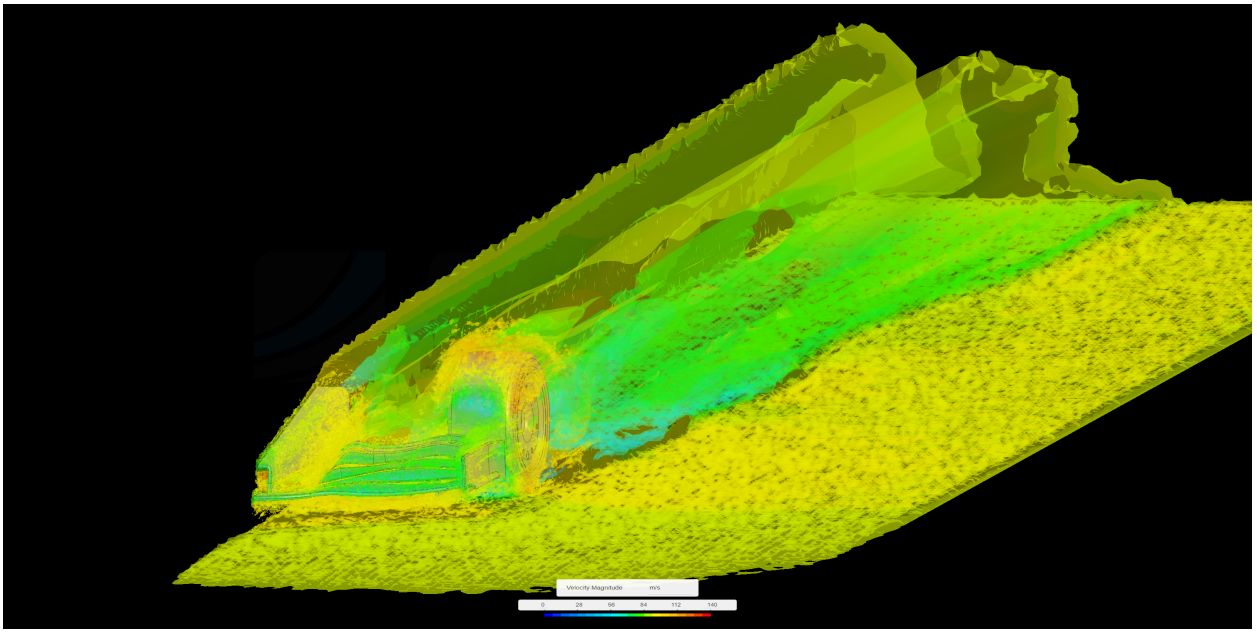

Figure C.11: General view of the vorticity in the 2021 front wing and tire simulation. *Source: Own Work.*

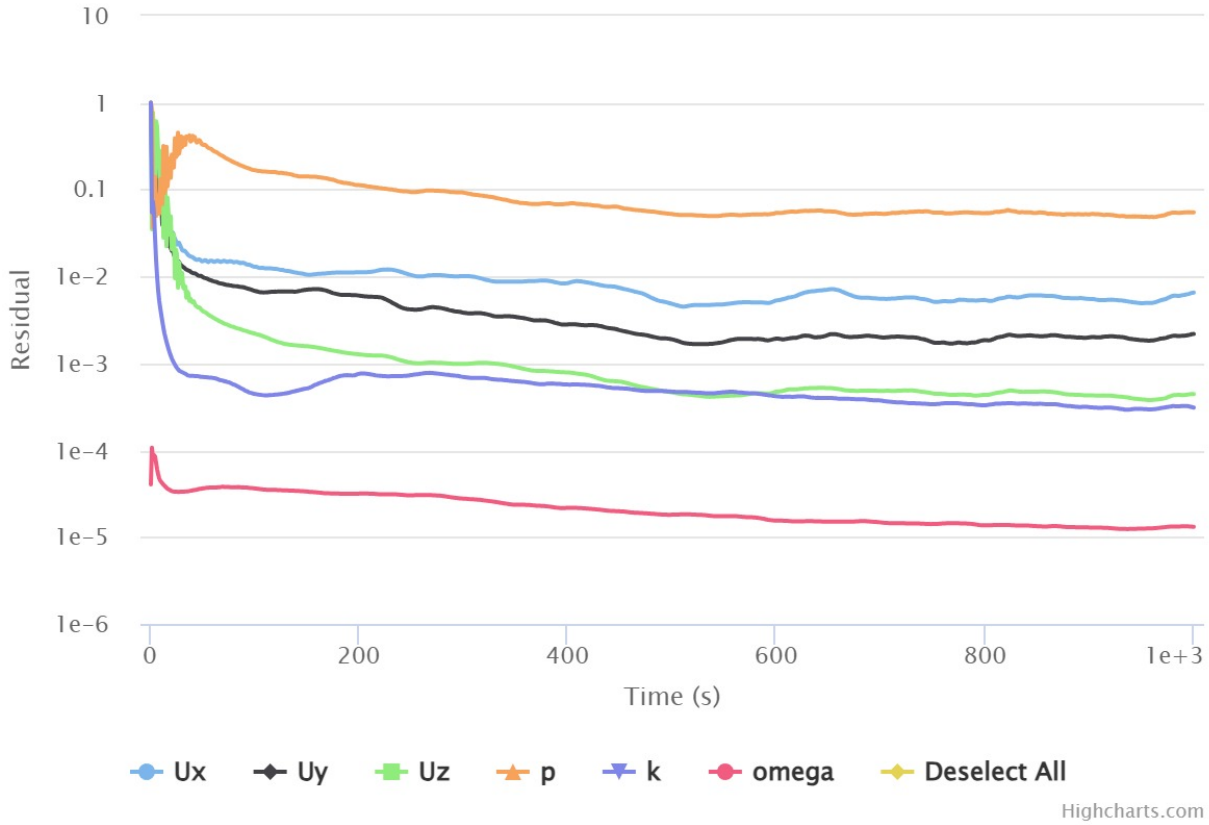

Figure C.12: Residual plots of the 2021 front wing and tire simulation. *Source: Own Work.*

C.3 2022 front wing simulation

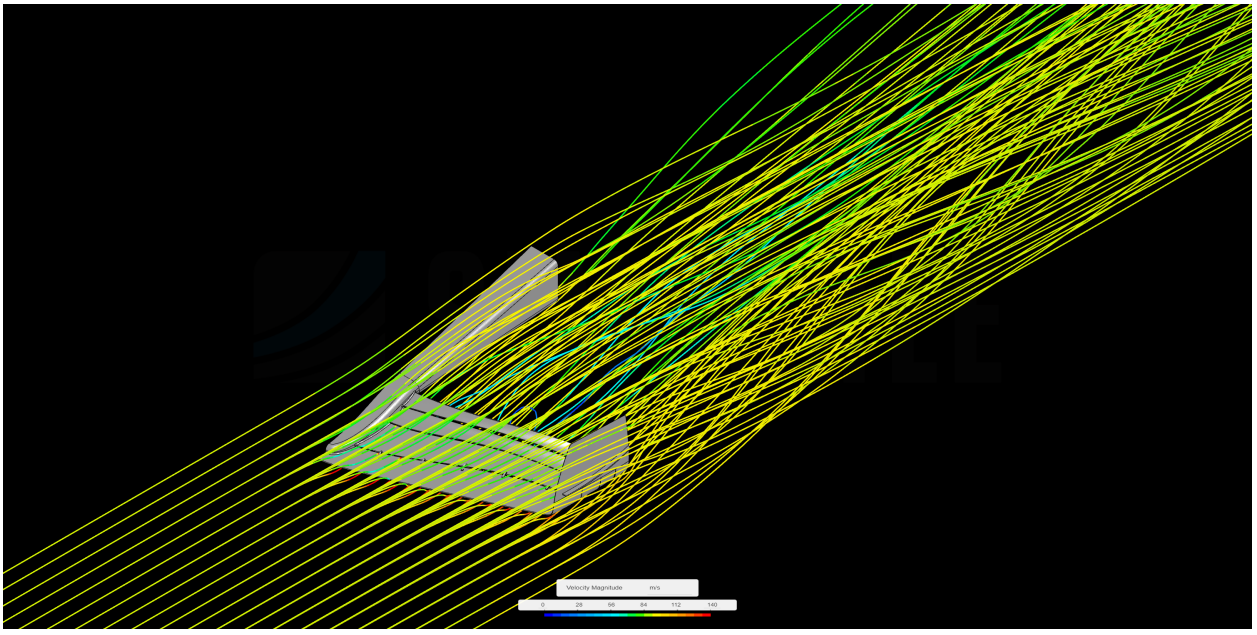

Figure C.13: Isometric view of the streamlines in the 2022 front wing simulation. *Source: Own Work.*

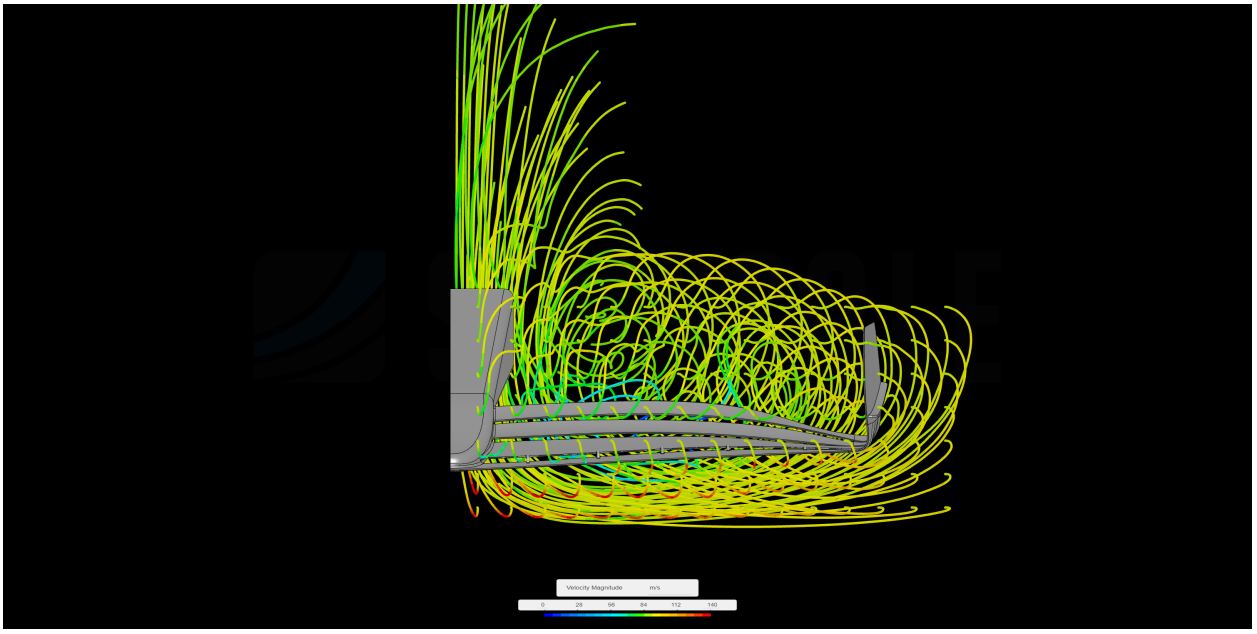

Figure C.14: Front view of the streamlines in the 2022 front wing simulation. *Source: Own Work.*

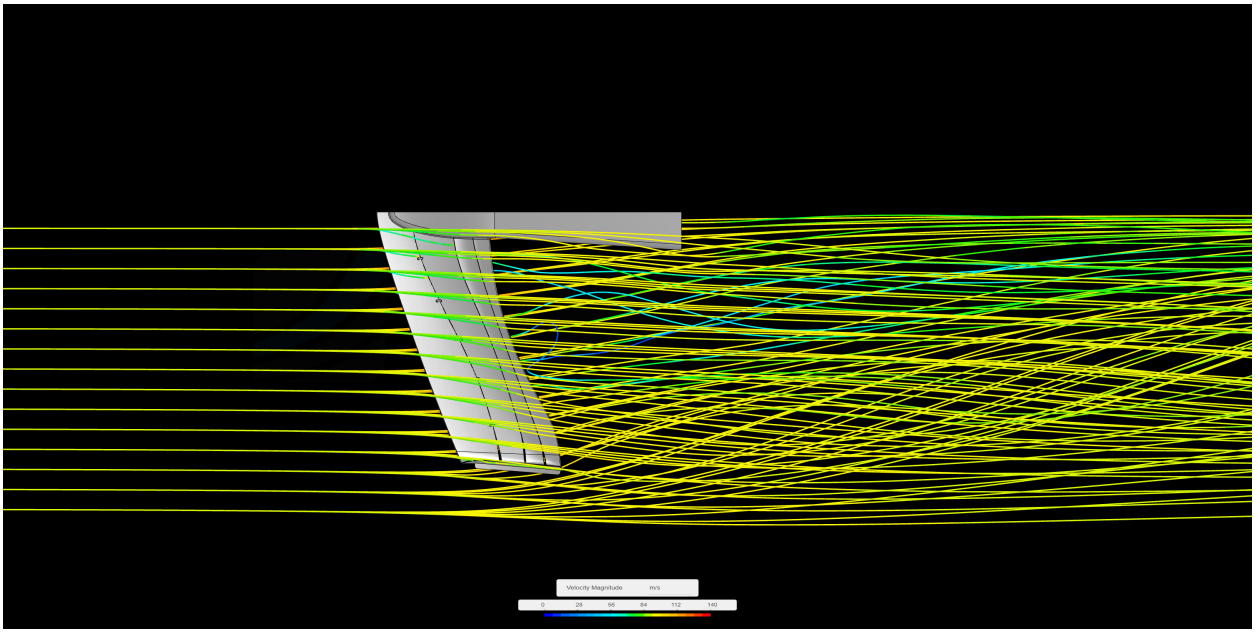

Figure C.15: Top view of the streamlines in the 2022 front wing simulation. *Source: Own Work.*

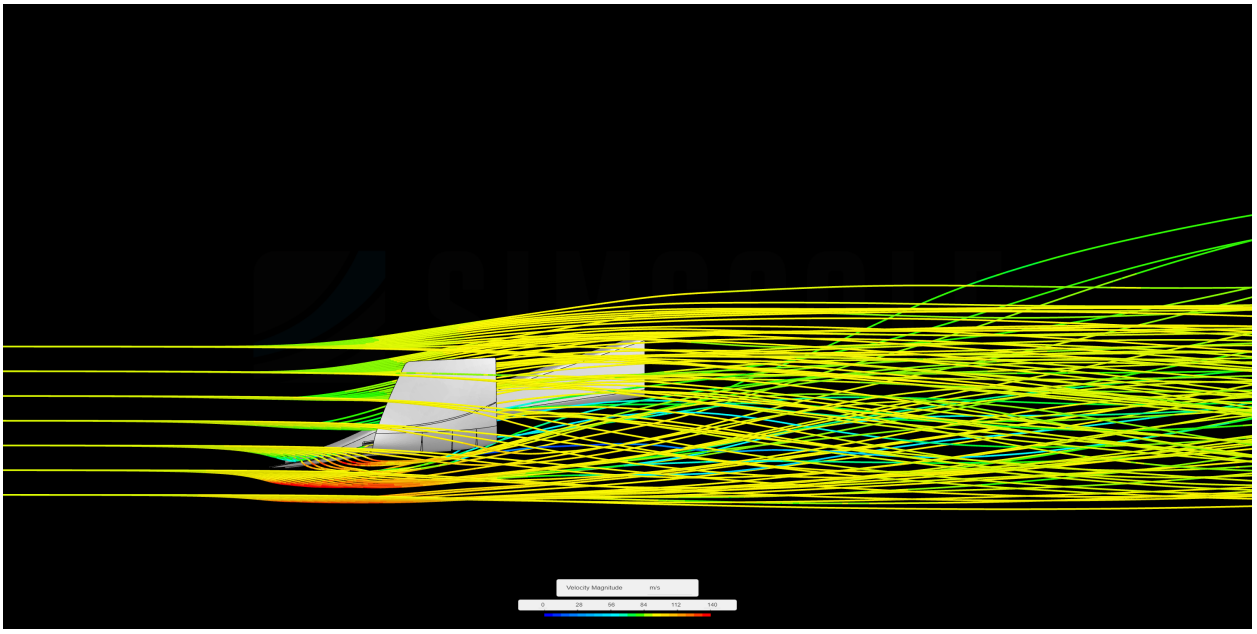

Figure C.16: Profile view of the streamlines in the 2022 front wing simulation. *Source: Own Work.*

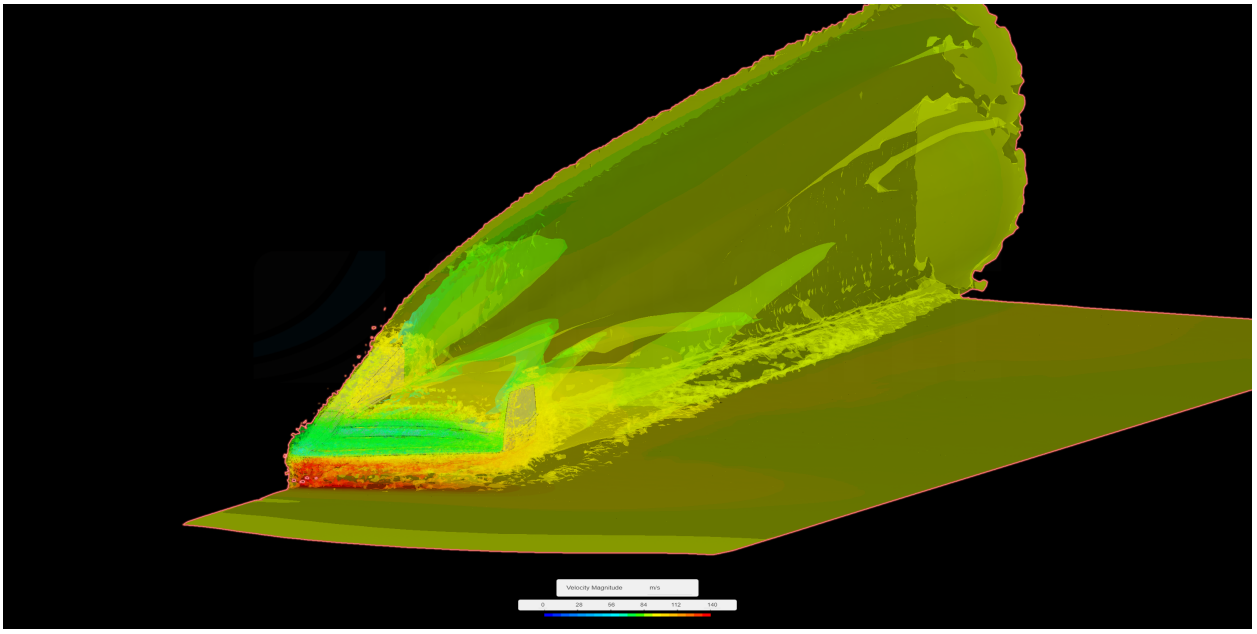

Figure C.17: General view of the vorticity in the 2022 front wing simulation. *Source: Own Work.*

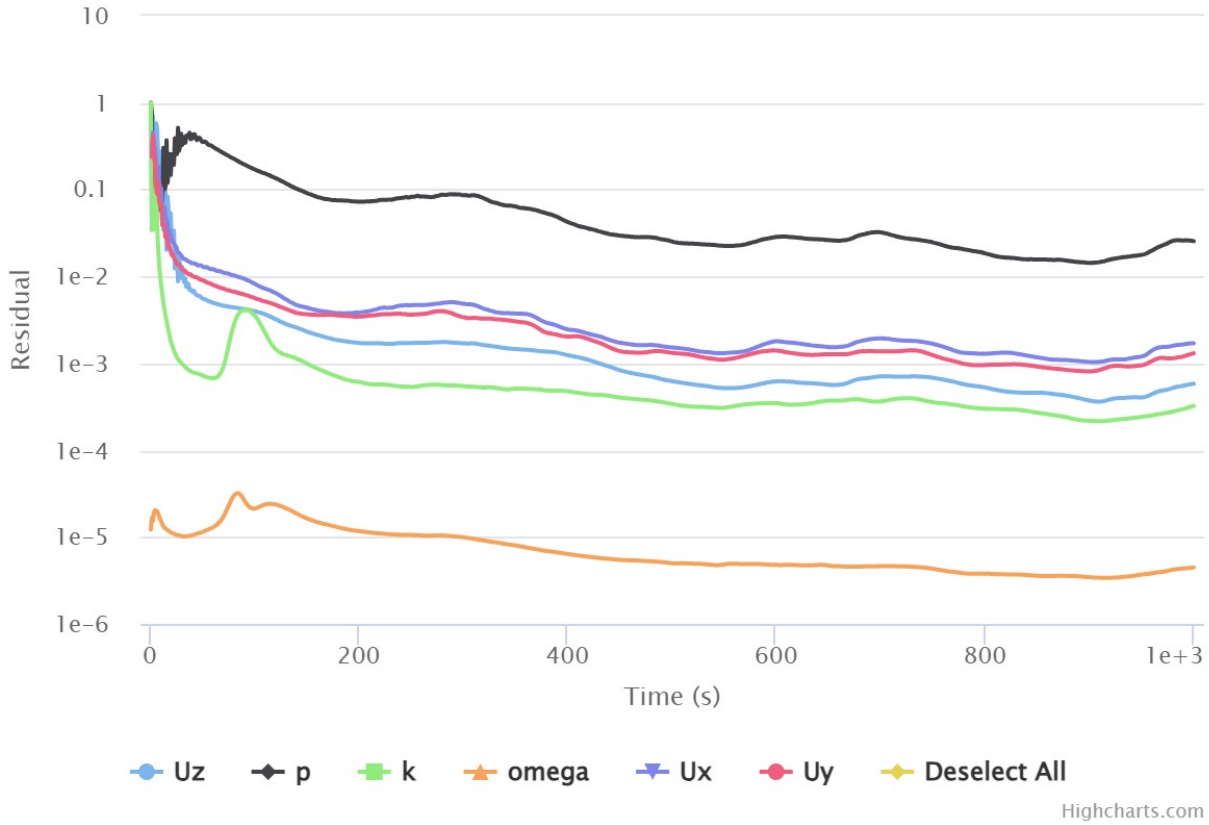

Figure C.18: Residual plots of the 2022 front wing simulation. *Source: Own Work.*

C.4 2022 front wing and tire simulation

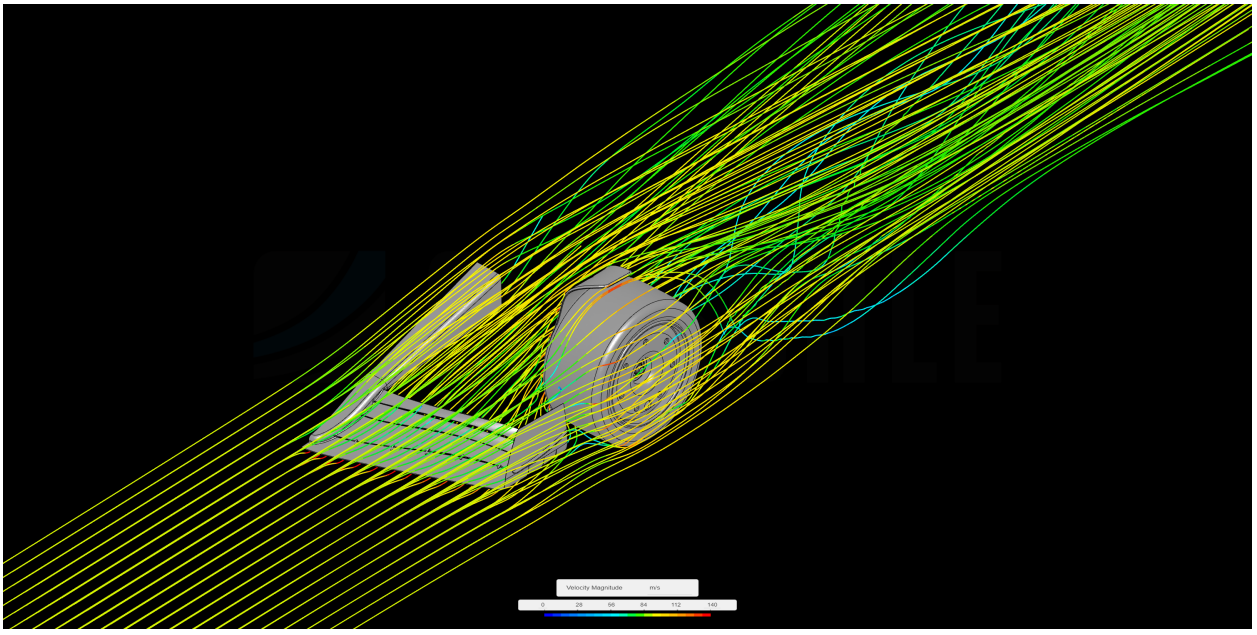

Figure C.19: Isometric view of the streamlines in the 2022 front wing and tire simulation. *Source: Own Work.*

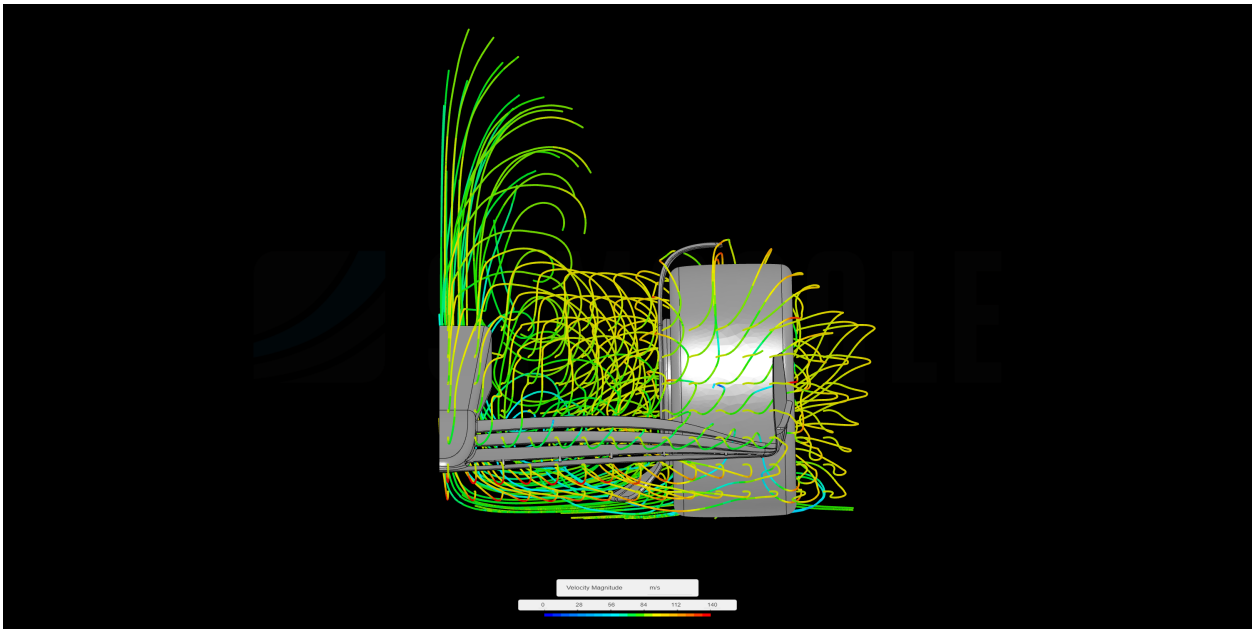

Figure C.20: Front view of the streamlines in the 2022 front wing and tire simulation. *Source: Own Work.*

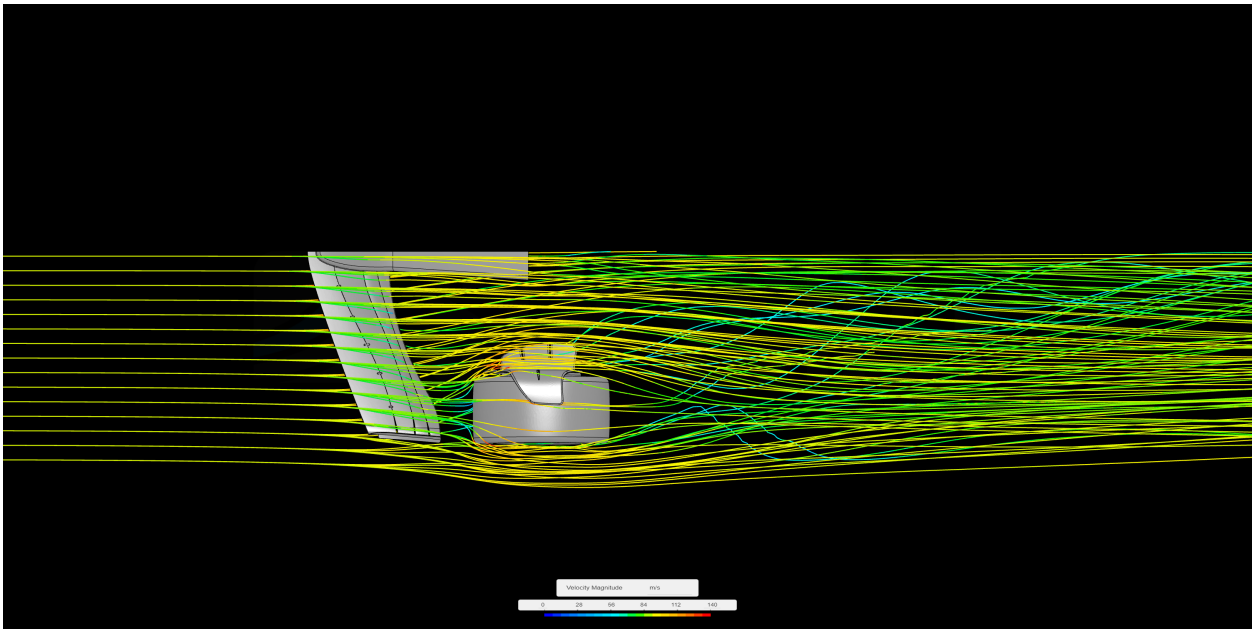

Figure C.21: Top view of the streamlines in the 2022 front wing and tire simulation. *Source: Own Work.*

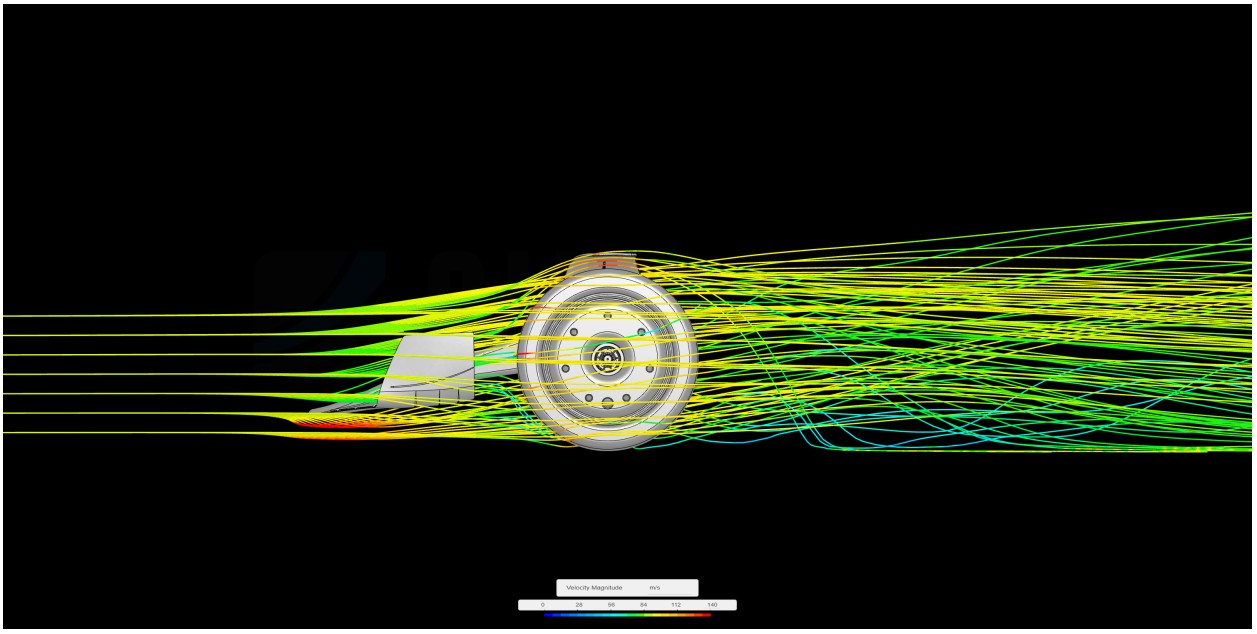

Figure C.22: Profile view of the streamlines in the 2022 front wing and tire simulation. *Source: Own Work.*

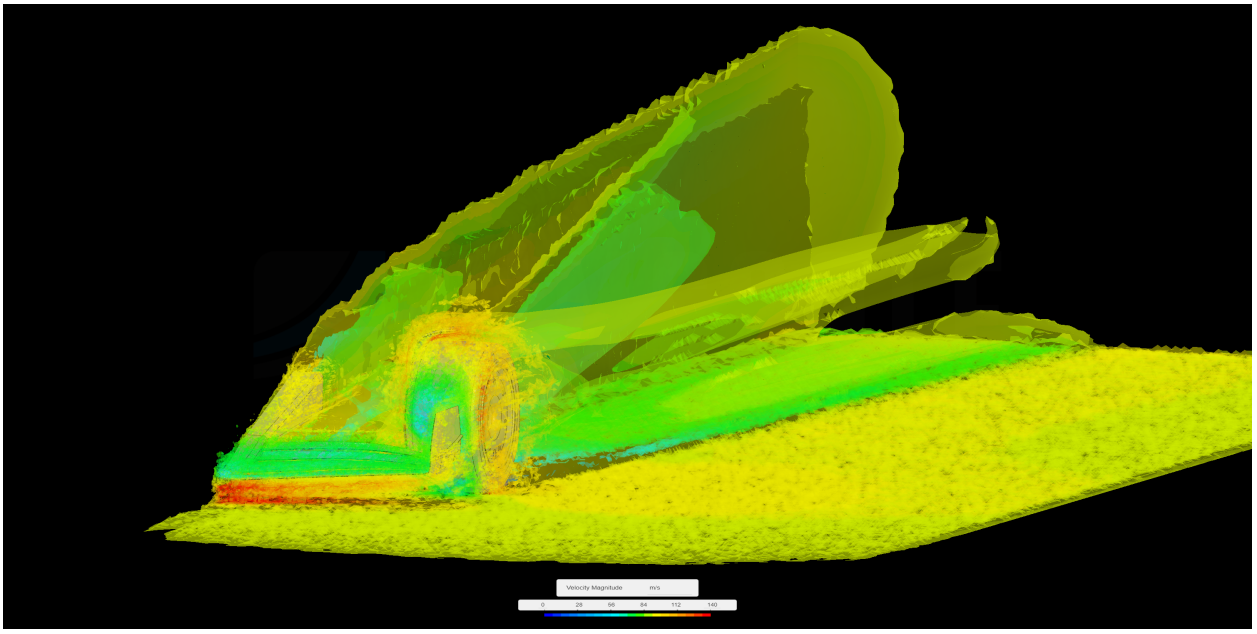

Figure C.23: General view of the vorticity in the 2022 front wing and tire simulation. *Source: Own Work.*

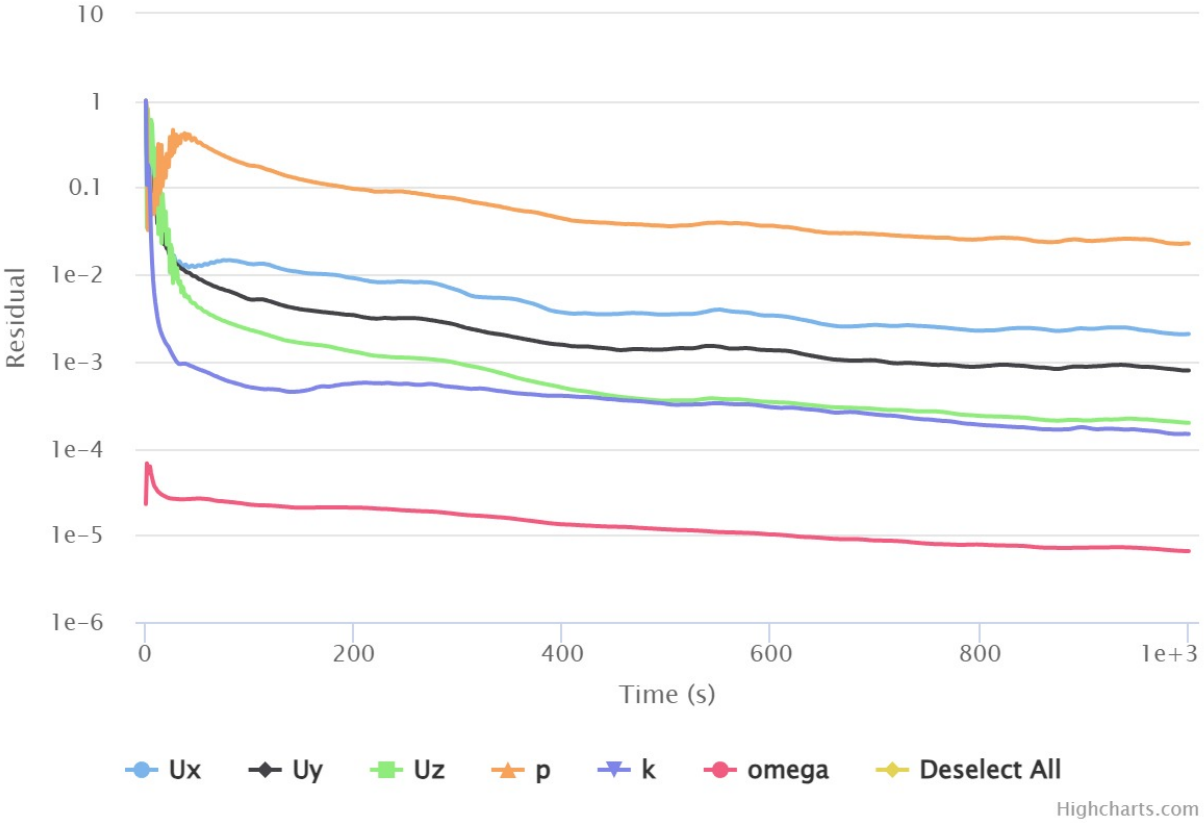

Figure C.24: Residual plots of the 2022 front wing and tire simulation. *Source: Own Work.*